INVESTIGATION OF THE EFFECT OF ATMOSPHERIC DUST ON THE DETERMINATION OF TOTAL OZONE FROM THE EARTH'S ULTRAVIOLET REFLECTIVITY MEASUREMENTS; TECHNICAL REPORT: II

(December 16, 1976)

Contract No. NAS5-23556

Prepared by

J. V. Dave

International Business Machines Corporation
Federal Systems Division
18100 Frederick Pike
Gaithersburg, Maryland 20760

For

National Aeronautics and Space Administration
Goddard Space Flight Center
Greenbelt, Maryland 20771

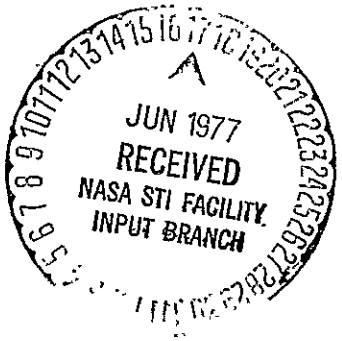

TABLE OF CONTENTS

Table of Contents, Cont'd.

Abstract

In this second technical report for the investigation of the effect of atmospheric dust on the estimation of total ozone from the earth's ultraviolet reflectivety along a local nadir direction, we will describe results of a detailed analysis of the simulated measurements for the BUV (Nimbus-4) configuration by using a total ozone estimation procedure similar to the one reported by Matoor, Heath, Kruegar (1971). Based on this detailed analysis, we will discuss the following two items: (1) A set of recommedations for increasing the accuracy and confidence level of the total ozone values estimated from the measurements of the earth's ultraviolet reflectivity at five different wavelengths (BUV configuration); and (2) a tentative procedure for the estimation of total ozone from measurements of reflectivity at six different wavelengths specified in the SBUV/TOMS (Nimbus-G) configuration.

The above-mentinoed analysis is based on simulated measurements for pseudo-spherical models of the earth's atmosphere resting on a Lambert surface and having arbitrary vertical profiles of ozone, but otherwise free of aerosols and/or water droplets.

I. INTRODUCTION

In the first technical report with the same title as this one, we described a set of computer programs (FORTRAN IV language) for evaluating the azimuth-independent component of the intensity of scattered radiation emerging at the top of a *pseudo-spherical* atmospheric model with arbitrary height-distributions of ozone, and/or aerosols. The model is assumed to rest on a Lambert ground of reflectivity R. By *pseudo-spherical*, we mean that the basic atmospheric model corresponds to that of a plane-parallel atmosphere of infinite extent along the horizontal directions, but of finite optical extent along the vertical; the sphericity is only partly accounted for by computing attenuation suffered by the incoming solar radiation (neglecting refraction) for the appropriate spherical case. Furthermore, the nadir angle of observation is also duly corrected for the satellite's altitude above the earth's surface.

These computer programs were primarily developed for assisting the NASA, Ultraviolet Ozone Team (Dr. D. F. Heath and others) in their total-ozone estimation work by performing analysis of the simulated measurements for various realistic models of the earth's atmosphere. Estimation of total ozone in an atmospheric column from multi-spectral measurements of the radiation backscattered by the earth-atmosphere system, is not a trivial problem for several reasons. First, a relatively noise-free set of spectrally pure measurements is required with an accurate knowledge of the instrument's position and attitude in space and time. Second, there are a good number of atmospheric unknowns which can modulate the

signal in an undeterminable manner. Besides the total ozone to be estimated, some of the other unknowns are its height distribution, reflectivity of the underlying surface and its wavelength dependence, surface pressure, aerosols, water droplets, ice crystals, and nonhomogeneities in the field of view due to one or more of these factors.

Some aspects of this complex problem were first investigated by Dave and Mateer [1967] with simulated measurements restricted to the Rayleigh models of the earth-atmosphere system. Based on this prior study, Mateer, Heath, and Krueger [1971] developed a procedure for estimating total ozone, in an atmospheric column underneath the NIMBUS-IV satellite, from measurements of the back-scattered ultraviolet radiation in five spectral regions (viz., 0.3125, 0.3175, 0.3312, 0.3398, and 0.3800 μm). They then used this procedure for estimating total ozone for a sample of 320 cases of approximate coincidences (in space as well as in time) of the NIMBUS-IV data, and *ground-truth* measurements of total ozone with the Dobson Spectrophotometer. They find that, on the average, the satellite values were lower than the corresponding Dobson values by about 0.025 atm-cm. Some cases are also reported where the difference between these two values is as large as 0.060 atm-cm. They believed that a part of this error is due to a lack of a perfect coincidence between the Dobson, and the satellite data. Based on their experience with the analysis of the NIMBUS-IV BUV data, this team of investigators have recommended an additional measurement at 0.3600 μm for the SBUV/TOMS experiments to be performed aboard the forthcoming NIMBUS-G satellite.

The purpose of this report is to discuss the results of a detailed analysis of the simulated measurements for the five-wavelength, BUV configuration. These simulated measurements are obtained by making use of the computer programs mentioned at the beginning of this section. This analysis is for models of the earth-atmosphere system resting on a Lambert surface whose reflectivity R may or may not vary with the wavelength, but the atmosphere free of any particulate matter comparable in size to, or larger than, the wavelengths of incident radiations under investigation. A set of five-wavelength simulated measurements is first analyzed in terms of the *best ozone estimate*, and the *effective albedo* by making use of a procedure identical to the one discussed by Mateer, Heath, and Krueger [1971]. Further analysis is then performed by imposing additional, valid and meaningful constraints for acceptance of the *best ozone estimate*. This analysis is followed by a set of recommendations which may be incorporated in the final, BUV, total-ozone estimation procedure for increasing the accuracy and confidence level of the satellite, total-ozone values. Experience gained from the aforementioned BUV simulation study, is then applied for developing and testing a total-ozone estimation procedure for the six-wavelength, SBUV/TOMS configuration.

II. TOTAL-OZONE ESTIMATION PROCEDURE

2.1 *General:* In §I, it was mentioned that a procedure for estimation of total ozone from five spectral measurements of the radiation backscattered by the earth-atmosphere system along the local nadir direction,

was developed and used by Mateer, Heath, and Krueger [1971]. Since a detailed written description of this procedure was not available at the beginning of this project, a tentative description was developed by the author after several telephone conversations with Mr. Larry Novak who is very closely associated with the BUV, total-ozone-analysis project at NASA/GSFC. This tentative description was sent to Dr. Robert S. Fraser (Consultant to the Technical Officer for this Contract) for a verification on August 12, 1976. An additional point to this tentative description was brought out by Mr. Novak in the material which Dr. Fraser enclosed with his letter to the author, and dated August 25, 1976. In the meantime, Mr. Novak also sent, to the author, a set of subroutines used in estimation of total ozone, and a copy of his preliminary documentation of these subroutines.

Some basic information required in following the total-ozone estimation procedure described in §2.4, is given in §2.2 and §2.3. Description of the procedure given in §2.4 is primarily for the purpose of bringing out details of the procedure as used in the interpretation of the simulated, BUV data. However, this description is kept general enough for use in modification to the original total-ozone estimation procedure (one being used at NASA/GSFC by Mr. Novak and others), and also for use in analysis of the simulated observations for the SBUV/TOMS configuration.

Because of a rather limited scope of this simulation experiment and controlability of several factors, some minor differences occur between

the original total-ozone estimation procedure (used at NASA/GSFC), and the one used for the first analysis of the simulated, BUV observations. These differences are brought out in §2.5 for the sake of completeness.

2.2 *Basic Tables:* The backbone of the total-ozone estimation procedure is several sets of tables of computed quantities $I_c(\lambda, \Omega, P_0, R_\lambda = 0.0, \theta_0)$, $T_c(\lambda, \Omega, P_0, \theta_0)$, and $\bar{S}_c(\lambda, \Omega, P_0)$ obtained with the help of computer programs described in the Technical Report I having the same title as this one. Each table in these sets is for a *pseudo-spherical* atmospheric model with a surface pressure of P_0 mb, and a total-ozone amount of Ω atm-cm. These models resting on a perfectly absorbing surface ($R_\lambda = 0.0$), are free of any aerosols, water droplets, ice crystals, or horizontal nonhomogeneities. The remaining two parameters, viz λ and θ_0 represent the wavelength (in μm, 1 μm = 10^{-4} cm), and the local solar zenith angle (in degrees) for the incident radiation under investigation. For all wavelengths, these quantities are computed after assuming that a $\pi \cos\theta_0$ units of solar energy is incident normal to a unit horizontal area located at the top of the model, in each spectral band.

The quantity $I_c(\lambda, \Omega, P_0, R_\lambda = 0.0, \theta_0)$ is the intensity of the scattered radiation emerging at the top of the atmospheric model along the local nadir direction when all four parameters in the parentheses are specified. The quantity $T_c(\lambda, \Omega, P_0, \theta_0)$ represents the total (direct + diffuse) transmission along the local nadir direction (in the same model) when the atmospheric model is illuminated isotropically, from below, by a Lambertian reflection of all direct solar energy and

the diffuse skylight energy (due to illumination of the model from top only) emerging at the bottom. The third quantity $\bar{S}_c(\lambda, \Omega, P_0)$ represents the diffuse flux reflectivity for an isotropic illumination of the model from below.

The following expression is then used for computations of $I_c(\lambda, \Omega, P_0, R_\lambda, \theta_0)$ when a given model rests on a ground obeying Lambert's law of reflection, and having a reflectivity R_λ at the wavelength λ:

$$I_c(\lambda, \Omega, P_0, R_\lambda, \theta_0) = I_c(\lambda, \Omega, P_0, R_\lambda = 0.0, \theta_0) + \frac{R_\lambda}{1 - R_\lambda \bar{S}_c(\lambda, \Omega, P_0)} T_c(\lambda, \Omega, P_0, \theta_0) . \quad (1)$$

In all, 20 sets of tables are prepared; the first ten sets are for P_0 = 1,000 mb, and the remaining ones are for P_0 = 400 mb. The total ozone amount for an atmospheric model with P_0 = 1,000 mb is given by one of the following values of the parameter Ω: Ω = 0.200, 0.250, 0.300, 0.350, 0.400, 0.450, 0.500, 0.550, 0.600, and 0.650 atm-cm. (The vertical distribution of ozone for each of these amounts is for a mid-latitude atmosphere. The actual distribution used is based on information provided by Dr. C. L. Mateer.)

The atmospheric models for P_0 = 400 mb are obtained after terminating the corresponding 1,000 mb models at a level which is 7 km above the mean sea-level. Thus, if the 1,000 mb has a total ozone amount of 0.200 atm-cm, the corresponding 400 mb model has an actual total ozone amount of 0.189 atm-cm. For clarity, we will denote the actual total

ozone amount in a model by the symbol Ω, and the total ozone amount in the model when its lower boundary is extended to the mean sea-level, by the symbol Ω_{in}. Thus, for the above-mentioned case, $\Omega = \Omega_{in} = 0.200$ atm-cm for the $P_0 = 1{,}000$ mb model; but $\Omega = 0.189$ atm-cm, and $\Omega_{in} = 0.200$ atm-cm for the $P_0 = 400$ mb model. Values of Ω and Ω_{in} for the remaining models are given in §3.1. For convenience, all ten sets of tables for a given value of P_0 are arranged in the increasing order of the parameter Ω.

In order to confirm with the original, BUV total-ozone estimation procedure, we have used the value of Ω_{in} in the place of that of Ω during the analysis of simulated observations. This ingenious step permits an estimation of total ozone in the entire (right down to the mean sea-level) atmospheric column underneath the satellite even when an optically thick cloud layer is located between the satellite and the ground. Presence of such a cloud layer is not expected to affect the amount of ozone within, or under, the cloud layer.

A given set of tables contains values of I_c, T_c, and $\bar{S}_c$ at six wavelengths (viz, 0.3125, 0.3175, 0.3312, 0.3398, 0.3600, and 0.3800 μm), and those of I_c and T_c at ten values of θ_0 (viz, 0°, 45°, 60°, 70°, 75.6°, 79.6°, 82.5°, 84.7°, 86.7°, and 90°). The 0.3600 μm table is for use in the analysis of the simulated measurements for the SBUV/TOMS configuration.

If the conditions for which these basic tables are prepared are satisfied within acceptable limits, and if values of the parameters P_0,

θ_0, and R_λ are available when the intensity measurements $[I_m(\lambda, \theta_0)]$ along a local nadir direction are taken, a value of Ω for the atmospheric column underneath the satellite at the time of observation may be estimated by making use of secondary tables of $I_c(\lambda, \Omega, P_0, R_\lambda, \theta_0)$ vs. P_0, vs. Ω (or Ω_{in}), and vs. θ_0. Some interpolation between tabulated values of various variables will be necessary for this purpose. Out of the several values of Ω so obtained (one corresponding to each wavelength of measurement), one with the highest sensitivity of I_c to changes in Ω, in the range of immediate interest, may be selected as the best ozone estimate. [Only two parameters are listed for the measured intensity, $I_m(\lambda, \theta_0)$. This is because the third parameter Ω is to be determined. Furthermore, as it will be discussed later, values of the remaining two parameters (viz, P_0 and R_λ) are also unknown within any meaningful accuracy for either the BUV, or SBUV/TOMS configuration.]

Before closing this subsection, we would like to add that the above-mentioned basic tables can also be used to obtain a value of R_λ after rewriting Eq. (1) as follows:

$$R_\lambda = \frac{f(\lambda, \Omega, P_0, R_\lambda = 0.0, \theta_0)}{T_c(\lambda, \Omega, P_0, \theta_0) + \bar{S}_c(\lambda, \Omega, P_0)\, f(\lambda, \Omega, P_0, R_\lambda = 0.0, \theta_0)}, \quad (2)$$

where

$$f(\lambda, \Omega, P_0, R_\lambda = 0.0, \theta_0) = I_m(\lambda, \theta_0) - I_c(\lambda, \Omega, P_0, R_\lambda = 0.0, \theta_0). \quad (3)$$

The Ω dependence of the terms on the righthand side of Eq. (2) vanishes when the wavelength for which the measurement is available, is located

outside the bands of absorption by ozone (e.g., 0.3800 μm).

2.3 *The Quantity N:* It is a well-known fact that the atmospheric conditions for which the basic tables (§2.2) are prepared, are rarely satisfied in practice. Furthermore, values of $I_m(\lambda, \theta_0)$ may have some biased error due to calibration problems and/or deterioration. It is therefore customary to use the ratio of the intensity at two wavelengths with significantly different amounts of absorption by ozone, but located sufficiently close enough to minimize the effects of other uncertainties. A more convenient quantity used in the ozone estimation field is given by the following equation:

$$N_c(\lambda_i, \lambda_j; R_{\lambda_i}, R_{\lambda_j}; \Omega_{in}, P_0, \theta_0) = 100 \times \log_{10}\left[\frac{I_c(\lambda_i, \Omega_{in}, P_0, R_{\lambda_i}, \theta_0)}{I_c(\lambda_j, \Omega_{in}, P_0, R_{\lambda_j}, \theta_0)}\right], \tag{4}$$

and

$$N_m(\lambda_i, \lambda_j; \theta_0) = 100 \times \log_{10}\left[\frac{I_m(\lambda_i, \theta_0)}{I_m(\lambda_j, \theta_0)}\right]. \tag{5}$$

For a given set of the remaining parameters, the quantity N_c generally increases with increase in Ω_{in} (see §IV). Therefore, a value of Ω can be estimated from a measured value of $N_m(\lambda_i, \lambda_j, \theta_0)$ and appropriate sets of tables of N_c vs. P_0, vs. θ_0, and vs. Ω_{in} (some interpolation would be required) provided information about the parameters R_{λ_i}, R_{λ_j}, P_0, and θ_0 is available at the time and the place of observation. For

the BUV (or SBUV/TOMS) configuration, the criterion for selecting the wavelength pair mentioned at the beginning of this subsection is satisfied by two pairs, viz, 0.3312 - 0.3125 μm, and 0.3398 - 0.3175 μm. The N_c values for the third pair, viz, 0.3398 - 0.3312 μm, are generally too insensitive to changes in Ω_{in}.

Another quantity of interest to us is the slope of the N_c vs. Ω_{in} curve in the region surrounding the point where an Ω value is estimated. It will be given by

$$S^Z_{x,y} = \frac{N_c(\Omega_{k+1}) - N_c(\Omega_k)}{\Omega_{k+1} - \Omega_k}, \tag{6}$$

where

$$\Omega_k \leq \Omega^Z_{x,y} \leq \Omega_{k+1}.$$

In Eq. (6), we have omitted the parameters λ_i, λ_j, R_{λ_i}, R_{λ_j}, P_0 and θ_0 for the quantity N_c in the numerator, for brevity. The quantities Ω_k and Ω_{k+1} are two successive values of Ω_{in} for which basic tables are available.

The subscript x (to Ω or S) stands for the wavelength pair used; x = 1 for the first pair, viz, 0.3312 - 0.3125 μm; and x = 2 for the second pair, viz, 0.3398 - 0.3175 μm. The subscript y stands for the value of P_0 identifying the set of basic tables. The superscript Z identifies the nature of R_{λ_i}, R_{λ_j} information (see §2.4).

2.4 *Basic Procedure:* For estimation of total ozone in a simulated BUV configuration, simultaneous measurements of the intensity of back-scattered radiation along the local nadir direction are available at five wavelengths; i.e., we have values of $I_m(\lambda, \theta_0)$ for λ = 0.3125, 0.3175, 0.3312, 0.3398, and 0.3800 μm. Value of θ_0 for the place, and the time of observation is also known. We then proceed as follows to obtain values of the *best ozone estimate* (Ω_e), and the *effective albedo* ($\bar{R}$).

Step I: Use the measured value of $I_m(0.3800, \theta_0)$ for evaluation of the righthand side of Eq. (2) by making use of the 1,000 mb tables for the appropriate θ_0. (We do not have information on P_0; the 1,000 mb table is used arbitrarily.) Furthermore, there may be other unknown factors, e.g., absorption and/or back-scattering by aerosols, or the Lambert's law may not be valid. We have therefore not computed $R_{0.3800}$ in this step. The computed quantity will therefore be referred to as the *coarse effective albedo,* and it will be represented by the symbol $R^C_{0.3800,1000}$.

Step II: Assume that the *coarse effective albedo* so measured is independent of λ. Therefore,

$$R^C_{\lambda,1000} = R^C_{0.3800,1000} \tag{7}$$

for λ = 0.3125, 0.3175, 0.3312, and 0.3398 μm.

Step III: Use values of the quantity $R^C_{\lambda,1000}$ in the place of reflectivities R_{λ_i} and R_{λ_j} in Eq. (4). Then obtain values of the quan-

tities $\Omega^C_{x,1000}$ and $S^C_{x,1000}$ for $x = 1$, and 2 by making use of the $P_0 = 1{,}000$ mb tables, information content of §2.3, and values of $N_m(\lambda_i, \lambda_j, \theta_0)$ obtained from appropriate values of $I_m(\lambda, \theta_0)$.

Note: (1) The quantity $\Omega^C_{x,1000}$ is set to 0.0, and $S^C_{x,1000}$ is set to -100.0 when the quantity N_m is found to be greater than all N_c values available for the given combination of various parameters.

(2) As mentioned earlier, the quantity N_c generally increases with Ω_{in}. Thus, if the N_m value under scrutiny is less than N_c for $\Omega_{in} = 0.200$ atm-cm, values of $\Omega^C_{x,1000}$ and $S^C_{x,1000}$ are obtained by carrying out a backward extrapolation with values of N_c at $\Omega_{in} = 0.200$ and 0.250 atm-cm.

Step IV: Select one of the two $\Omega^C_{x,1000}$ values for a use in Step V with the help of the following criterion: Set x to 2. Reset x to 1 if, and only if, $S^C_{1,1000} > S^C_{2,1000}$.

If $\Omega^C_{1,1000} = \Omega^C_{2,1000} = 0.0$ (i.e., it was not possible to estimate total ozone for either of the pairs in Step III), initialize the following quantities as shown for clarification, and omit Steps V and VI. $\Omega^I_{x,1000} = 0.0$, $S^I_{x,1000} = -100.0$, for $x = 1, 2$; and $R^I_{\lambda,1000} = R^C_{\lambda,1000}$ for the first four wavelengths.

Step V: Use the value of $\Omega^C_{x,1000}$ selected in Step IV to compute a value of the *improved effective albedo*, $R^I_{0.3398,1000}$ as follows: Determine two successive values of Ω_{in} for which the basic tables are

available so that $\Omega_k < \Omega^C_{x,1000} \leq \Omega_{k+1}$. Obtain two values of $R^I_{0.3398,1000}$ (one with Ω_k and the other with Ω_{k+1}), by making use of $I_m\ (0.3398, \theta_0)$, 1,000 mb tables for the appropriate Ω_{in} and θ_0, and Eq. (2). These two values of $R^I_{0.3398,1000}$ are then used to obtain a final value of this quantity at $\Omega^C_{x,1000}$ after a linear interpolation between Ω_k and Ω_{k+1}.

Then, set $R^I_{\lambda,1000} = R^I_{0.3398,1000}$ for $\lambda = 0.3125$, 0.3175, and 0.3312 μm. *(Improved effective albedo* is also assumed to be independent of wavelength.)

Step VI: Repeat Step III after using $R^I_{\lambda,1000}$ in the place of $R^C_{\lambda,1000}$. We will then have values of the quantities $\Omega^I_{x,1000}$ and $S^I_{x,1000}$ for $x = 1$, and 2.

Step VII: Repeat Steps I through VI above by using the 400 mb tables instead of the 1,000 mb tables. We will then have values of $R^C_{\lambda,400}$ for all five values of λ, those of $R^I_{\lambda,400}$ for the first four values of λ, and of $\Omega^C_{x,400}$, $S^C_{x,400}$, $\Omega^I_{x,400}$ as well as $S^I_{x,400}$ for $x = 1$, and 2.

Step VIII: Determine the *effective albedo* ($\bar{R}$) as follows:

$$\bar{R} = 0.5 \left[R^I_{\lambda,1000} + R^I_{\lambda,400} \right], \tag{8}$$

using any value of the parameter λ as $R^I_{\lambda,y}$ is assumed to be independent of wavelength.

Step IX: This final step is for obtaining a value for the quantity Ω_e, the *best ozone estimate*, from the computed values of $\Omega^I_{x,y}$ for $x = 1$, and 2, and for $y = 1{,}000$ and 400 mb. The following paths are taken depending upon the availability of two, or all of $\Omega^I_{x,y}$ values (a zero value of $\Omega^I_{x,y}$ implies that that particular $\Omega^I_{x,y}$ is unavailable):

(i) All four values of $\Omega^I_{x,y}$ are available. Select the wavelength pair (a value for x) as follows: Set x to 2. Reset x to 1 if, and only if, $S^I_{1,1000} > S^I_{2,1000}$, and $S^I_{1,400} > S^I_{2,400}$. Then proceed to (v) below.

(ii) Only values of $\Omega^I_{1,1000}$ and $\Omega^I_{1,400}$ are available. Set x to 1, and proceed to (v) below.

(iii) Only values of $\Omega^I_{2,1000}$ and $\Omega^I_{2,400}$ are available. Set x to 2, and proceed to (v) below.

(iv) None of (i) to (iii) above. It is not possible to obtain a value of Ω_e. Set it to zero, and omit Step (v) below.

(v) $$\Omega_e = \Omega^I_{x,1000} \quad \text{for} \quad \bar{R} \leq 0.2 , \tag{9}$$

$$\Omega_e = \Omega^I_{x,400} \quad \text{for} \quad \bar{R} \geq 0.8 , \tag{10}$$

and for $0.2 < \bar{R} < 0.8$, the Ω_e is given by

$$\Omega_e = \frac{0.8 - \bar{R}}{0.6} \Omega^I_{x,1000} + \frac{\bar{R} - 0.2}{0.6} \Omega^I_{x,400} . \tag{11}$$

The foregoing description of the procedure is rather mechanical. We will now attempt to provide some rationale behind various steps of this basic procedure. As mentioned earlier, a value of P_0 for the place and time of observation is not available. It has therefore been thought appropriate to perform computations, at all times, for two pressure levels, the 1,000 mb value corresponding to an average sea-level atmospheric pressure, and the 400 mb value corresponding (hopefully) to the top of high clouds encountered in the earth's atmosphere most of the times.

Chances of encountering high reflectivities at high surface pressures are very small unless there is snow on the ground, or there are very low-level, optically thick clouds. Thus, a low value of $\bar{R}$ can be associated with a high value of P_0, and vice versa. Hence, Eqs. (9) to (11) represent a heuristic but ingenious attempt to relate $\bar{R}$ to P_0. (In the original BUV, total-ozone estimation procedure, it is recognized that higher values of $\bar{R}$ can frequently occur for higher values of P_0, especially at high latitudes in the winter months. For such cases, an additional special step is set up in that program.)

An assumption is made that the computed *effective albedo* is independent of wavelength. However, we are not certain of this assumption under all possible conditions. It is therefore prudent to measure *effective albedo* as close to the wavelength region of interest (0.3125 - 0.3398 μm) as possible. However, we have no information on ozone-amount and hence the wavelength for measuring *effective albedo* has to be

located outside the ozone absorption band, i.e., beyond 0.3650 μm. The nearest measurement for an *effective albedo* measurement is at 0.3800 μm which cannot be considered very close to the wavelength region of interest. Therefore, it is advisable to call the 0.3800 μm *effective albedo* measurement as the *coarse effective albedo*, use it to obtain a first guess of the total ozone value ($\Omega^C_{x,y}$), and use this $\Omega^C_{x,y}$ to compute (hopefully) a better *effective albedo* value closest to the spectral region of interest. This new *effective albedo* value called the *improved effective albedo* $R^I_{\lambda,y}$ be better calculated for the region of the least absorption by ozone to minimize errors due to uncertainties in the value of $\Omega^C_{x,y}$. Hence, the choice of the 0.3398 μm measurement for this purpose.

A computer program for estimating total ozone using the simulated BUV measurements and steps outlined above, is described in Appendix A.

2.5 *Differences from the Original Procedure:* Some minor differences occurring between the original total-ozone estimation procedure (see §2.1), and the one used for estimating total ozone from the simulated BUV data (see §2.4), are described below for the sake of completeness.

The basic tables described in §2.2 are prepared in the original version of the procedure for an atmosphere with 1,013 mb surface pressure, and for the same atmosphere chopped off at a level where the pressure is four-tenths of 1,013 mb. These two sets are then respectively referred to as 1.0 atmosphere table, and 0.4 atmosphere table. This difference is of no significant importance in our analysis.

Because of changes in the amounts and profile characteristics of ozone encountered from the equator to pole, the original procedure calls for three subsets of tables for each P_0 value. The subset used depends upon the geographic location of the area under observation; i.e., low latitude, midlatitude, or high latitude. Two additional subsets are also provided for use under special circumstances. A migration is generally permitted from one subset to another whenever the Ω_{in}-range of the subset selected at the first time, is found to be insufficient. The subset to which a migration is made depends upon several factors such as the nature of the original subset, the Ω_{in}-direction along which more tables are required, and the exact location of the site of observation. If a value of $\Omega^C_{x,y}$ and/or $\Omega^I_{x,y}$ cannot be determined after one such migration from one subset to another (a special case can arise where even one migration cannot be permitted), the corresponding $\Omega^Z_{x,y}$ is labeled as undeterminable. We have not incorporated this sophisticated maneuver in our procedure as our interest is primarily restricted to the analysis of problems arising from several ingenious but heuristic paths taken to hopefully minimize the effects due to unavailability of values of the basic parameters P_0 and R_λ, and those due to the breaking down of various assumptions (e.g., R_λ independent of λ; models free of aerosols and water droplets; horizontal homogeneity; and Lambert law of reflection) in real life.

The original procedure provides a subprocedure for an interpolation of tables between two successive values of θ_0 for which the basic

tables are available. This is because real observations can exist for any arbitrary value of θ_0. Our simulated observations are only made for those values of θ_0 for which the basic tables are available.

The specific BUV configuration results in measurements of $I_m(\lambda, \theta_0)$ at λ = 0.3125, 0.3175, 0.3312, and 0.3398 μm, not simultaneously, but at a time interval of about 2 sec. In order to correct for changes in the *effective albedo* due to the translation of the satellite, $I_m(0.3800, \theta_0)$ is measured four times, one coinciding with measurement of each of the four wavelengths in the region of ozone absorption. This additional complication results in different values of $R^C_{\lambda,y}$ and $R^I_{\lambda,y}$ at different wavelengths. The *effective albedo* $\bar{R}$ given by Eq. (8) is then redefined to include weighting for $R^I_{\lambda,y}$ values for the pair selected in Step IX. It should be pointed out that this use of different *coarse* or *improved effective albedoes* at different wavelengths is in no way connected with a real possible dependence of R_λ on λ.

In the original procedure, a quadratic interpolation procedure is used for computation of $R^I_{0.3398,y}$ in Step V.

Finally, the basic tables in the original procedure are prepared after taking into account polarization of the scattered radiation when a given atmospheric model is illuminated by F_{0_λ} units of solar energy passing normally, in unit time, through a unit area located at the top of the atmosphere. Thus, as the incident energy is wavelength dependent, the term inside the large parentheses in Eq. (4) or (5) has to be multiplied by the term $F_{0_{\lambda_j}}/F_{0_{\lambda_i}}$. The atmospheric models in the orig-

inal procedure extend to a height of 80 km, while those used by us extend to a height of 70 km, only. There is also some difference in the manner in which the basic models are subdivided into layers.

III. INPUT DATA

3.1 *Atmospheric Models:* The atmospheric models with a surface pressure (P_0) of 1,000 mb are divided into 32 layers, and those with P_0 = 400 mb are divided into 25 layers. Values of the geometric thickness in km, pressure thickness in mb, and ozone amounts in atm-cm for each of the 32 layers of the 1,000 mb models are given in Tables I and II. Only the ozone amount of a layer changes from one model to the other. Ozone amounts in different layers of the first four models (viz, models with a total ozone amount Ω_{in} given by Ω_{in} = 0.200, 0.250, 0.300, and 0.350 atm-cm) are given in Table I. Table II contains values of $\Delta\Omega$ for each of the 32 layers for models with Ω_{in} = 0.400, 0.450, 0.500, 0.550, 0.600, and 0.650 atm-cm.

Total ozone amounts mentioned in the preceding paragraph are for the 1,000 mb models. As mentioned earlier (§2.2), the 400 mb models are obtained after deleting the bottom-most seven layers of the 1,000 mb models. Thus, $\Omega = \Omega_{in}$ for the models with P_0 = 1,000 mb, but $\Omega < \Omega_{in}$ for the models with $P_0 < 1{,}000$ mb. Table III contains information about P_0, Ω, and Ω_{in} for 22 different models for which computations are performed.

Table I. Values of the geometric thickness in km, pressure thickness in mb, and ozone amount in atm-cm for various layers of the model No. 2, 3, 4, and 5 with 0.200, 0.250, 0.300, and 0.350 atm-cm of total ozone, respectively. Geometric and pressure thickness remain unchanged from one model to the other.

Layer number	Thickness		Amount of ozone (atm-cm) in the layer for the model			
	Geometric (km)	Pressure (mb)	No. 2	No. 3	No. 4	No. 5
1	10.0	0.17	0.00002	0.00002	0.00002	0.00002
2	10.0	0.74	0.00016	0.00016	0.00016	0.00016
3	5.0	0.80	0.00290	0.00290	0.00290	0.00290
4	5.0	1.53	0.00722	0.00722	0.00725	0.00732
5	5.0	3.16	0.01735	0.01750	0.01769	0.01768
6	5.0	6.55	0.03630	0.03340	0.03792	0.03925
7	5.0	13.75	0.05376	0.06650	0.06900	0.07050
8	1.0	4.30	0.01100	0.01500	0.01750	0.01850
9	1.0	5.10	0.01040	0.01460	0.01830	0.01940
10	1.0	6.00	0.00975	0.01360	0.01710	0.01990
11	1.0	7.20	0.00890	0.01220	0.01590	0.01940
12	1.0	8.30	0.00800	0.01120	0.01472	0.01820
13	1.0	9.60	0.00690	0.00920	0.01330	0.01650
14	1.0	11.20	0.00510	0.00710	0.01120	0.01390
15	1.0	12.60	0.00360	0.00510	0.00845	0.01180
16	1.0	14.50	0.00195	0.00400	0.00640	0.00920

. . . *to be continued*

Table I, cont'd.

Layer number	Thickness		Amount of ozone (atm-cm) in the layer for the model			
	Geometric (km)	Pressure (mb)	No. 2	No. 3	No. 4	No. 5
17	1.0	17.50	0.00105	0.00240	0.00471	0.00802
18	1.0	21.50	0.00090	0.00120	0.00380	0.00720
19	1.0	24.50	0.00070	0.00100	0.00340	0.00640
20	1.0	27.50	0.00050	0.00080	0.00260	0.00590
21	1.0	31.50	0.00040	0.00070	0.00210	0.00510
22	1.0	35.50	0.00031	0.00065	0.00195	0.00440
23	1.0	40.50	0.00035	0.00065	0.00186	0.00340
24	1.0	45.00	0.00056	0.00080	0.00180	0.00250
25	1.0	51.00	0.00075	0.00125	0.00181	0.00200
26	1.0	61.00	0.00105	0.00150	0.00194	0.00220
27	1.0	69.00	0.00125	0.00190	0.00225	0.00260
28	1.0	75.00	0.00167	0.00230	0.00248	0.00300
29	1.0	87.00	0.00180	0.00245	0.00289	0.00310
30	1.0	97.00	0.00190	0.00265	0.00294	0.00320
31	1.0	100.00	0.00180	0.00265	0.00286	0.00320
32	1.0	111.00	0.00170	0.00240	0.00280	0.00315

Table II. Values of the ozone amount in atm-cm for various layers of the model no. 6, 7, 8, 9, 10, and 11 with Ω = 0.400, 0.450, 0.500, 0.550, 0.600, and 0.650 atm-cm of total ozone, respectively.

Layer number	Amount of ozone (atm-cm) in the layer for the model					
	No. 6	No. 7	No. 8	No. 9	No. 10	No. 11
1	0.00002	0.00002	0.00002	0.00002	0.00002	0.00002
2	0.00016	0.00016	0.00016	0.00016	0.00016	0.00016
3	0.00290	0.00290	0.00290	0.00290	0.00290	0.00290
4	0.00732	0.00742	0.00742	0.00742	0.00742	0.00742
5	0.01810	0.01780	0.01790	0.01790	0.01790	0.01790
6	0.03905	0.03950	0.03950	0.03950	0.03950	0.03950
7	0.07290	0.07380	0.07390	0.07390	0.07390	0.07390
8	0.01980	0.01990	0.02000	0.02000	0.02000	0.02000
9	0.02170	0.02220	0.02280	0.02340	0.02400	0.02460
10	0.02340	0.02440	0.02570	0.02700	0.02830	0.02960
11	0.02120	0.02380	0.02700	0.03020	0.03340	0.03660
12	0.02020	0.02290	0.02500	0.02710	0.02920	0.03130
13	0.01860	0.02110	0.02400	0.02690	0.02980	0.03270
14	0.01720	0.01880	0.02200	0.02520	0.02840	0.03160
15	0.01440	0.01700	0.01900	0.02100	0.02300	0.02500
16	0.01220	0.01550	0.01800	0.02050	0.02300	0.02550

. . . *to be continued*

Table II, cont'd.

Layer number	Amount of ozone (atm-cm) in the layer for the model					
	No. 6	No. 7	No. 8	No. 9	No. 10	No. 11
17	0.01150	0.01490	0.01800	0.02110	0.02420	0.02730
18	0.01110	0.01480	0.01900	0.02320	0.02740	0.03160
19	0.01070	0.01500	0.02000	0.02500	0.03000	0.03500
20	0.01030	0.01540	0.02100	0.02660	0.03220	0.03780
21	0.00950	0.01430	0.01900	0.02370	0.02840	0.03310
22	0.00710	0.01080	0.01400	0.01720	0.02040	0.02360
23	0.00520	0.00710	0.00900	0.01090	0.01280	0.01470
24	0.00310	0.00410	0.00500	0.00600	0.00700	0.00800
25	0.00245	0.00320	0.00410	0.00500	0.00590	0.00680
26	0.00185	0.00300	0.00380	0.00460	0.00540	0.00620
27	0.00195	0.00290	0.00350	0.00410	0.00470	0.00530
28	0.00250	0.00310	0.00350	0.00390	0.00430	0.00470
29	0.00310	0.00330	0.00350	0.00370	0.00390	0.00410
30	0.00360	0.00360	0.00370	0.00390	0.00410	0.00430
31	0.00345	0.00370	0.00390	0.00410	0.00430	0.00450
32	0.00345	0.00360	0.00370	0.00390	0.00410	0.00430

Table III. Surface pressure (P_0 in mb), actual total ozone amount (Ω in atm-cm), and the total ozone amount when the model is extended to the mean sea-level (Ω_{in} in atm-cm) for various atmospheric models.

Model number	P_0 in mb	Ω in atm-cm	Ω_{in} in atm-cm
1	1,000	0.0	0.0
2	1,000	0.200	0.200
3	1,000	0.250	0.250
4	1,000	0.300	0.300
5	1,000	0.350	0.350
6	1,000	0.400	0.400
7	1,000	0.450	0.450
8	1,000	0.500	0.500
9	1,000	0.550	0.550
10	1,000	0.600	0.600
11	1,000	0.650	0.650
12	400	0.0	0.0
13	400	0.189	0.200
14	400	0.234	0.250
15	400	0.282	0.300
16	400	0.330	0.350
17	400	0.380	0.400
18	400	0.427	0.450
19	400	0.474	0.500
20	400	0.522	0.550
21	400	0.569	0.600
22	400	0.617	0.650

3.2 *Optical Data:* Table IV contains information on the normal Rayleigh scattering optical thickness of the standard atmosphere $[\tau_b^{(s,R)}]$, and absorption coefficient of one atm-cm of ozone to the base e for all six wavelengths at which computations are carried out.

Table IV. Normal Rayleigh scattering optical thickness $[\tau_b^{(s,R)}]$ of the standard atmosphere, and absorption coefficient (α) of one atm-cm of ozone to the base e at six different wavelengths for which computations are performed.

Wavelength (μm)	$\tau_b^{(s,R)}$	α
0.3125	1.0200	1.6700
0.3175	0.9570	0.9100
0.3312	0.8000	0.1750
0.3398	0.7180	0.0482
0.3600	0.5634	0.0012
0.3800	0.4494	0.0000

IV. SOME CHARACTERISTICS OF THE QUANTITY N_c

4.1 *Variations of N_c with Ω_{in}:* In §2.3, it was mentioned that the quantity $N_c(\lambda_i, \lambda_j; R_{\lambda_i}, R_{\lambda_j}; \Omega_{in}, P_0, \theta_0)$ generally increases with an increase in Ω_{in}, the total ozone content of the atmospheric model when other parameters appearing within the parentheses are held constant.

This characteristic of the N_c vs. Ω_{in} curve then forms the basis for estimation of total ozone from the measured value of this quantity, i.e., $N_m(\lambda_i, \lambda_j, \theta_0)$ given by Eq. (5). We shall therefore examine this property of the N_c vs. Ω_{in} curves, in some detail, in this subsection.

Variations of N_c as a function of the total ozone content (Ω_{in}) in the atmospheric model are shown in Figs. 1 and 2 for the first (0.3312 - 0.3125 μm), and the second (0.3398 - 0.3175 μm) pair, respectively for P_0 = 1,000 mb, and $R_{\lambda_i} = R_{\lambda_j} = 0.0$. Different curves are for different values of the parameter θ_0. For the first pair, the quantity N_c increases with an increase in Ω_{in} for values of θ_0 up to 75.6°. The $\theta_0 = 79.6°$ curve of N_c vs. Ω_{in} of Fig. 1 shows only a very small increase in N_c as Ω_{in} is increased from 0.550 to 0.600 atm-cm (the corresponding values of N_c are 100.33 and 100.70 units, respectively). A further increase in Ω_{in} from 0.600 to 0.650 atm-cm results in a very small decrease in N_c from 100.70 to 100.68 units. For still higher values of θ_0, the N_c vs. Ω_{in} curve depicts a clear maximum which shifts from 0.500, to 0.400, to 0.350 atm-cm as θ_0 is increased from 82.5°, to 84.7°, to 86.7°. The $\theta_0 = 90°$ curve shows a continuous decrease in N_c as Ω_{in} is increased from 0.200 atm-cm to 0.650 atm-cm. For the second pair (Fig. 2), the quantity N_c increases with an increase in Ω_{in} at all ten θ_0s. However, the curves for $\theta_0 = 86.7°$ and 90.0° are rather flat for high values of Ω_{in}. As for example, $N_c(90°, 0.600$ atm-cm) = 77.11 units, and $N_c(90°, 0.650$ atm-cm) = 77.22 units. The curves of N_c vs. Ω_{in} for the first pair are generally more sensitive

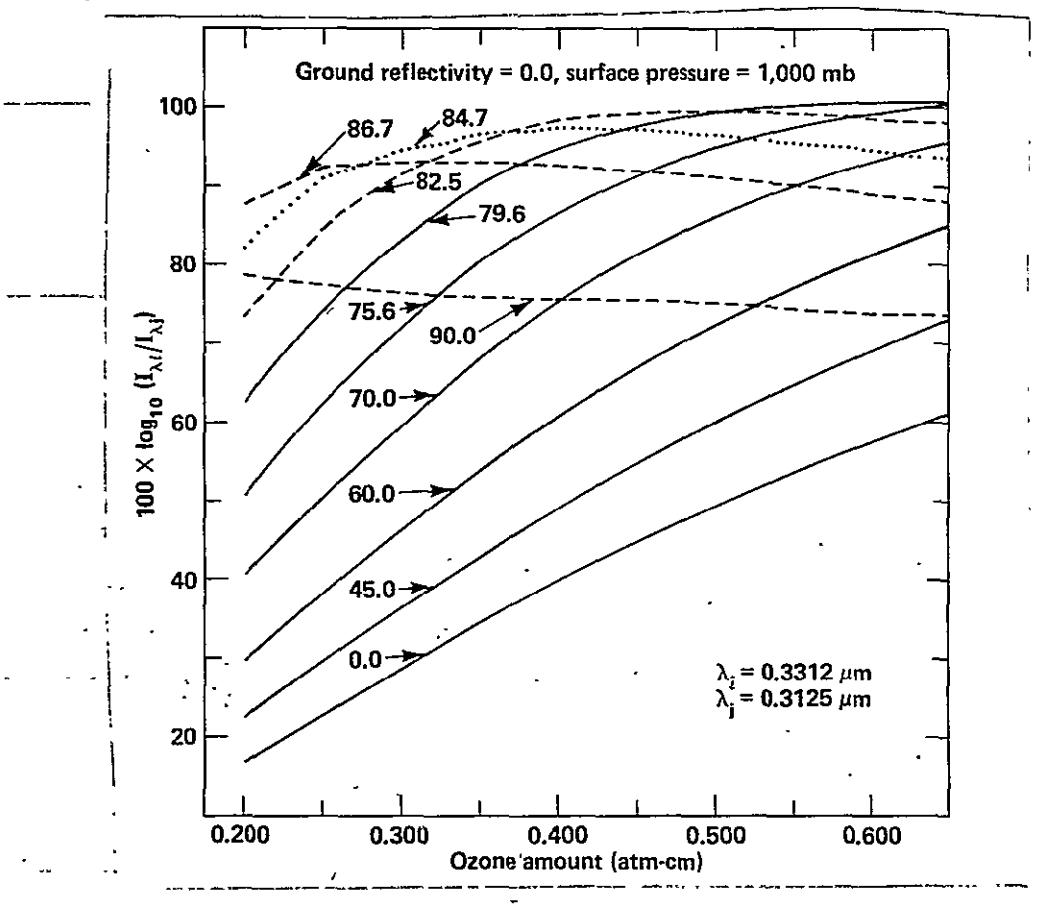

Fig. 1 Variations of the computed quantity N_c [see Eq. (4)] as a function of the total ozone amount (Ω_{in}) in the atmospheric model. Different curves are for different values of the parameter θ_0, solar zenith angle, λ_i = 0.3312 μm, λ_j = 0.3125 μm, $R_{\lambda_i} = R_{\lambda_j}$ = 0.0, and P_0 = 1,000 mb.

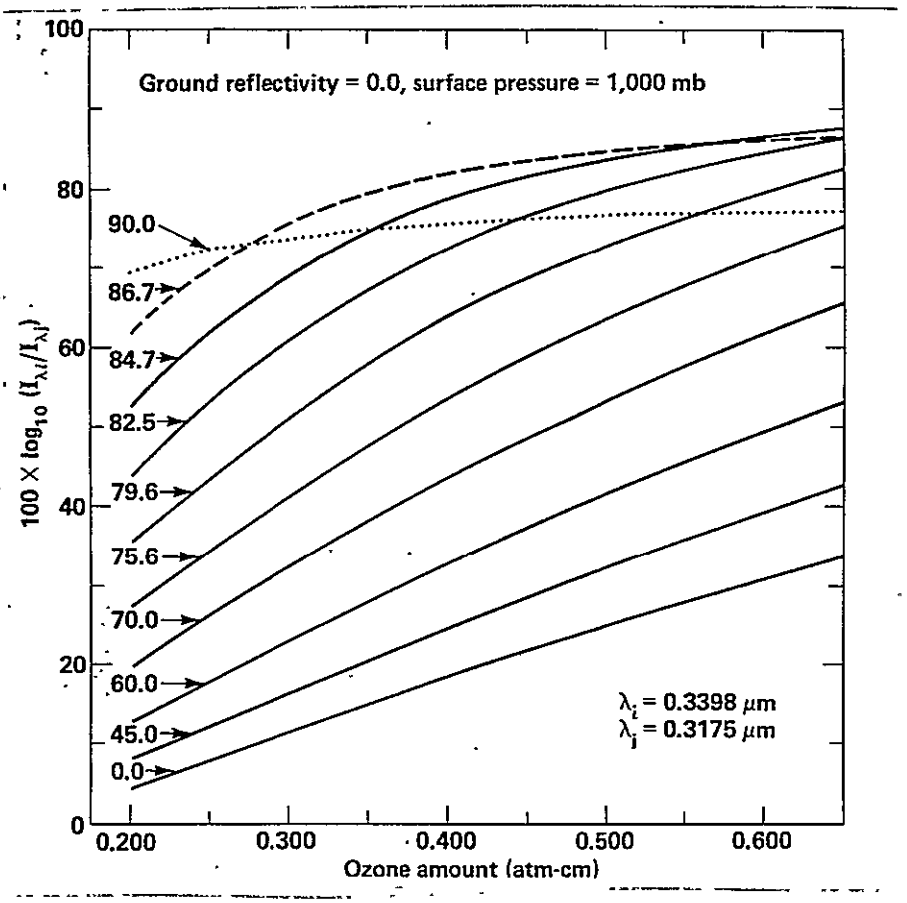

Fig. 2 Variations of the computed quantity N_c [see Eq. (4)] as a function of the total ozone amount (Ω_{in}) in the atmospheric model. Different curves are for different values of the parameter θ_0, solar zenith angle. λ_i = 0.3398 μm, λ_j = 0.3175 μm, $R_{\lambda_i} = R_{\lambda_j} = 0.0$, and P_0 = 1,000 mb.

to a change in Ω_{in} for the small values of θ_0, than the corresponding curves for the second pair. As for example, an increase in total ozone from 0.200 atm-cm to 0.250 atm-cm results in an increase in N_c(0.3312, 0.3125, 0°) from 16.80 to 22.72 units, but an increase in N_c(0.3398, 0.3175, 0°) from 4.57 to 8.10 units, only.

The higher sensitivity of the N_c vs. Ω_{in} curves (to changes in Ω_{in}) for the first pair at small θ_0 values compared to that of the corresponding curves for the second pair, is due to a relatively stronger absorption by ozone for the spectral regions of the first pair compared to that of the second pair. The loss of sensitivity of the first pair at large θ_0 to changes in ozone content, is primarily due to a rise in the height of the effective scattering layer through the ozone layer. Further information on this particular aspect can be found in a paper by Dave and Mateer [1967].

Results similar to those presented in Figs. 1 and 2 but for $R_{\lambda_i} = R_{\lambda_j} = 1.0$ were also analyzed for both the wavelength pairs. However, no graphical results are presented for these cases in this report. An increase in the surface reflectivity resulted in a very significant change in the slopes of the N_c vs. Ω_{in} curves at large θ_0 for the first pair. The $\theta_0 = 79.6°$ N_c vs. Ω_{in} curve for $R_{\lambda_i} = R_{\lambda_j} = 1.0$ did not show any decrease in N_c with increase in Ω_{in}. The maxima of the N_c vs. Ω_{in} curves for $\theta_0 = 82.5°$, 84.7°, and 86.7° shifted to the right for the first pair as the reflectivity of the underlying surface was increased from 0.0 to 1.0. The $\theta_0 = 90°$ curve for the first pair

with $R_{\lambda_i} = R_{\lambda_j} = 0.0$ (Fig. 1) shows a continuous decrease in N_c with increase in Ω_{in}, while the same curve but for $R_{\lambda_i} = R_j = 1.0$ showed a weak maximum around $\Omega_{in} = 0.500$ atm-cm. Similar improvements in the sensitivity of N_c to changes in Ω_{in} at large θ_0, due to an increase in reflectivity were also seen for the second pair after comparing results in Figs. 2, with those for $R_{\lambda_i} = R_{\lambda_j} = 1.0$, and $P_0 = 1{,}000$ mb.

From the preceding discussion on the trends of N_c vs. Ω_{in} variations, it is clear that the first wavelength pair loses its sensitivity completely to changes in Ω_{in}, for high Ω_{in} at $\theta_0 = 82.5°$ when $R_{\lambda_i} = R_{\lambda_j} = 1.0$, but at $\theta_0 = 79.6°$ when $R_{\lambda_i} = R_{\lambda_j} = 0.0$. The arbitrary method of determining the *coarse*, or the *improved effective albedo* described in §2.4, results in a requirement of generation of the N_c vs. Ω_{in} curves with negative values of R_λ. To this effect, it should be pointed out that for $R_{\lambda_i} = R_{\lambda_j} = -0.1$, the quantity $N_c(0.3312, 0.3125, \Omega_{in}, 1{,}000 \text{ mb}, 75.6°)$ is equal to 92.33, 94.70, 96.36, and 97.46 units, for $\Omega_{in} = 0.500$, 0.550, 0.600, and 0.650 atm-cm, respectively.

Trends in variations of N_c with Ω_{in} for the $P_0 = 400$ mb models are, in general, very similar to those discussed in the preceding paragraphs for corresponding models with $P_0 = 1{,}000$ mb. Representative results for the first and the second pairs are shown in Figs. 3 and 4, respectively for $P_0 = 400$ mb, and $R_{\lambda_i} = R_{\lambda_j} = 0.0$.

In Fig. 5, we have plotted values of $N_c(0.3398, 0.3175)$ and $N_c(0.3398, 0.3312)$ as a function of Ω_{in}, for $R_{\lambda_i} = R_{\lambda_j} = 0.0$, $\theta_0 = 86.7°$ and 90°, and $P_0 = 1{,}000$ and 400 mb. The results for the new pair

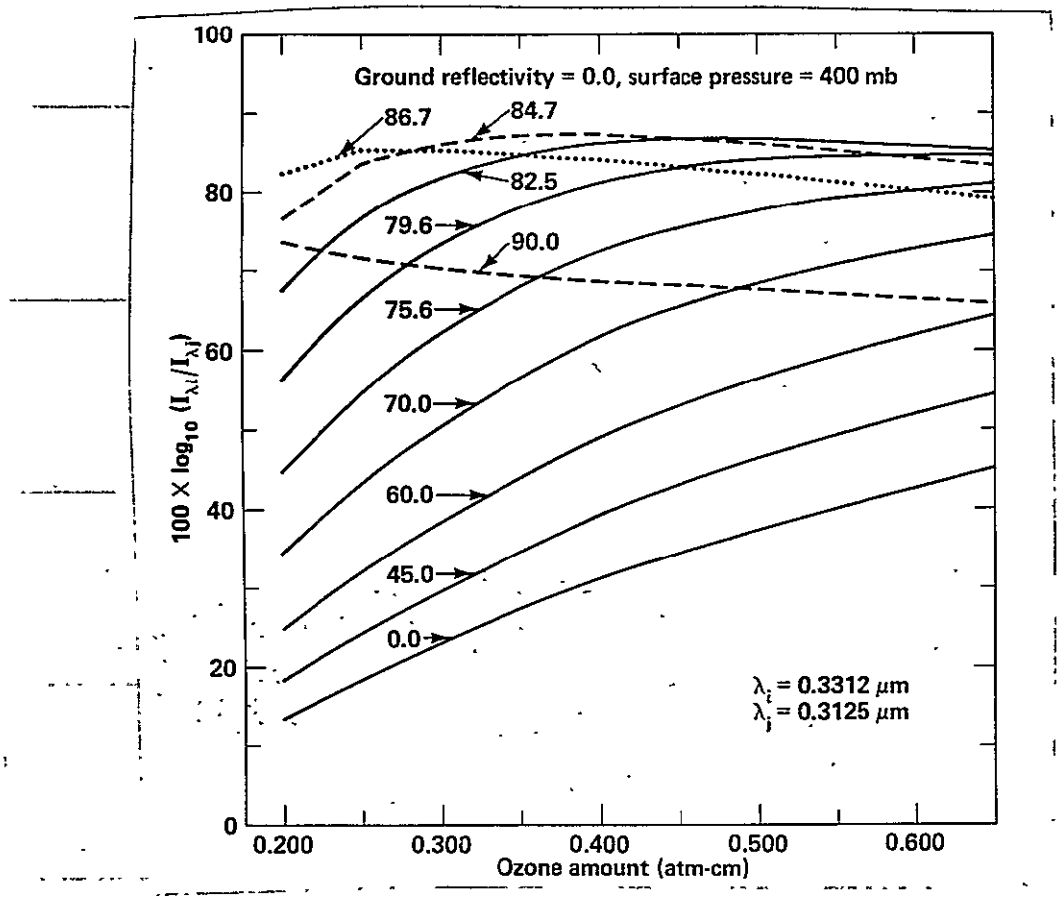

Fig. 3 Variations of the computed quantity N_c [see Eq. (4)] as a function of the total ozone amount (Ω_{in}) in the atmospheric model. Different curves are for different values of the parameter θ_0, solar zenith angle. λ_i = 0.3312 μm, λ_j = 0.3125 μm, $R_{\lambda_i} = R_{\lambda_j}$ = 0.0, and P_0 = 400 mb.

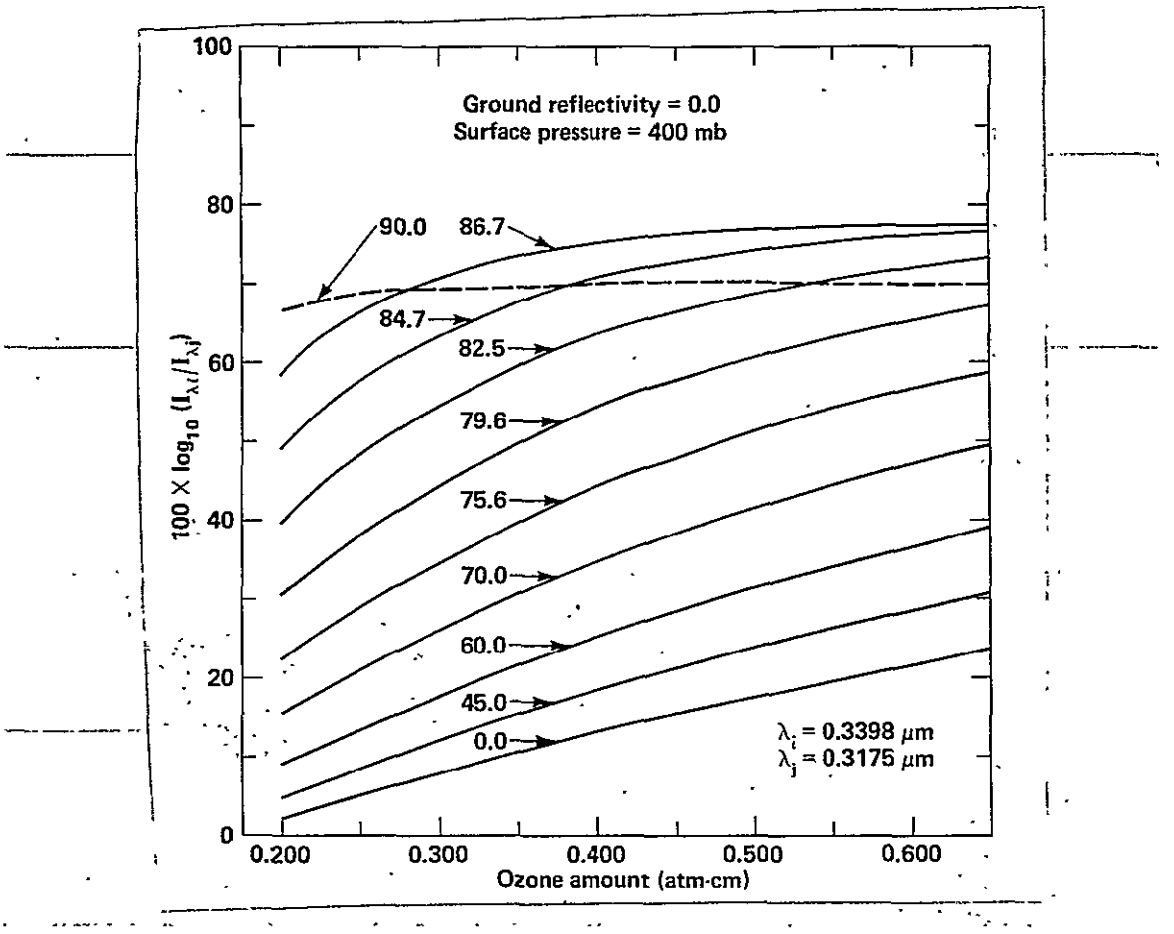

Fig. 4 Variations of the computed quantity N_c [see Eq. (4)] as a function of the total ozone amount (Ω_{in}) in the atmospheric model. Different curves are for different values of the parameter θ_0, solar zenith angle. λ_i = 0.3398 μm, λ_j = 0.3175 μm, $R_{\lambda_i} = R_{\lambda_j}$ = 0.0, and P_0 = 400 mb.

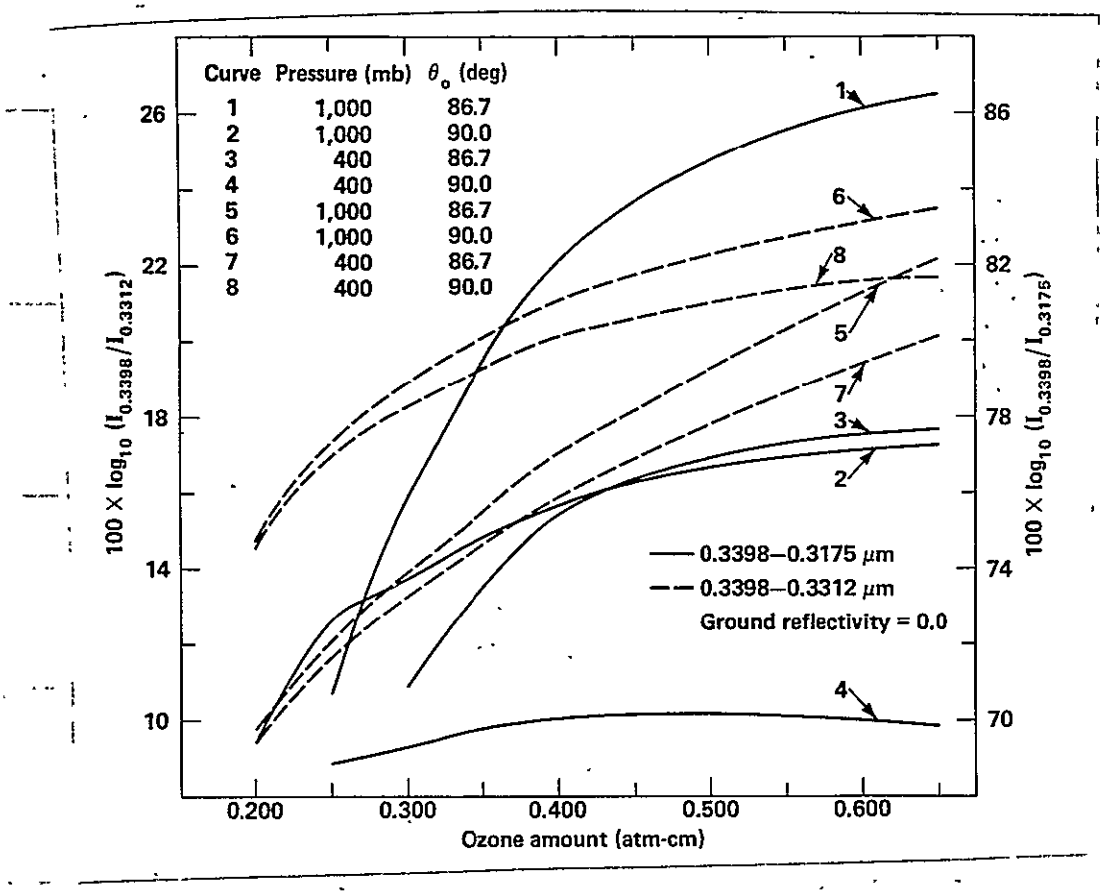

Fig. 5 Variations of the computed quantity N_c [see Eq. (4)] as a function of the total ozone amount (Ω_{in}) in the atmospheric model. Solid curves are for the 0.3398–0.3175 μm pair, and the broken curves are for the 0.3398 – 0.3312 μm pair. $R_{\lambda_i} = R_{\lambda_j} = 0.0$. Only the curves for $\theta_0 = 86.7°$ and 90° are shown. P_0 = 1,000 mb as well as 400 mb.

(viz, third pair; 0.3398 - 0.3312 μm) are shown by broken curves, while those for the second pair (viz, 0.3398 - 0.3175 μm) are shown by solid curves. A comparison of the curve number m with the curve number $m + 4$ suggests a small but significant increase in the slope of the $N_c - \Omega_{in}$ curve as we transpose from the second, to the third pair. Thus, in principle, there is a small advantage in use of the third pair when Ω_{in} and θ_0 assume large values. However, there are several additional factors such as the rapid changes in brightness within the field of view and the reliability of the θ_0 value at the place and time of observation, which may control the desire of estimating total ozone in such extreme cases.

Values of $N_c(0.3398, 0.3175, 84.7°)$ are plotted in Fig. 6 as a function of the total ozone (Ω_{in} in atm-cm) for $P_0 = 1{,}000$ mb (solid curves), and $P_0 = 400$ mb (broken curves). There are three sets of curves, one set for each of the following values of the ground reflectivity ($R_{\lambda_i} = R_{\lambda_j} = R$): 0.0, 0.5, and 1.0. This diagram is provided primarily for realizing the spread between $\Omega^Z_{2,y}$ for a given measurement, N_m. As for example, for $R_{\lambda_i} = R_{\lambda_j} = 0.0$, a value of N_m of 60 units yields $\Omega^Z_{2,1000} = 0.238$ atm-cm, and $\Omega^Z_{2,400} = 0.272$ atm-cm. On the other hand, for $R_{\lambda_i} = R_{\lambda_j} = 0.5$, we have $\Omega^Z_{2,1000} = 0.212$ atm-cm, and $\Omega^Z_{2,400} = 0.220$ atm-cm. If we enter this diagram with $N_m = 80$ units and $R_{\lambda_i} = R_{\lambda_j} = 0.0$, we will come out with a value of 0.423 atm-cm for $\Omega^Z_{2,1000}$, but $\Omega^Z_{2,400}$ will be undeterminable. It may be necessary to construct more diagrams like this one for a better understanding of the results obtained with the total-ozone estimation procedure described in §II.

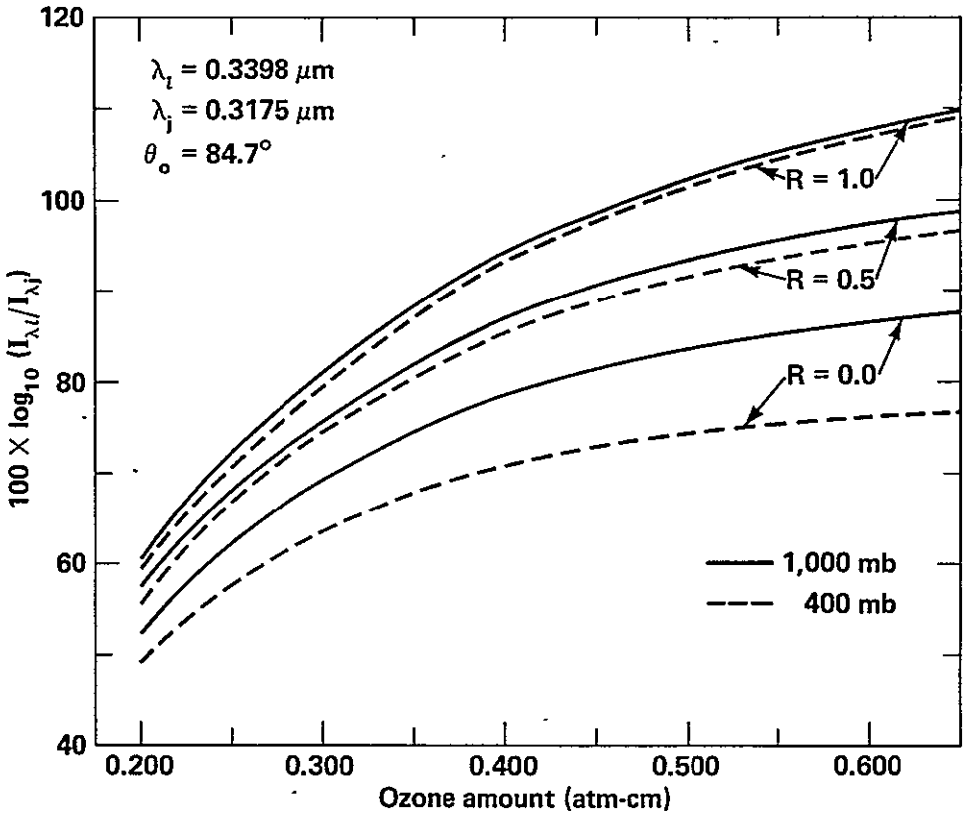

Fig. 6 Variations of the computed quantity N_c [see Eq. (4)] as a function of the total ozone amount (Ω_{in}) in the atmospheric model for a solar zenith angle of 84.7°. λ_i = 0.3398 μm, and λ_j = 0.3175 μm. The solid (broken) curves are for the models with 1,000 mb (400 mb) surface pressure. Values of $R_{\lambda_i} = R_{\lambda_j} = R$ are as shown in the diagram.

4.2 *Values of N_c as Obtained with Different Procedures:* In §2.5, we pointed out several differences between computational procedures used for evaluation of the quantity $N_c(\lambda_i, \lambda_j; R_{\lambda_i}, R_{\lambda_j}; \Omega_{in}, P_0, \theta_0)$ for the original NASA/GSFC total-ozone estimation procedure for the analysis of the actual BUV data, and for that used by us in the analysis of the simulated observations. It was therefore considered desirable to compare values of this quantity as obtained from these two procedures.

Values of $N_c(\lambda_i, \lambda_j; R_{\lambda_i}, R_{\lambda_j}; \Omega_{in}, P_0, \theta_0)$ for the following parameters were computed using the NASA/GSFC procedure by Dr. Ashok Kaveeshwar associated with the BUV ozone-estimation project, and using the procedure for the analysis of the simulated BUV data (as described in this report) by the author: 0.3312 - 0.3125, 0.3398 - 0.3175, and 0.3398 - 0.3312 μm wavelength pairs; $R_{\lambda_i} = R_{\lambda_j} = R$ given by $R = -0.1\ (0.1)\ 1.0$; ten values of θ_0 listed earlier; P_0 = 1,000 mb and 400 mb for the author's calculations, i.e., 1.0 and 0.4 atmospheres for the NASA/GSFC work (see the second paragraph of §2.5); and $\Omega_{in} = 0.200\ (0.050)\ 0.450$ atm-cm. These sets of tables of N_c were then exchanged for independent intercomparisons.

The results of these independent intercomparisons showed that values of the quantity N_c as obtained from these two independent procedures described above, agree within ± 0.5 units on the average for cases with the solar zenith angle (θ_0) not exceeding about 70°. For still larger values of θ_0, this difference increases to about ± 2 units. Considering several differences between two procedures, it was decided by us

(Drs. Mateer, Novak, and Kaveeshwar, as well as the author) that the agreement between these two sets of N_c is very good, indeed. Furthermore, it should be added that values of I_c, T_c, etc., for the analysis of the simulated observations are to be computed using the same procedure. Thus, the aforementioned procedure dependence of N_c cannot be expected to have any effect on the results of investigations carried out under this contract.

The above-mentioned procedure dependence of N_c can be due to one, or both, of the following causes:

(1) Difference in vertical profiles of ozone as used by two procedures. The author has based ozone profiles for his work on the data used in the NASA/GSFC work. (These data were supplied to the author, in the numerical form, by Dr. C. L. Mateer.) However, because of the manner in which an atmospheric model is divided into layers by two procedures, it is possible that some minor differences have popped in.

(2) Neglect of polarization of the atmospheric radiation: Values I_c for N_c for the NASA/GSFC procedure were obtained after taking into account polarization of the scattered radiation. However, as mentioned earlier, this aspect of atmospheric scattering was neglected in the investigation of the analysis of the simulated data. Dr. R. S. Fraser has shown that a significant portion of the above-mentioned difference is due to the neglect of polarization of the scattered radiation.

V. SIMULATION FOR THE BUV CONFIGURATION

5.1 *Results for the R-Independent-of-λ Cases:* Values of the *effective albedo* [$\bar{R}$ given by Eq. (8)] and the *best ozone estimate* [Ω_e given by Eq. (9), or (10), or (11)] were evaluated for the atmospheric models no. 2 to 11, and 13 to 22 (see Table III) for ten different values of the solar zenith angle (θ_0 = 0°, 45°, 60°, 70°, 75.6°, 79.6°, 82.5°, 84.7°, 86.7°, and 90°), and for eight different values of the reflectivity (R = 0.0, 0.1, 0.2, 0.3, 0.4, 0.6, 0.8, and 1.0) of the Lambert surface underlying the model. Results presented in this section (§5.1) as well as in the next section (§5.2) are for the cases where the quantity R is assumed to remain constant with changes in the wavelength (λ).

Four sets of programs were written for this purpose. They are referred to as SITC1, SITC2, SITC3, and SITC4, or—for brevity—as C1, C2, C3, and C4. (It may be noted that programs SITAA and SITBB described in the first technical report are for computing values of I_c, T_c, etc., for a given model.)

The program SITC1 faithfully follows the steps described in §2.4. As mentioned earlier, this basic procedure of §2.4 is expected to be identical to the one being used at NASA/GSFC for the estimation of total ozone from the BUV data. Some minor differences between the original NASA/GSFC procedure and the one used by us for the analysis of the simulated observations, are listed in §2.5.

The program SITC2 is a copy of the SITC1 program modified to set $\Omega^C_{1,400}$, $\Omega^C_{1,1000}$ of Step III, and $\Omega^I_{1,400}$ and $\Omega^I_{1,1000}$ of Step VI, to zero whenever θ_0 exceeds 79.6°. This is to avoid the possibility of obtaining erroneous values of $\Omega^Z_{x,y}$, arising from peculiar properties of N_c vs. Ω curves discussed in §4.1. In an oral presentation of the results discussed in this §V to Dr. Mateer on September 20, 1976, we found that the original NASA/GSFC procedure contains an additional step which can be interpreted to carry out the same function (i.e., of setting $\Omega^Z_{1,y}$ to zero when θ_0 is large) in an indirect manner. We therefore feel that, based on this additional information, the SITC2 program more closely resembles the original NASA/GSFC procedure than the SITC1 program.

The SITC3 program is a copy of the SITC2 program modified to set $\Omega^I_{x,y}$ to zero whenever $\left|\Omega^I_{x,y} - \Omega^C_{x,y}\right| \geq 0.030$ atm-cm. This criterion is based on the following argument: As mentioned in §2.4, $\Omega^C_{x,y}$ is obtained by making use of the *coarse effective albedo* $R^C_{0.3800,y}$, and $\Omega^I_{x,y}$ is obtained by making use of the *improved effective albedo* $R^I_{0.3398,y}$. A large absolute difference between $\Omega^C_{x,y}$ and $\Omega^I_{x,y}$ implies either a large difference between two computed values of the albedos, or alternately, a strong sensitivity of the N_c vs. Ω curve to small changes in R. In either case, there is sufficient ground to discard the corresponding value of $\Omega^I_{x,y}$.

The SITC4 program is a copy of the SITC3 program modified to accept the appropriate value of $\Omega^I_{x,1000}$ as Ω_e provided $\bar{R} \leq 0.2$ [see Eq. (9)],

and the appropriate value of $\Omega^{I}_{x,400}$ as Ω_e provided $\bar{R} \geq 0.8$ [see Eq. (10)]. This modification is introduced to free the procedure of an unnecessarily strict acceptance criterion. When $\bar{R} \leq 0.2$ ($\bar{R} \geq 0.8$), a value of $\Omega^{I}_{x,400}$ ($\Omega^{I}_{x,1000}$) is not required in computations of Ω_e; see Step IX of §2.4.

The purpose of this simulation is to compare the value of Ω_e with the corresponding total ozone amount in the atmospheric model when its lower boundary is extended right down to the mean sea-level, i.e., the quantity Ω_{in}, and to compare $\bar{R}$ with the corresponding value of R. Results of this latter comparison will be presented in §5.2. It is clear that this comparison task is by no means a trivial one (4 procedures × 20 models × 10 values of θ_0 × 8 values of R), and hence a good degree of discretion is used in the presentation of results. For convenience, we will refer to the quantity $1{,}000 \times (\Omega_e - \Omega_{in})$ as the *deviation*, Δ. A positive (negative) value of the quantity Δ implies an overestimation (underestimation) of total ozone by the procedure.

Values of the quantity Δ are tabulated in Tables V, VI, and VII for the atmospheric models no. 3, 6, and 9, respectively. These atmospheric models are for a surface pressure (P_0) of 1,000 mb. Their respective total ozone contents (Ω_{in}) are 0.250, 0.400, and 0.550 atm-cm. For each case, results are presented for all ten values of θ_0, but for only four values of R, viz, 0.0, 0.2, 0.6, and 1.0. Similar results for the atmospheric models no. 14, 17, and 20 [respective ozone amounts (Ω_{in}) 0.250, 0.400, and 0.550 atm-cm when corrected for the ozone con-

Table V. Values of the *deviation* [$\Delta = 1{,}000 \times (\Omega_e - \Omega_{in})$] for the atmospheric model no. 3; $\Omega_{in} = 0.250$ atm-cm; $P_0 = 1{,}000$ mb.

θ_0 in deg.	*Deviation* Δ obtained with the procedure							
	C1	C2	C3	C4	C1	C2	C3	C4
	R = 0.0				R = 0.2			
0.0	0	0	0	0	-1	-1	-1	-1
45.0	0	0	0	0	-1	-1	-1	-1
60.0	0	0	0	0	-1	-1	-1	-1
70.0	0	0	0	0	0	0	0	0
75.6	0	0	0	0	0	0	0	0
79.6	0	0	0	0	0	0	0	0
82.5	0	0	0	0	0	0	0	0
84.7	0	0	0	0	0	0	0	0
86.7	0	0	0	0	0	0	0	0
90.0	0	0	-	0	-1	-1	-1	-1
	R = 0.6				R = 1.0			
0.0	11	11	11	11	28	28	28	28
45.0	9	9	9	9	25	25	25	25
60.0	8	8	8	8	21	21	21	21
70.0	6	6	6	6	16	16	16	16
75.6	5	5	5	5	12	12	12	12
79.6	4	4	4	4	10	10	10	10
82.5	4	3	3	3	10	7	7	7
84.7	3	3	3	3	8	8	8	8
86.7	3	3	3	3	9	9	9	9
90.0	5	5	5	5	18	18	18	18

Table VI. Values of the *deviation* [$\Delta = 1{,}000 \times (\Omega_e - \Omega_{in})$] for the atmospheric model no. 6; $\Omega_{in} = 0.400$ atm-cm; $P_0 = 1{,}000$ mb.

θ_0 in deg.	*Deviation* Δ obtained with the procedure							
	C1	C2	C3	C4	C1	C2	C3	C4
	R = 0.0				R = 0.2			
0.0	0	0	0	0	0	0	0	0
45.0	0	0	0	0	0	0	0	0
60.0	0	0	0	0	0	0	0	0
70.0	0	0	0	0	0	0	0	0
75.6	0	0	0	0	-1	-1	-1	-1
79.6	0	0	0	0	0	0	0	0
82.5	0	0	0	0	0	0	0	0
84.7	0	0	0	0	0	0	0	0
86.7	0	0	-	0	0	0	0	0
90.0	-	-	-	0	-4	-4	-	-
	R = 0.6				R = 1.0			
0.0	15	15	15	15	33	33	33	33
45.0	13	13	13	13	30	30	30	30
60.0	11	11	11	11	26	26	26	26
70.0	9	9	9	9	20	20	20	20
75.6	6	6	6	6	16	16	16	16
79.6	5	5	5	5	12	12	12	12
82.5	5	5	5	5	11	11	11	11
84.7	6	6	6	6	13	13	13	13
86.7	8	8	8	8	18	18	18	18
90.0	8	8	8	8	24	24	24	24

Table VII. Values of the *deviation* [$\Delta = 1{,}000 \times (\Omega_e - \Omega_{in})$] for the atmospheric model no. 9; $\Omega_{in} = 0.550$ atm-cm; $P_0 = 1{,}000$ mb.

θ_0 in deg.	*Deviation* Δ obtained with the procedure							
	C1	C2	C3	C4	C1	C2	C3	C4
	R = 0.0				R = 0.2			
0.0	0	0	–	0	0	0	0	0
45.0	0	0	–	0	1	1	1	1
60.0	0	0	–	0	1	1	1	1
70.0	0	0	–	0	-1	-1	-1	-1
75.6	0	0	–	0	0	0	0	0
79.6	0	0	–	0	0	0	0	0
82.5	0	0	–	0	0	0	0	0
84.7	91	0	–	0	67	0	–	–
86.7	-251	–	–	0	–	-3	–	–
90.0	-181	–	–	0	-183	–	–	–
	R = 0.6				R = 1.0			
0.0	21	21	21	21	43	43	43	43
45.0	19	19	19	19	40	40	40	40
60.0	16	16	16	16	34	34	34	34
70.0	12	12	12	12	26	26	26	26
75.6	10	10	10	10	22	22	22	22
79.6	9	9	9	9	17	17	17	17
82.5	9	9	9	9	17	17	17	17
84.7	11	11	11	11	21	21	21	21
86.7	–	13	13	13	28	28	28	28
90.0	3	3	–	–	33	33	33	33

tents of the deleted layers; see §3.1] with a surface pressure of 400 mb are presented in Tables VIII, IX, and X, respectively. Presence of the symbol "-" (dash) in the place of a numerical value for Δ implies that it was not possible to obtain a value of Ω_e for that particular case.

From the values of Δ given in Table V for the atmospheric model no. 3 with $R = 0.0$, we find that the total ozone amount in this particular case can generally be estimated very accurately [$\Delta = 1{,}000\ (\Omega_e - \Omega_{in}) = 0$] for all ten positions of the sun by making use of any of the four procedures (C1 through C4) described above. The only exception is the subcase of $\theta_0 = 90°$ with the procedure C3 where it is not possible to estimate Ω_e as $\Omega^I_{2,400}$ could not be determined. We find that $R^C_{0.3800,400} = 0.147$, $\Omega^C_{2,400} = 0.270$ atm-cm, $R^I_{0.3398,400} = 0.221$, and $\Omega^I_{2,400} = 0.231$ atm-cm. Thus, $\left|\Omega^I_{2,400} - \Omega^C_{2,400}\right| > 0.030$ atm-cm, and hence, $\Omega^I_{2,400}$ is set to zero. However, the *effective albedo* $\bar{R}$ is < 0.2 for this subcase, and hence $\Omega^I_{2,1000} = 0.250$ atm-cm is returned as a value of Ω_e by the C4 procedure. For the atmospheric model no. 3 resting on a Lambertian surface with $R = 0.2$, the *deviation* Δ is either 0, or -1, for all procedures and all values of θ_0. Hence, we can state the total-ozone estimation procedure is capable of returning *very accurate* ($\Delta = \pm 2$) values of Ω_e provided Ω_{in} is small (0.200 - 0.300 atm-cm), P_0 is very high (very close to 1,000 mb), and $R \leq 0.2$. [Evidently, this last statement (and also similar generalized statements appearing later in this report) is made after examining results in

Table VIII. Values of the *deviation* $[\Delta = 1{,}000 \times (\Omega_e - \Omega_{in})]$ for the atmospheric model no. 14; Ω_{in} = 0.250 atm-cm; P_0 = 400 mb.

θ_0 in deg.	*Deviation* Δ obtained with the procedure							
	C1	C2	C3	C4	C1	C2	C3	C4
	R = 0.0				R = 0.2			
0.0	77	77	-	-	23	23	23	23
45.0	60	60	-	-	21	21	21	21
60.0	43	43	-	-	17	17	17	17
70.0	26	26	-	-	11	11	11	11
75.6	16	16	16	16	6	6	6	6
79.6	33	33	10	10	3	3	3	3
82.5	24	23	23	23	10	10	10	10
84.7	22	21	21	21	9	9	9	9
86.7	26	26	26	26	11	11	11	11
90.0	206	206	-	-	50	50	-	-
	R = 0.6				R = 1.0			
0.0	-5	-5	-5	-5	0	0	0	0
45.0	-4	-4	-4	-4	0	0	0	0
60.0	-3	-3	-3	-3	0	0	0	0
70.0	-3	-3	-3	-3	0	0	0	0
75.6	-2	-2	-2	-2	0	0	0	0
79.6	-2	-2	-2	-2	0	0	0	0
82.5	-1	-1	-1	-1	0	0	0	0
84.7	-1	-1	-1	-1	0	0	0	0
86.7	-1	-1	-1	-1	0	0	0	0
90.0	-1	-1	-1	-1	0	0	0	0

Table IX. Values of the *deviation* [$\Delta = 1{,}000 \times (\Omega_e - \Omega_{in})$] for the atmospheric model no. 17; $\Omega_{in} = 0.400$ atm-cm; $P_0 = 400$ mb.

θ_0 in deg.	*Deviation* Δ obtained with the procedure							
	C1	C2	C3	C4	C1	C2	C3	C4
	R = 0.0				R = 0.2			
0.0	69	69	-	-	19	19	19	19
45.0	51	51	-	-	16	16	16	16
60.0	32	32	-	-	12	12	12	12
70.0	13	13	-	-	6	6	6	6
75.6	0	0	-	-	0	0	0	0
79.6	41	41	-	-	13	13	13	13
82.5	30	30	-	-	10	10	10	10
84.7	36	36	-	-	11	11	11	11
86.7	-	83	-	-	90	23	-	-
90.0	-98	-	-	-	153	153	-	-
	R = 0.6				R = 1.0			
0.0	-7	-7	-7	-7	0	0	0	0
45.0	-6	-6	-6	-6	0	0	0	0
60.0	-5	-5	-5	-5	0	0	0	0
70.0	-4	-4	-4	-4	0	0	0	0
75.6	-3	-3	-3	-3	0	0	0	0
79.6	-2	-2	-2	-2	0	0	0	0
82.5	-2	-2	-2	-2	0	0	0	0
84.7	-2	-2	-2	-2	0	0	0	0
86.7	-2	-2	-2	-2	0	0	0	0
90.0	-3	-3	-3	-3	0	0	0	0

Table X. Values of the *deviation* [$\Delta = 1{,}000 \times (\Omega_e - \Omega_{in})$] for the atmospheric model no. 20; $\Omega_{in} = 0.550$ atm-cm; $P_0 = 400$ mb.

θ_0 in deg.	*Deviation* Δ obtained with the procedure							
	C1	C2	C3	C4	C1	C2	C3	C4
	R = 0.0				R = 0.2			
0.0	44	44	–	–	9	9	9	9
45.0	25	25	–	–	6	6	–	–
60.0	3	3	–	–	1	1	–	–
70.0	94	94	–	–	30	30	–	–
75.6	64	64	–	–	17	17	–	–
79.6	53	53	–	–	10	10	–	–
82.5	83	39	–	–	9	9	–	–
84.7	-208	82	–	–	–	20	–	–
86.7	-315	–	–	–	-280	93	–	–
90.0	-225	–	–	–	-207	–	–	–
	R = 0.6				R = 1.0			
0.0	-10	-10	-10	-10	0	0	0	0
45.0	-9	-9	-9	-9	0	0	0	0
60.0	-7	-7	-7	-7	0	0	0	0
70.0	-5	-5	-5	-5	0	0	0	0
75.6	-4	-4	-4	-4	0	0	0	0
79.6	-4	-4	-4	-4	0	0	0	0
82.5	-4	-4	-4	-4	0	0	0	0
84.7	-5	-5	-5	-5	0	0	0	0
86.7	–	-6	-6	-6	0	0	0	0
90.0	-2	-2	–	–	0	0	0	0

appropriate intermediate ranges.] If we moderate our definition of *very accurate* from $\Delta = \pm 2$ to $\Delta = \pm 4$ units, the Ω_{in} range can be extended to about 0.350 atm-cm, and the R range to about 0.4. For $R \geq 0.6$, all total-ozone estimation procedures yield a significantly overestimated value of Ω_e. The degree of overestimation is independent of the procedure used but, it increases with an increase in R, and is very significant indeed, at small ($\theta_0 \leq 45°$) and large ($\theta_0 \sim 90°$) values of θ_0. This is because the estimation procedure is forced to accept $\Omega^I_{x,400}$ instead of $\Omega^I_{x,1000}$ [see Eq. (10)] at high values of R due to our lack of knowledge of the quantity P_0. It may be noted that for the model no. 3 with $\theta_0 = 0°$ and R = 1.0, all estimation procedures come up with $\Omega^I_{1,1000} = 0.250$ atm-cm, but $\Omega^I_{1,400} = 0.278$ atm-cm. Thus, we see a clear need of having some information about the parameter P_0 at the time of observation for increasing the accuracy of Ω_e, especially if the sun is very close to the local zenith.

Numerical results presented in Tables VI and VII for the atmospheric models no. 6 and 9, respectively, support the analysis given in the preceding paragraph, in a general sense. For the model no. 6 with $\theta_0 = 90°$ and R = 0.0, a value of Ω_e could be obtained with the C4 procedure. On the other hand, the restriction imposed by the C3 procedure results in an inability to accept an otherwise good value of $\Omega^I_{x,y}$ for the $\theta_0 = 90°$, R = 0.2 subcase. For the model no. 9 (Table VII) with 0.550 atm-cm total ozone, the C1 procedure yields very erroneous values for Ω_e when the sun is near the horizon, and the ground reflec-

tivity is small. A value of 91 for the $R = 0.0$, $\theta_0 = 84.7°$ subcase occurs because $R^I_{0.3398,1000}$ and $R^I_{0.3398,400}$ are evaluated to be - 0.091 and 0.248, respectively. Corresponding values of $\Omega^I_{2,1000}$ and $\Omega^I_{2,400}$ then turn out to be 0.641 and 0.535 atm-cm, respectively. A large negative value for Δ for the $R = 0.0$, $\theta_0 = 86.7°$ subcase (and also for the subcases $R = 0.0$, $\theta_0 = 90°$, and $R = 0.2$, $\theta_0 = 90°$) is due to the presence of a maximum in the N_c vs. Ω_{in} curve discussed in §4.1, associated with the existence of the condition of $S^I_{1,1000}$ being greater than $S^I_{2,1000}$ in the region of immediate interest. Thus, we have several examples stressing the need of using only the second wavelength pair for large values of θ_0. As mentioned earlier, the NASA/GSFC procedure for estimation of total ozone from the BUV measurements, does contain a step to perform the same function in an indirect manner.

From the results presented in Tables VIII to X for atmospheric models with a surface pressure of 400 mb, we find that the *deviation* Δ vanishes for all subcases with $R = 1.0$. Results for the same models but with $R = 0.8$ for which no numerical data are presented in this report, also show Δ to be zero for all subcases. This is because the estimation procedure is forced to select values of $\Omega^I_{x,400}$ as Ω_e for $R \geq 0.8$, and the surface pressure for these models also happens to be 400 mb. For $R = 0.6$, the quantity Δ carries a negative value which increases with an increase in θ_0, and also with a decrease in Ω_{in}. The maximum underestimation in total ozone is by about 2%. For still lower values of R ($R = 0.2$, and 0.0), we find the total ozone amount

to be overestimated by as much as 31% in some extreme cases (e.g., Δ = 77 units for the $R = 0.0$, $\theta_0 = 0°$ subcase for the model no. 14) by the C1 and C2 procedures. Many of such bad cases can be discarded by imposing the extra constraint added in arriving at SITC3 from SITC2. It should be pointed out that, once in a while, this extra constraint does result in discarding of a good case also; as for example, a use of C1 or C2 procedure yields a value of zero for Δ for the subcase $R = 0.0$, $\theta_0 = 75.6°$ of the model no. 17, but a use of C3 or C4 procedure leads to the inability in estimation of Ω_e.

Somewhat detailed discussion in the preceding paragraphs can be summarized as follows:

- After exercising due precautions for not using the N_c vs. Ω curves exhibiting a maximum, two problem areas have developed due to a need for estimating total ozone in the absence of any information about the surface pressure. The first problem area consists of cases associated with values of the parameters P_0 and R in the upper parts of their respective ranges. For such cases, we find that the estimated ozone amount (Ω_e) can be greater than the input ozone amount by as much as 0.045 atm-cm. The exact degree of overestimation depends upon values of the various parameters such as P_0, R, θ_0, and Ω_{in}.

- The second problem area consists of cases associated with values of the parameters P_0 and R in the lower part of their respective ranges. For such cases, we again find that the total ozone amount

can be overestimated by as much as 0.075 atm-cm. Some of these cases can be discarded by setting $\Omega^{I}_{x,y}$ to zero whenever $\left|\Omega^{I}_{x,y} - \Omega^{C}_{x,y}\right| \geq 0.030$ atm-cm for a given x,y combination (see discussion of SITC3 procedure).

5.2 *Effective Albedo:* The total-ozone estimation procedure also computes another quantity called the *effective albedo* which is denoted by the symbol $\bar{R}$ [see Eq. (8)]. From the procedure outlined in §2.4 for the evaluation of $\bar{R}$, it is clear that $\bar{R}$ is not related to the Lambert reflectivity (R) of the surface underneath the atmosphere, only. Because of the use of tables for arbitrarily chosen surface pressures of 1,000 and 400 mb, and also because of the use of $\Omega^{C}_{x,y}$ in evaluation of $R^{I}_{0.3398,y}$, $\bar{R}$ can also depend upon the surface pressure (P_0) of the model under investigation, and upon the solar zenith angle (θ_0). However, because of our knowledge that the Lambert's law is not valid for realistic surfaces, there seems to be a considerable temptation for relating $\bar{R}$ to the optical characteristics of the surface only. The following discussion is provided to assist the reader in seeing some pseudoproperties of $\bar{R}$ which are in no way connected to the actual optical characteristics of the surface underlying the atmospheric model.

Values of the *coarse effective albedo* ($R^{C}_{0.3800,1000}$ and $R^{C}_{0.3800,400}$), *improved effective albedo* ($R^{I}_{0.3398,1000}$ and $R^{I}_{0.3398,400}$), as well as of the *effective albedo* ($\bar{R}$) as obtained during various stages of calculations in the total-ozone estimation procedure are given in Table XI, for two arbitrarily selected (Nos. 4 and 18) atmospheric models with R = 0.0

Table XI. Values of *albedo* obtained during various stages of calculations in the total-ozone estimation procedure, for two arbitrarily chosen models.

Model No.	R	θ_0	$R^C_{0.3800,1000}$	$R^I_{0.3398,1000}$	$R^C_{0.3800,400}$	$R^I_{0.3398,400}$	$\bar{R}$
4	0.0	45.0	0.000	0.000	0.120	0.188	0.094
		70.0	0.000	0.000	0.167	0.243	0.122
		90.0	0.000	0.000	0.147	0.226	0.113
	1.0	45.0	1.000	1.000	1.006	1.003	1.002
		70.0	1.000	1.000	0.966	0.970	0.985
		90.0	1.000	1.000	0.985	0.997	0.999
18	0.0	45.0	-0.168	-0.333	0.000	0.000	-0.167
		70.0	-0.268	-0.517	0.000	0.000	-0.259
		90.0	-0.223	-0.487	0.000	0.000	-0.244
	1.0	45.0	0.995	0.997	1.000	1.000	0.999
		70.0	1.035	1.031	1.000	1.000	1.016
		90.0	1.015	1.004	1.000	1.000	1.002

and 1.0, and θ_0 = 45°, 70°, and 90°. For the model No. 4 with 1,000 mb surface pressure, values of $R^C_{0.3800,1000}$ and $R^I_{0.3398,1000}$ agree with the corresponding value of R as the surface pressures of the model and tables used are exactly the same. Such is also the case for values of $R^C_{0.3800,400}$ and $R^I_{0.3398,400}$ for the atmospheric model No. 18. However, for the determination of $R^C_{0.3800,400}$ and $R^I_{0.3398,400}$ for the model No. 4, we enter the 400 mb tables with a relatively large value of $I_m(0.3800, \theta_0)$ and $I_m(0.3398, \theta_0)$, respectively. This step then results

in an overestimation of the *improved effective albedoes*. The degree of overestimation is naturally controlled by the slope of $I_c(\lambda, \Omega_{in}, P_0, R_\lambda, \theta_0)$ vs. R_λ curves, and the separation of such curves for $P_0 = 1{,}000$ and 400 mb, in the region of immediate interest. Hence, we have pseudo-dependence of $R^C_{0.3800,400}$, $R^I_{0.3398,400}$, and $\bar{R}$ on the parameter θ_0, for the atmospheric model No. 4. The above-mentioned arguments can also be used after appropriate changes to explain under-estimation and θ_0-dependence of $R^C_{0.3800,1000}$, $R^C_{0.3398,1000}$ and $\bar{R}$ values for the atmospheric model No. 18.

A detailed analysis of $\bar{R}$ values for all 20 models confirmed the presence of the above-mentioned pseudo-dependence of $\bar{R}$ on θ_0, and on R, in all cases. Besides, a small, but significant, dependence of $\bar{R}$ on Ω_{in} was also noted. We will not go into this aspect any further. However, we will consider the variations of mean $\bar{R}$ (mean over 10 values of θ_0, and over 10 atmospheric models with the same surface pressure, but for a given value of R) as a function of R, for models with 1,000 mb, and 400 mb surface pressures. For $P_0 = 1{,}000$ mb, this quantity mean $\bar{R}$ is found to assume a value of 0.108, 0.189, 0.270, 0.353, 0.438, 0.613, 0.797, and 0.993 for R = 0.0, 0.1, 0.2, 0.3, 0.4, 0.6, 0.8, and 1.0, respectively. Thus, the range of mean $\bar{R}$ is smaller than that of R even though values of mean $\bar{R}$ for small values of R are greater than the corresponding values of R. For $P_0 = 400$, mean $\bar{R}$ assumes a value of -0.235, -0.077, 0.071, 0.210, 0.340, 0.582, 0.803, and 1.007 for the values of R given by R = 0.0, 0.1, 0.2, 0.3, 0.4, 0.6, 0.8,

and 1.0, respectively. Thus, the current total-ozone estimation procedure tends to expand (shrink) the range of mean $\bar{R}$ compared to that of R if the models being analyzed by it have low (high) surface pressures.

From the results presented in the preceding paragraphs, it is clear that the negative values of the *effective albedo* is an artifact of the total-ozone estimation procedure. The analysis of the actual BUV measurements has provided some negative values of $\bar{R}$ in the range -0.05 to 0.0. Absence of very large negative values (~ -0.1 or smaller) in the results of the analysis of actual measurements, can be partly attributed to the lack of perfectly absorbing ($R = 0.0$) natural surfaces. Several values of the *effective albedo* measured over the polar regions by the BUV configuration, are found to fall in the range $1.1 - 1.6$. It is possible that some of these large values of $\bar{R}$ are due to a specular reflection, or some other physical reason, or due to a combination of circumstances. However, one more aspect of the estimation procedure has to be considered before assigning these large values of $\bar{R}$ to natural causes. This aspect is related to the possible errors in estimation of the parameter θ_0 at the place and time of observation due to some biased errors as a result of the nonparallelness of the axis of the satellite and the optical axis of the cone of observation, or due to some random errors resulting from changes in the orbital parameters. From the plots of $I_c(0.3800, \Omega = 0.0, 1{,}000\ \text{mb}, R_\lambda, \theta_0)$ vs. θ_0 shown in Fig. 7 for four different values of R_λ (= R), we can see that an error of about 1° in θ_0 for large ($\sim 84°$ or greater) values of θ_0 can result in errors of ± 0.2 in the estimation of R.

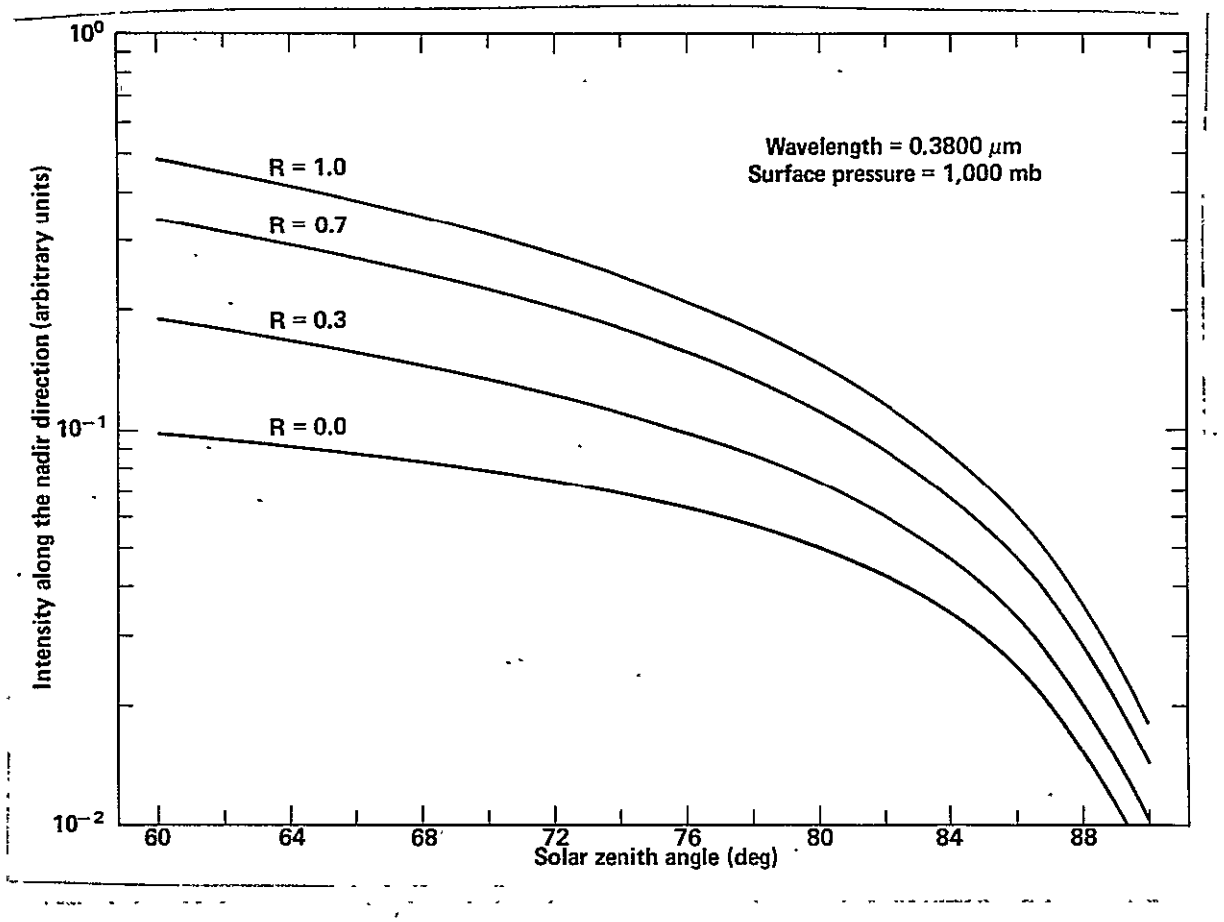

Fig. 7 Variations of the intensity of the scattered radiation emerging along the local nadir direction [$I_c(\lambda, \Omega, P_0, R_\lambda, \theta_0)$] as a function of the solar zenith angle (θ_0) for λ = 0.3800 μm, and P_0 = 1,000 mb (atmospheric model Nos. 2 through 11). Different curves are for different values of the reflectivity (R_λ) of the surface underlying the atmosphere.

5.3 *Results for the Cases with R Dependent up to λ:* In §5.1, we justified the constraint of setting $\Omega^{I}_{x,y}$ to zero if $\left|\Omega^{I}_{x,y} - \Omega^{C}_{x,y}\right| \geq$ 0.030 atm-cm in the SITC3 (or C4) procedure on the ground of a possible large difference between values of $R^{C}_{0.3800,y}$ and $R^{I}_{0.3398,y}$, or on the ground of a large sensitivity of $\Omega^{I}_{x,y}$ to small changes in albedo. This constraint is on a very sound basis if we have an *a priori* information that R_{λ} is independent of λ. If we do have information on variations of R_{λ} with λ for various surfaces, we can modify the total-ozone estimation procedure to take advantage of this additional information. The question then arises as to how much error is introduced in Ω_{e} as a result of a given R_{λ} vs. λ variation, and to what extent the criterion of the SITC3 procedure assists in improving values of Ω_{e} so obtained.

Very little information is available in the open literature about the spectral dependence of various types of natural surfaces in the region of immediate interest, viz, 0.3100 - 0.3800 μm. We have therefore attempted to obtain a preliminary answer to this question by using simulated Lambert reflectivity characteristics shown in Fig. 8. In fact, we have used three distinct types of characteristics. The first type of characteristics represents surfaces whose Lambert reflectivity increases with an increase in wavelength (curves marked A, B, and C). Three different slopes of R_{λ} vs. λ are considered, viz, $\Delta R = 0.01$, 0.02, and 0.05 for a 0.01 μm change in wavelength. The second type of characteristics represents surfaces whose Lambert reflectivity

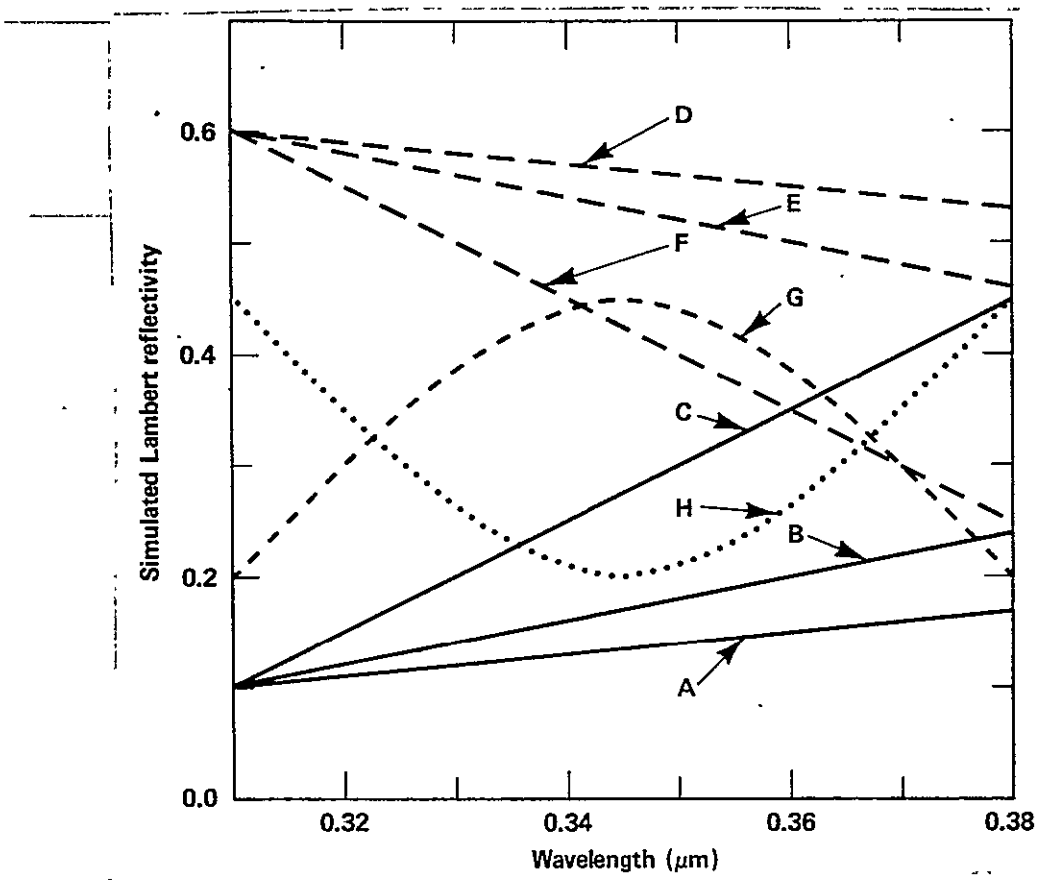

Fig. 8 Variations of the simulated Lambert reflectivity (R_λ) as a function of the wavelength (λ).

decreases with an increase in wavelength (curves marked D, E, F). Again, the same three slopes are considered, but with an opposite sign. The third type of characteristics would represent surfaces whose R_λ vs. λ curves would have either a maximum (curve G), or a minimum (curve H), in the middle of the spectral region of interest.

The SITC2 and SITC4 procedures (see §5.1) were modified to handle this generalized input, and renamed SITC6 and SITC8, respectively. The new procedures are capable of handling cases where the Lambert reflectivity (R_λ) of the surface underlying the atmospheric model, can be a function of wavelength (λ). Atmospheric models Nos. 2 through 11, and 13 through 22 were again used to obtain values of Ω_e and $\bar{R}$ for ten different values of θ_0, and eight different R_λ vs. λ characteristics using the SITC6 and SITC8 procedures. For brevity, we will restrict our discussion to a mean value of Ω_e where this mean is taken over a maximum of 20 subcases for a given value of the input ozone amount (Ω_{in}), but for 10 values of θ_0 and 2 values of the surface pressure (P_0). Number of subcases for which the *best ozone estimate* (Ω_e) could be evaluated for a given value of Ω_{in} and the corresponding mean value of Ω_e as obtained with the SITC6 and SITC8 procedures are given in Tables XII, XIII, and XIV for the three different types of reflectance characteristics, respectively, described in the preceding paragraph.

From the results presented in Table XII for the models resting on a Lambert surface whose reflectivity increases with an increase in wavelength, it can be seen that the constraint of the SITC8 procedure dis-

Table XII. Number of subcases for which the *best ozone estimate* (Ω_e) could be evaluated out of a maximum of 20 subcases (10 values of θ_0, and 2 values of P_0) for a given input ozone amount (Ω_{in}), and the corresponding mean Ω_e for these subcases as obtained with the SITC6 and SITC8 procedures. Ground Reflectivity: R_λ is assumed to increase linearly with an increase of λ (curves A, B, and C of Fig. 8).

Number of subcases for which Ω_e could be evaluated.

Ω_{in} atm-cm	Ref. Curve A		Ref. Curve B		Ref. Curve C	
	SITC6	SITC8	SITC6	SITC8	SITC6	SITC8
0.200	20	17	20	17	20	15
0.250	20	17	20	15	20	13
0.300	20	15	20	12	19	8
0.350	19	10	19	9	19	8
0.400	19	9	19	8	19	5
0.450	19	9	19	8	17	0
0.500	18	8	17	7	17	0
0.550	17	7	17	6	15	0
0.600	15	7	14	5	11	0

Corresponding value of mean Ω_e in atm-cm.

0.200	0.215	0.211	0.220	0.214	0.233	0.221
0.250	0.270	0.262	0.275	0.264	0.292	0.272
0.300	0.324	0.312	0.332	0.311	0.337	0.315
0.350	0.366	0.362	0.372	0.357	0.390	0.367
0.400	0.420	0.405	0.428	0.408	0.455	0.417
0.450	0.477	0.455	0.485	0.458	0.495	-
0.500	0.527	0.505	0.531	0.509	0.554	-
0.550	0.575	0.555	0.585	0.559	0.592	-
0.600	0.606	0.606	0.605	0.608	0.601	-

Table XIII. Number of subcases for which the *best ozone estimate* (Ω_e) could be evaluated out of a maximum of 20 subcases (10 values of θ_0, and 2 values of P_0) for a given input ozone amount (Ω_{in}), and the corresponding mean Ω_e for these subcases as obtained with the SITC6 and SITC8 procedures.

Ground Reflectivity: R_λ is assumed to decrease linearly with an increase of λ (curves D, E, and F of Fig. 8).

Number of subcases for which Ω_e could be evaluated.

Ω_{in} atm-cm	Ref. Curve D		Ref. Curve E		Ref. Curve F	
	SITC6	SITC8	SITC6	SITC8	SITC6	SITC8
0.200	20	20	20	20	20	18
0.250	20	20	20	20	20	18
0.300	20	20	20	18	20	17
0.350	20	19	20	18	20	13
0.400	20	18	20	16	18	4
0.450	20	18	20	14	17	0
0.500	20	16	19	12	16	0
0.550	19	14	17	12	13	0
0.600	16	13	13	10	8	0

Corresponding value of mean Ω_e in atm-cm.

0.200	0.196	0.196	0.192	0.192	0.178	0.180
0.250	0.247	0.247	0.243	0.243	0.230	0.231
0.300	0.297	0.297	0.291	0.293	0.276	0.278
0.350	0.346	0.347	0.341	0.343	0.323	0.324
0.400	0.396	0.397	0.389	0.392	0.376	0.381
0.450	0.445	0.446	0.436	0.442	0.421	-
0.500	0.493	0.497	0.485	0.491	0.470	-
0.550	0.543	0.547	0.537	0.541	0.519	-
0.600	0.595	0.597	0.591	0.591	0.572	-

Table XIV. Number of subcases for which the *best ozone estimate* (Ω_e) could be evaluated out of a maximum of 20 subcases (10 values of θ_0, and 2 values of P_0) for a given input ozone amount (Ω_{in}), and the corresponding mean Ω_e for these subcases as obtained with the SITC6 and SITC8 procedures.

Ground Reflectivity: Variations of R_λ vs. λ used for these results are as shown by the curves G, and H of Fig. 8.

Number of subcases for which Ω_e could be evaluated.

Ω_{in} atm-cm	Ref. Curve G		Ref. Curve H	
	SITC6	SITC8	SITC6	SITC8
0.200	19	15	20	15
0.250	18	7	20	14
0.300	18	5	20	9
0.350	17	0	20	6
0.400	15	0	20	4
0.450	9	0	19	0
0.500	5	0	18	0
0.550	0	0	18	0
0.600	0	0	16	0

Corresponding value of mean Ω_e in atm-cm.

0.200	0.241	0.231	0.166	0.173
0.250	0.292	0.275	0.218	0.226
0.300	0.342	0.325	0.265	0.275
0.350	0.394	-	0.315	0.329
0.400	0.448	-	0.369	0.376
0.450	0.499	-	0.410	-
0.500	0.537	-	0.458	-
0.550	-	-	0.508	-
0.600	-	-	0.556	-

cards a large number of subcases at large values of the parameter Ω_{in}. This is especially true when the slope of the R_λ vs. λ curve is also the steepest of all (curve C). Use of the SITC6 (or SITC8) procedure for atmospheric models resting on a Lambert surface with its reflectivity increasing with an increase in wavelength, results in an overestimation of mean Ω_e (in fact, most of the individual values of Ω_e were found to be greater than the corresponding value of Ω_{in}). In general, values of the mean Ω_e obtained with the SITC8 procedure are significantly closer to the corresponding Ω_{in} values than those obtained with the SITC6 procedure.

Results presented in Table XIII for the models resting on a Lambert surface whose reflectivity decreases with an increase in wavelength, also support the observations for the models with the first surface characteristics reported in the preceding paragraph except that the quantity $[(\text{mean } \Omega_e) - \Omega_{in}]$ now carries a negative sign. Furthermore, the magnitude of $(\text{mean } \Omega_e) - \Omega_{in}$ is also generally smaller for this latter characteristic than the preceding one.

When the spectral reflectance curves of the Lambert surface underlying an atmospheric model exhibit a strong maximum or a minimum in the middle of the spectral region of interest, use of the SITC8 procedure results in discarding of a large number of subcases (Table XIV). Furthermore, the quantity $[(\text{mean } \Omega_e) - \Omega_{in}]$ is positive (negative) when the reflectance characteristics of the underlying surface are represented by the curve G (H) of Fig. 8. It may also be noted that the values of

$|(\text{mean } \Omega_e) - \Omega_{in}|$ for the results presented in Table XIV are generally greater than those in Table XII, or XIII.

Other additional aspects which should be looked into in this type of analysis are the maximum, mean, and the R.M.S. deviations of Ω_e around its mean value. From a cursory analysis of the detailed output, we feel that the use of the SITC8 procedure would also result in a significant improvement in this area.

5.4 *Effect of Raising the Ground:* Results presented in §5.1, §5.2, and §5.3 are restricted to dust-free atmospheric models with a surface pressure (P_0) of 1,000 or 400 mb. In fact, these models are the same as those used for the preparation of basic tables for the total-ozone estimation procedure (see §2.2). In order to investigate the effect of raising the lower boundary of the atmospheric model above the mean sea-level, the atmospheric model No. 3 and 7 with Ω_{in} = 0.250 and 0.450 atm-cm were used to generate several additional models whose lower boundaries are located at h km above the mean sea-level. The following values are used for the parameter h: 0, 2, 4, 6, 7, 9, 11, 13, and 15 km. It may be noted that the model with its lower boundary located at 7 km above the mean sea-level has a surface pressure (P_0) of 400 mb. Information about the surface pressure (P_0 in mb), and the total ozone content (Ω in atm-cm) of these additional atmospheric models along with their corresponding serial numbers as used in generation of the output, is given in Table XV.

Table XV. Values of the height (h in km) of the lower boundary of the atmospheric model above the mean sea-level, surface pressure (P_0 in mb) at this lower boundary, and the actual total ozone amount [Ω in atm-cm] for several additional models. Information about models No. 3, 7, 14, and 18 is reproduced here from Table III for assuring completeness of presentation.

Model Number	Height (km)	Surface Pressure (mb)	Ozone Amount (atm-cm)
3	0	1,000	0.250
31	2	789	0.245
32	4	605	0.240
33	6	461	0.236
14	7	400	0.234
34	9	304	0.232
35	11	228	0.231
36	13	169	0.229
37	15	123	0.227
7	0	1,000	0.450
38	2	789	0.443
39	4	605	0.436
40	6	461	0.430
18	7	400	0.427
41	9	304	0.419
42	11	228	0.402
43	13	169	0.372
44	15	123	0.342

Values of the *deviation* Δ [$= 1{,}000 \times (\Omega_e - \Omega_{in})$] are given in Table XVI for all atmospheric models with $\Omega_{in} = 0.250$ atm-cm, and for all ten values of θ_0, but for the wavelength-independent reflectivity of 0.1, and 0.2 only. (The SITC4 procedure was used for this purpose.) Similar results but for $R = 0.8$ and 1.0 are given in Table XVII. For $R = 0.0$ and 0.1, the *deviation* Δ increases with an increase in the height of the lower boundary of the model above the mean sea-level. Large values of Δ are generally seen at small values of θ_0, and at high values of h. For $\theta_0 = 0°$, 45°, and 60°, it is not possible to estimate a value of Ω_e for values of $h > 9$ km when $R = 0.1$. For $R = 0.8$ and 1.0, the *deviation* Δ (which is positive for $h = 0$ km) decreases with an increase in the value of the parameter h, passes through a zero value at $h = 0$ km, and assumes negative values thereafter.

From the values of the quantity Δ given in Table XVIII for all atmospheric models with $\Omega_{in} = 0.450$ atm-cm, and with low values ($R \approx 0.1$ and 0.2) for the Lambert reflectivity of the underlying surface, we find that it is not possible to obtain a value of Ω_e in many subcases. This is not the case for large values of R (0.8 and 1.0) for which numerical results are presented in Table XIX. Comparison of results presented in Tables XVII and XIX shows a very significant increase in the magnitude of Δ for given R, θ_0, h combinations as Ω_{in} is increased from 0.250 to 0.450 atm-cm.

The following analysis was performed for a part of the output for the atmospheric models listed in Table XV at the request of Dr. A. J.

Table XVI. Effect of raising the lower boundary by h km on the *deviation* [$\Delta = 1{,}000 \times (\Omega_e - \Omega_{in})$] for an atmospheric model with $\Omega_{in} = 0.250$ atm-cm.

θ_0	*Deviation* for the model with h =								
	0 km	2 km	4 km	6 km	7 km	9 km	11 km	13 km	15 km
	R = 0.1; Independent of λ.								
0.0	0	9	22	36	44	–	–	–	–
45.0	0	7	18	30	37	–	–	–	–
60.0	0	5	13	23	28	–	–	–	–
70.0	0	3	8	14	18	27	–	–	–
75.6	0	2	4	8	11	17	–	–	–
79.6	0	1	3	5	6	9	13	–	–
82.5	0	3	8	12	15	23	–	–	–
84.7	0	4	8	12	14	19	24	–	–
86.7	0	4	10	15	18	22	25	–	–
90.0	0	17	–	–	–	–	–	–	–
	R = 0.2; Independent of λ.								
0.0	-1	5	12	19	23	31	38	43	47
45.0	-1	4	10	17	21	28	34	39	42
60.0	-1	3	8	13	17	23	29	33	36
70.0	0	2	5	8	11	16	21	25	28
75.6	0	1	3	5	6	10	14	17	19
79.6	0	1	1	3	3	5	7	10	11
82.5	0	2	5	8	10	14	19	25	–
84.7	0	2	5	8	9	11	14	18	22
86.7	0	3	7	10	11	13	14	14	14
90.0	-1	11	26	–	–	–	–	–	–

Table XVII. Effect of raising the lower boundary by h km on the *deviation* [$\Delta = 1{,}000 \times (\Omega_e - \Omega_{in})$] for an atmospheric model with $\Omega_{in} = 0.250$ atm-cm.

θ_0	*Deviation* for the model with h =								
	0 km	2 km	4 km	6 km	7 km	9 km	11 km	13 km	15 km
	R = 0.8; Independent of λ.								
0.0	24	16	8	2	0	-3	-5	-7	-9
45.0	20	14	8	2	0	-3	-5	-7	-9
60.0	16	12	6	2	0	-3	-4	-6	-9
70.0	12	9	5	1	0	-2	-3	-5	-8
75.6	10	7	4	1	0	-1	-2	-4	-6
79.6	8	6	3	1	0	-1	-1	-2	-3
82.5	6	4	2	0	0	0	0	0	-1
84.7	6	4	2	1	0	0	0	0	1
86.7	7	5	3	1	0	-1	-1	-2	-1
90.0	15	10	5	1	0	-1	-2	-6	-15
	R = 1.0; Independent of λ.								
0.0	28	19	10	2	0	-3	-5	-6	-8
45.0	25	17	9	2	0	-3	-5	-7	-9
60.0	21	14	8	2	0	-3	-5	-7	-10
70.0	16	11	6	2	0	-2	-4	-6	-8
75.6	12	8	5	1	0	-2	-3	-4	-6
79.6	10	7	4	1	0	-1	-1	-2	-3
82.5	7	5	2	0	0	0	0	0	0
84.7	8	5	2	0	0	0	0	1	2
86.7	9	6	3	1	0	-1	-1	0	1
90.0	18	12	6	1	0	-1	-2	-5	-14

Table XVIII. Effect of raising the lower boundary by h km on the *deviation* [$\Delta = 1{,}000 \times (\Omega_e - \Omega_{in})$] for an atmospheric model with $\Omega_{in} = 0.450$ atm-cm.

θ_0	*Deviation* for the model with h =								
	0 km	2 km	4 km	6 km	7 km	9 km	11 km	13 km	15 km
	R = 0.1; Independent of λ.								
0.0	0	7	18	–	–	–	–	–	–
45.0	0	5	14	–	–	–	–	–	–
60.0	0	3	8	–	–	–	–	–	–
70.0	0	9	3	–	–	–	–	–	–
75.6	0	5	14	–	–	–	–	–	–
79.6	0	4	10	–	–	–	–	–	–
82.5	0	4	10	–	–	–	–	–	–
84.7	0	7	14	–	–	–	–	–	–
86.7	0	14	–	–	–	–	–	–	–
90.0	0	–	–	–	–	–	–	–	–
	R = 0.2; Independent of λ.								
0.0	0	3	8	13	15	18	–	–	–
45.0	0	3	7	11	12	–	–	–	–
60.0	0	1	4	7	8	–	–	–	–
70.0	1	0	1	25	–	–	–	–	–
75.6	0	3	9	15	–	–	–	–	–
79.6	0	2	5	9	–	–	–	–	–
82.5	0	3	5	7	8	–	–	–	–
84.7	0	4	8	11	–	–	–	–	–
86.7	–	9	–	–	–	–	–	–	–
90.0	–	–	–	–	–	–	–	–	–

Table XIX. Effect of raising the lower boundary by h km on the *deviation* [$\Delta = 1{,}000 \times (\Omega_e - \Omega_{in})$] for an atmospheric model with $\Omega_{in} = 0.450$ atm-cm.

θ_0	*Deviation* for the model with h =								
	0 km	2 km	4 km	6 km	7 km	9 km	11 km	13 km	15 km
	R = 0.8; Independent of λ.								
0.0	32	22	12	4	0	−9	−30	−63	−94
45.0	29	20	11	4	0	−9	−29	−62	−93
60.0	24	17	10	4	0	−8	−28	−60	−91
70.0	19	14	8	3	0	−7	−25	−56	−86
75.6	15	10	6	2	0	−5	−21	−51	−79
79.6	12	9	5	2	0	−5	−19	−47	−75
82.5	12	8	5	2	0	−4	−15	−40	−66
84.7	14	10	6	2	0	−4	−15	−37	−60
86.7	19	14	8	3	0	−6	−21	−46	−67
90.0	24	16	9	3	0	−8	−30	−67	–
	R = 1.0; Independent of λ.								
0.0	37	24	13	4	0	−9	−30	−63	−94
45.0	34	23	13	4	0	−9	−30	−63	−94
60.0	29	20	12	4	0	−9	−29	−62	−93
70.0	23	16	9	3	0	−7	−26	−58	−88
75.6	18	12	7	3	0	−6	−22	−53	−81
79.6	14	9	5	2	0	−5	−20	−49	−77
82.5	14	9	4	1	0	−3	−15	−40	−67
84.7	16	10	5	2	0	−3	−14	−36	−59
86.7	22	14	8	3	0	−5	−19	−44	−64
90.0	28	19	10	3	0	−7	−28	−65	–

Fleig: The total-ozone estimation procedure may provide values of $\Omega^I_{x,1000}$ and $\Omega^I_{x,400}$ for $x = 1$, and 2. Based on the value of θ_0 and the slope of the N_c vs. Ω_{in} curve in the region of immediate interest, we select one of the two wavelength pairs, and then obtain a value of Ω_e with the help of the procedure discussed in §2.4, and §5.1. If values of $\Omega^I_{x,1000}$ and $\Omega^I_{x,400}$ are available for a given subcase and for the wavelength pair used in the determination of Ω_e, we can then obtain a value of Ω_e' from the knowledge of the P_0 parameter for a given model, and a linear interpolation or a linear extrapolation of $\Omega^I_{x,y}$ vs. P_0, or vs. log P_0, or vs. h curves. After several trials, we found that a linear interpolation or extrapolation in P_0 provides the best results.

Values of Ω_e' were obtained after following the procedure outlined in the preceding paragraph for the atmospheric models No. 31, 32, 36, and 37 illuminated by the sun at 0°, 45°, 60°, 70°, and 75.6° from the local zenith. For all cases for which it was possible to obtain a value of Ω_e', we found the *deviation* Δ' $[= 1{,}000 \times (\Omega_e' - \Omega_{in})]$ to be in the range ± 4 units. Thus, for the model No. 32 with $R = 0.0$ and $\theta_0 = 0°$, we have $\Delta = 34$ units but $\Delta' = -3$ units only. For the model No. 37 with $R = 0.2$ and $\theta_0 = 0°$, we have $\Delta = 47$ units but $\Delta' = 0$. For the model No. 37 with $\theta_0 = 0°$, we have $\Delta = -9$ units and $\Delta' = 0$ for $R = 0.8$, but $\Delta = -8$ units and $\Delta' = 4$ units for $R = 1.0$. These results suggest that a knowledge of P_0 associated with the availability of the values of $\Omega^I_{x,1000}$ and $\Omega^I_{x,400}$ for a given subcase,

helps considerably in increasing the reliability of the *best ozone estimate* provided Ω_{in} is small.

For the moderate values of Ω_{in} (i.e., Ω_{in} = 0.450 atm-cm), it was not possible to obtain a value of Ω_e' in many instances due to the unavailability of both $\Omega^I_{x,1000}$ and $\Omega^I_{x,400}$. For subcases for which the quantity Ω_e' could be determined, the corresponding Δ' was found to be close to zero only if P_0 for that particular subcase was located between 1,000 and 400 mb. The results were of rather poor quality whenever a linear extrapolation was required. As for example, for the model No. 41 and 42 with $\theta_0 = 0°$, and R = 0.4, the quantity Δ has a value of - 12 and - 28 units, respectively, while the respective values of the quantity Δ' are - 5 and - 21 units.

Results presented in the last two paragraphs demonstrate the need of developing a new total-ozone estimation procedure with basic sets of tables for additional values of the parameter P_0 if the value of the surface pressure at the time of observation is available from independent sources. It may suffice to have three additional basic sets, viz, for P_0 = 800, 600, and 200 mb.

5.5 *Convergence of the Best-Ozone-Estimate Value:* The total-ozone estimation procedure described in §2.4 can be briefly outlined as follows:

(a) Measured values of the intensity of the scattered radiation emerging at the top of the atmosphere along the local nadir direction $[I_m(\lambda, \theta_0)]$ are available for 5 different values of λ (viz, 0.3125,

0.3175, 0.3312, 0.3398, and 0.3800 μm), and a given value of θ_0.

(b) Use 1,000 mb tables for the given θ_0 to compute $R^C_{0.3800,1000}$ from $I_m(0.3800, \theta_0)$. Assign the computed value of $R^C_{0.3800,1000}$ to $R^C_{\lambda,1000}$ for the remaining four wavelengths.

(c) Compute $\Omega^C_{x,1000}$ using values of $R^C_{\lambda,1000}$ and $I_m(\lambda, \theta_0)$ at the first four wavelengths listed in (a) above.

(d) Use $\Omega^C_{x,1000}$ to obtain $R^I_{0.3398,1000}$ from the value of $I_m(0.3398, \theta_0)$, and assign $R^I_{0.3398,1000}$ value to $R^I_{\lambda,1000}$ for the first three wavelengths.

(e) Compute $\Omega^I_{x,1000}$ using values of $R^I_{\lambda,1000}$ and $I_m(\lambda, \theta_0)$.

(f) Repeat (b) to (e) above to compute $R^C_{\lambda,400}$, $\Omega^C_{x,400}$, $R^I_{\lambda,400}$, and $\Omega^I_{x,400}$.

(g) Evaluate Ω_e using values of $R^I_{\lambda,1000}$, $R^I_{\lambda,400}$, $\Omega^I_{x,1000}$, and $\Omega^I_{x,400}$ after selecting the proper wavelength pair, i.e., a value for the subscript x.

These steps of the procedure suggest a possibility of obtaining a converged value of Ω_e by setting up an iteration scheme. The value of Ω_e at step (g) can be taken as $\Omega^{I2}_{x,y}$ to evaluate $R^{I2}_{\lambda,y}$ following step (d). Steps (e), (f), and (g) can then be executed to arrive at the second value of the *best ozone estimate* represented by the symbol Ω^2_e. This iteration procedure can then be repeated to obtain values of Ω^3_e, Ω^4_e, $\cdots$, Ω^n_e.

Values of Ω_e^n for $n = 1, 2, 3, 4, 5,$ and 6 were computed for the atmospheric model No. 2 through 11, and 13 through 22 by using the iteration procedure outlined in the preceding paragraph at the suggestion and request of Dr. A. J. Fleig. These computations were carried out for all 10 values of θ_0, and 8 values of R listed earlier. A modified version of the SITC4 procedure was used for this purpose.

Out of a total 800 subcases for the 1,000 mb models (10 models × 10 values of θ_0 × 8 values of R), it was not possible to evaluate even Ω_e^1 (or Ω_e) for 110 subcases (see §5.1). Values of Ω_e^n were found to remain unchanged with an increase in the order of iteration for 615 subcases. For 59 subcases, the quantity $\left|\Omega_e^6 - \Omega_{in}\right|$ for a given R, θ_0, Ω_{in} combination was found to be greater than the corresponding value of $\left|\Omega_e^1 - \Omega_{in}\right|$ by 0.001 or 0.002 atm-cm suggesting a deterioration in the value of Ω_e^n with an increase in the order of iteration. For 10 other subcases, this deterioration was found to be as much as 0.007 atm-cm. For two subcases with $\Omega_{in} = 0.650$ atm-cm, we could estimate Ω_e^1, but not Ω_e^2. Only for four subcases out of a total of 800, the iteration procedure assisted in improving the final value of the *best-ozone-estimate* (i.e., $\left|\Omega_e^6 - \Omega_{in}\right| < \left|\Omega_e^1 - \Omega_{in}\right|$ for a given R, θ_0, Ω_{in} combination) by 0.002 atm-cm, at the most.

Similar analysis of the results of iteration for the atmospheric models with 400 mb surface pressure, yielded somewhat more encouraging information than the one reported in the preceding paragraph for the 1,000 mb models. Out of a total of 800 subcases, it was not possible to

evaluate even Ω_e^1 for 251 subcases. For 419 subcases, values of Ω_e^n were found to remain unchanged with an increase in the order of iteration, n. For 18 subcases with $\Omega_{in} = 0.650$ atm-cm, we could evaluate Ω_e^1, but not Ω_e^2. An oscillatory character of Ω_e^n vs. n was observed in seven cases; e.g., for the subcase defined by $\Omega_{in} = 0.400$ atm-cm, R = 0.2, and $\theta_0 = 75.6°$, the quantity Ω_e^n was found to change from 0.400, to 0.421, to 0.398, to 0.421, to 0.398, and back to 0.421 atm-cm as the superscript n is increased, by one, from 1 through 6, respectively. For 63 subcases, the final value of the *best ozone estimate* showed some small improvement, i.e., $\left|\Omega_e^6 - \Omega_{in}\right| - \left|\Omega_e^1 - \Omega_{in}\right| \leq 0.002$ atm-cm. A small deterioration in the value of Ω_e^n with an increase in the order of iteration was noticed in 28 subcases. The remaining 14 subcases were found to exhibit either a very significant deterioration (five cases), or a very significant improvement (nine cases). As for example, we found $\Omega_e^1 = 0.614$ atm-cm, $\Omega_e^2 = 0.591$ atm-cm, $\Omega_e^3 = 0.592$ atm-cm, $\Omega_e^4 = 0.592$ atm-cm, $\Omega_e^5 = 0.592$ atm-cm, and $\Omega_e^6 = 0.592$ atm-cm for the subcase defined by $\Omega_{in} = 0.600$ atm-cm, R = 0.3, and $\theta_0 = 60°$.

From the results presented in the preceding two paragraphs, we conclude that the use of an iterative procedure to obtain an improved value of the *best ozone estimate* by plugging in the current value of the *best ozone estimate* to get a new value of the *improved effective albedo*, is ineffective in most cases. For a few cases for which some effect is noticeable, the converged value may or may not represent a real improvement.

5.6 *Recommendations:* An oral presentation of some of the results discussed in §5.1 to §5.3 was given by the author to Dr. C. L. Mateer on September 20 - 21, 1976 at the Atmospheric Environment Service, Toronto, Canada, and to a group of scientists (Drs. A. J. Fleig, R. S. Fraser, and others) on September 22 - 24, 1976 at NASA/GSFC, Greenbelt, Maryland. A set of tentative recommendations was made by the author at these meetings, and discussed extensively. Results of further investigations based on these discussions are given in §5.4 and §5.5. A final set of recommendations which can assist in increasing the reliability and confidence level of total ozone values derived from the BUV measurements, is given below. Some of these recommendations include suggestions by various participants at these two meetings, and are not strictly confined to the primary purpose of this contract.

Recommendation I: In §4.1, we presented results to show that the N_c vs. Ω_{in} curve for the first wavelength pair (0.3312 - 0.3125 μm), and for $\theta_0 > 79.6°$ has a maximum which is shifted to lower values of Ω_{in} with an increase in θ_0. In §5.1, we presented several examples pointing out the large errors which can be introduced in the *best ozone estimate* (Ω_e) value (in some cases), due to an inadvertent use of the N_c vs. Ω_{in} curves with a maximum. As mentioned earlier (¶4 of §5.1), Dr. Mateer pointed out that the NASA/GSFC total-ozone procedure does contain an additional step which can be expected to perform the function of avoiding the use of such N_c vs. Ω_{in} curves. However, use of an explicit criterion discarding the use of the first pair during analysis of

observations for all values of θ_0 greater than a prespecified upper limit, seems very appropriate and it will avoid misunderstanding and duplication of effort on the part of future investigators. The specification of this upper limit would depend upon the $R^Z_{0.3312,P_0}$, $R^Z_{0.3125,P_0}$ (Z = C or I) combinations which can be encountered, and on the range of Ω_{in} for a given set of basic tables. From the results presented in §5.1, we can set this upper limit around 80°.

Recommendation II: The process of digitization of the signal representing a given $I_m(\lambda, \theta_0)$ measurement is known to introduce some error. This information should be used to determine the R.M.S. error in a given measurement of the quantity N_m [see Eq. (5)]. If the error of measurement in N_m is ΔN_m units, and if the quantity $\Omega^Z_{x,y}$ is to be determined within $\Delta\Omega$ atm-cm, we recommend discarding of a value of $\Omega^Z_{x,y}$ when the corresponding slope of the N_c vs. Ω_{in} curve in the region of interest [the quantity $S^Z_{x,y}$ given by Eq. (6)] is less than $\Delta N_m/\Delta\Omega$ units per atm-cm.

Recommendation III: This recommendation is for the inclusion of the criterion for discarding a value of $\Omega^I_{x,y}$ when the corresponding $\left|\Omega^I_{x,y} - \Omega^C_{x,y}\right|$ is greater than, or equal to, some preset limit. This limit was set, somewhat arbitrarily, at 0.030 atm-cm for our investigations reported under the heading of the SITC3 procedure (see ¶5 of §5.1). Some advantages of using this criterion are brought during the discussion of numerical results presented in Tables V through X. It is desirable to modify this criterion to $\left[\left|\Omega^I_{x,y} - \Omega^C_{x,y}\right|/\Omega^I_{x,y}\right]$ being greater

than or equal to a preset limit. Several tests with different values for the limit for this ratio are in order.

Recommendation IV: This recommendation is related to the relaxation of the unnecessarily strict criterion for accepting a value of Ω_e when the *effective albedo* ($\bar{R}$) falls outside the range 0.2 - 0.8. Further information on this aspect can be obtained in the sixth paragraph of §5.1. It is further recommended that if $\bar{R} \leq 0.2$ and if values of $\Omega^I_{1,1000}$ and $\Omega^I_{2,1000}$ are available, the value of $\Omega^I_{1,1000}$ should be accepted as Ω_e only if $S^I_{1,1000} > S^I_{2,1000}$ for this particular condition. A similar check must also be inserted for the selection between $\Omega^I_{1,400}$ and $\Omega^I_{2,400}$ as a final value for Ω_e when $\bar{R} \geq 0.8$.

Recommendation V: In §5.1, we have shown that the analysis of simulated BUV measurements in the total absence of any information about the surface pressure at the time and place of observation, leads to a very significant over-estimation of the total ozone amount if the sun is near the local zenith or local horizon, and if the associated values of the surface pressure and the ground reflectivity are also near the upper or the lower ends of their respective ranges. (Some of these cases of over-estimation can be objectively declared as "unable to determine the *best ozone estimate*" by following the third recommendation.) Further errors in the evaluation of $\bar{R}$ and hence of Ω_e are introduced due to errors in the determination of the value of θ_0 at the place and time of observation (§5.2) when the sun is near the local horizon. We therefore recommend that extra precautions be exercised before accepting the values of Ω_e for values of $\theta_0 > 85°$. It should be further pointed out that

the second wavelength pair (viz, 0.3398 - 0.3175 μm combination) also loses its sensitivity to changes in Ω_{in} for large values of Ω_{in} and θ_0. Under such circumstances, we recommend that the possibility of using the third wavelength pair (viz, 0.3398 - 0.3312 μm; see Fig. 5) be also looked into. For the future satellite experiments aimed at measuring total ozone at middle and high latitudes with the sun near the local horizon, we suggest an additional measurement of intensity in a narrow spectral interval between 0.3175 μm and 0.3312 μm.

Recommendation VI: In the preceding paragraph, we listed several conditions under which the total ozone in an atmospheric column can be overestimated due to a lack of any information about the surface (or cloud top) pressure at the place and time of observation. The degree of this overestimation can be reduced by a very significant amount by following the step outlined in §5.4 provided the surface pressure lies in between the two values of P_0 for which basic tables of the total-ozone estimation procedure are available. (If necessary, basic tables for additional values of the parameter P_0 can be prepared without much difficulty.) In principle, it is possible to obtain some indication of the surface pressure for each set of the BUV measurements from the analysis of the infrared measurements taken by another spectrometer on the NIMBUS-IV satellite. We therefore recommend an extensive effort to obtain such information about the surface pressure, and appropriate modifications in the total-ozone estimation procedure for taking advantage of this additional piece of information. It should be pointed out that we

do not require a very accurate measurement of the surface (or cloud top) pressure at the place and time of observation; an error of ± 50 mb, or even ± 100 mb, is acceptable.

Recommendation VII: Another problem area is the lack of any information on the spectral dependence of reflectivity of the underlying surface in the 0.3100 - 0.3400 μm region. The type of the errors that can be introduced in a value of the *best ozone estimate* (Ω_e) due to a lack of our knowledge on R_λ vs. λ, is brought out in §5.3 by carrying out a complete analysis for eight different simulated variations of the Lambert reflectivity with wavelength. An extensive project to obtain R_λ vs. λ characteristics of various types of natural surfaces using aircraft measurements, satellite measurements, laboratory measurements, and numerical simulation is in order.

Very recently, Dr. Fraser provided the author with a copy of the rough draft of a manuscript entitled, "The Apparent Spectral Ultraviolet Reflectances of Various Natural Surfaces" by P. M. Furukawa and D. F. Heath. The observations for this apparent spectral reflectance investigation were taken with single monochromators mounted on NASA's CV-990 aircraft. We find from this report that the apparent spectral reflectivity of a cloud layer is only slightly dependent on wavelength in the spectral region 0.3312 - 0.3800 μm, but decreases very rapidly as the wavelength is decreased from 0.3312 μm to 0.3100 μm. This sharp discontinuity in the apparent reflectance vs. λ curve for a cloud layer is attributed by the authors, to some absorption by liquid water in that

part of the spectrum. Further information on this aspect is very essential. In the absence of such information, it is desirable to extend the total-ozone estimation procedure for simulated (and then actual) measurements in the following manner:

Let us assume that a value of Ω_e is obtained from the value of $\Omega^I_{2,1000}$ and $\Omega^I_{2,400}$ by using the SITC4 (or its equivalent) procedure. For this purpose, we have made use of measurements of $I_m(\lambda, \theta_0)$ at λ = 0.3175, 0.3398, and 0.3800 μm. This value of Ω_e can then be used to obtain values of the *second improved effective albedo* represented by $R^{I2}_{\lambda,y}$ from those of $I_m(\lambda, \theta_0)$ at λ = 0.3125, 0.3312, and 0.3398 μm. A value of $R^{I2}_{0.3175,y}$ can then be obtained after a linear interpolation. Values of $R^{I2}_{0.3175,y}$ and $R^{I2}_{0.3398,y}$ can then be used to obtain values of $\Omega^{I2}_{2,y}$, and finally, a new value of Ω_e. If the original Ω_e is obtained from measurements at the first wavelength pair, the procedure would require an extrapolation for obtaining $R^{I2}_{0.3125,y}$ from the values of $R^{I2}_{0.3175,y}$ and $R^{I2}_{0.3398,y}$.

The extension of the SITC4 procedure in a manner outlined in the preceding paragraph must be tested extensively with simulated observations. Its adoption to the analysis of the actual observations should await results of this extensive testing.

Recommendation VIII: It is recommended that selected BUV data for which approximate coincidences of the *ground-truth* measurements of total ozone using the Dobson Spectrometer (only the so-called "direct sun measurements using A-D pairs") are available, be thoroughly analyzed after

including as many of the above-mentioned recommendations as possible. Effect of each of these recommendations can then be tested on actual data. Such a study is bound to assist considerably in increasing the reliability and confidence level of the BUV, total-ozone data provided the sample is sufficiently large and representative. It can also draw our attention to other problem areas. To this effect, it is desirable to see if any significant differences between the *ground-truth* and the BUV ozone values are related to changes in the underlying terrain due to the motion of the satellite. For this purpose, we can make use of a spread amongst four values of $R^{C}_{0.3800,y}$ obtained from each of the four measurements of $I_m(0.3800, \theta_0)$ taken through the duration of a given set of observations [i.e., during measurements of $I_m(\lambda, \theta_0)$ at λ = 0.3125, 0.3175, 0.3312, and 0.3398 μm which are taken at an interval of about 2 seconds].

VI. SIMULATION FOR THE SBUV/TOMS CONFIGURATION

6.1 *Procedure used for Analysis of the SBUV/TOMS Measurements:* The main difference between the section of the BUV experiment on the NIMBUS-IV satellite, and of the SBUV/TOMS experiment on the NIMBUS-G satellite aimed at the estimation of total ozone in an atmospheric column, is in the number of wavelengths for which measurements are available for this purpose. For the BUV configuration, measurements are available at the wavelength (λ) given by λ = 0.3125, 0.3175, 0.3312, 0.3398, and 0.3800 μm. For the other configuration, it is planned to have an additional

measurement at 0.3600 μm. There are some other important differences (e.g., observations along the off-nadir directions), but our study does not cover them.

This additional measurement is made in the spectral region with a very small absorption by ozone (Table IV), and hence it can be used for evaluation of $R^{C}_{0.3600,y}$ by making use of the Eq. (2). In this section, we will outline the procedure used by us for the analysis of the simulated SBUV/TOMS measurements along the local nadir, for the estimation of the quantities Ω_e *(best ozone estimate)*, and $\bar{R}_\lambda$ *(effective albedo)*. This procedure to be referred to as the SITD1 procedure, is essentially a modification of the SITC4 procedure discussed in the sixth paragraph of §5.1. In turn, this SITC4 procedure was obtained after inserting three important modifications in the SITC1 procedure outlined in §2.4. We will therefore ask the reader to refer to the discussion of §2.4 whenever appropriate.

Step I: Use the measured values of $I_m(\lambda, \theta_0)$ at $\lambda = 0.3600$ and 0.3800 μm for evaluating the *coarse effective albedoes* $R^{C}_{0.3600,1000}$ and $R^{C}_{0.3800,1000}$, respectively by making use of the 1,000 mb tables for the appropriate θ_0. The tables for $\Omega_{in} = 0.400$ atm-cm are arbitrarily chosen for the evaluation of the quantity $R^{C}_{0.3600,1000}$ as no information on the total ozone amount is available at this point. The rationale behind the use of the 1,000 mb tables and for referring the quantities computed with the help of Eq. (2) as the *coarse effective albedoes* can be found in the discussion under the heading "Step I" in §2.4.

Step II: Obtain values of $R^{C}_{\lambda,1000}$ at $\lambda = 0.3125$, 0.3175, 0.3312, and 0.3398 μm after a linear extrapolation of the $R^{C}_{\lambda,1000}$ vs. λ curve obtained from values of $R^{C}_{0.3800,1000}$ and $R^{C}_{0.3600,1000}$.

Step III: Follow Step III of §2.4 to obtain values of $\Omega^{C}_{x,1000}$ and $S^{C}_{x,1000}$ for $x = 1$ only if $\theta_0 \leq 79.6°$, and for $x = 2$ for all values of θ_0.

Step IV: This Step is exactly identical to Step IV in §2.4.

Step V: Follow Step V of §2.4 for obtaining values of the *improved effective albedo* ($R^{I}_{\lambda,1000}$) at $\lambda = 0.3398$, and 0.3600 μm. Then, obtain values of $R^{I}_{\lambda,1000}$ at $\lambda = 0.3125$, 0.3175, and 0.3312 μm using a quadratic extrapolation based on the values of $R^{I}_{\lambda,1000}$ at $\lambda = 0.3398$, 0.3600, and 0.3800 μm. (Note that $R^{I}_{0.3800,1000} = R^{C}_{0.3800,1000}$).

Step VI: Repeat Step III above using values of $R^{I}_{\lambda,1000}$ instead of those for $R^{C}_{\lambda,1000}$. We will then have values of the quantities $\Omega^{I}_{x,1000}$ and $S^{I}_{x,1000}$ for $x = 1$, and 2.

Step VII: Repeat Steps I through VI above by using the 400 mb tables instead of the 1,000 mb tables. We will then have values of $R^{C}_{\lambda,400}$ and $R^{I}_{\lambda,400}$ at all six wavelengths, and of the quantities $\Omega^{C}_{x,400}$ and $S^{C}_{x,400}$, as well as $\Omega^{I}_{x,400}$ and $S^{I}_{x,400}$ for $x = 1$, and 2.

Step VIII: Determine values of the *effective albedo* $\bar{R}_{\lambda}$ by making use of the following equation:

$$\bar{R}_{\lambda} = 0.5 \left[R^{I}_{\lambda,1000} + R^{I}_{\lambda,400} \right] . \qquad (12)$$

Step IX: Set $\Omega^I_{x,y}$ to zero if $\left|\Omega^I_{x,y} - \Omega^C_{x,y}\right| \geq 0.030$ atm-cm for a given x,y combination. A zero value of $\Omega^I_{x,y}$ implies that that particular value of $\Omega^I_{x,y}$ is unavailable. At that time, the corresponding value of the slope ($S^I_{x,y}$) is set to - 100.

Step X: This final step is for obtaining a value for the quantity Ω_e, the *best ozone estimate*, from the computed values of $\Omega^I_{x,y}$ for x = 1, and 2, and for y = 1,000, and 400 mb. The following paths are taken depending upon the number of $\Omega^I_{x,y}$'s carrying values greater than zero:

(i) All four values of $\Omega^I_{x,y}$ are available. Select the first wavelength pair only if $S^I_{1,1000} > S^I_{2,1000}$ and $S^I_{1,400} > S^I_{2,400}$. If not, select the second wavelength pair.

(ii) If only $\Omega^I_{1,1000}$ and $\Omega^I_{1,400}$ are available, then select the first wavelength pair.

(iii) If only $\Omega^I_{2,1000}$ and $\Omega^I_{2,400}$ are available, then select the second wavelength pair.

(iv) If the conditions listed under (i), (ii), or (iii) above are not satisfied, proceed as follows after assigning a zero value to Ω_e:

For $\bar{R}_{0.3398} \leq 0.2$,

$$\Omega_e = \text{Greater of } \left[\Omega^I_{1,1000}, \Omega^I_{2,1000}\right]. \qquad (13)$$

For $\bar{R}_{0.3398} \geq 0.8$,

$$\Omega_e = \text{Greater of } \left[\Omega^I_{1,400},\ \Omega^I_{2,400}\right] . \tag{14}$$

The zero value assigned to Ω_e remains unchanged for $0.2 < \bar{R}_{0.3398} < 0.8$.

(v) If one of the conditions listed under (i), (ii), or (iii) above is satisfied, determine the mean *effective albedo* $\bar{R}_{\lambda_i,\lambda_j}$ for the wavelength pair selected as follows:

$$\bar{R}_{\lambda_i,\lambda_j} = 0.5 \left[\bar{R}_{\lambda_i} + \bar{R}_{\lambda_j}\right] . \tag{15}$$

$\lambda_i = 0.3312$ μm, and $\lambda_j = 0.3125$ μm if the first wavelength is selected; and $\lambda_i = 0.3398$ μm and $\lambda_j = 0.3175$ μm if the second wavelength pair is selected. Then, obtain a value for Ω_e as follows:

$$\Omega_e = \Omega^I_{x,1000} \qquad \text{for } \bar{R}_{\lambda_i,\lambda_j} \le 0.2 , \tag{16}$$

$$\Omega_e = \Omega^I_{x,400} \qquad \text{for } \bar{R}_{\lambda_i,\lambda_j} \ge 0.8 , \tag{17}$$

and for $0.2 < \bar{R}_{\lambda_i,\lambda_j} < 0.8$,

$$\Omega_e = \frac{0.8 - \bar{R}_{\lambda_i,\lambda_j}}{0.6}\,\Omega^I_{x,1000} + \frac{\bar{R}_{\lambda_i,\lambda_j} - 0.2}{0.6}\,\Omega^I_{x,400} . \tag{18}$$

6.2 *Effective Albedo:* From the outline of the procedure used for the estimation of total ozone with the SBUV/TOMS configuration given in the preceding section, we find that any real- or pseudo-dependence of the *effective albedo* on wavelength will be brought forward by this analysis.

In §5.2, we presented results to show that the BUV total-ozone estimation procedure can introduce an artificial dependence of $\bar{R}$ on θ_0 and Ω_{in}, and that values of $\bar{R}$ so computed can fall outside the normal range (0.0 - 1.0). In this section, we will present several typical examples to show that a pseudo dependence of $\bar{R}_\lambda$ vs. λ can be exhibited in the results of analysis made with the total-ozone estimation procedure of §6.1, even when the simulated measurements are for an atmospheric model resting on a Lambert surface whose reflectivity R is assumed to be independent of wavelength.

Let us consider the atmospheric model No. 2 (see Table III) resting on a Lambert surface with a spectrally independent reflectivity (R) of 0.1. This model has a surface pressure (P_0) of 1,000 mb, and a total ozone content (Ω_{in}) of 0.200 atm-cm. We will further restrict our discussion to the case when the sun is at 70° from the local zenith, i.e., $\theta_0 = 70°$. For this particular subcase, we find that the values of the quantity $R^C_{\lambda,1000}$ for λ = 0.3125, 0.3175, 0.3312, 0.3398, 0.3600, and 0.3800 μm to be given by 0.102, 0.102, 0.102, 0.101, 0.101, and 0.100, respectively. A weak spectral dependence of the coarse albedo on λ in this particular case is due to the use of tables for 0.400 atm-cm total ozone (Step I of §6.1). This weak spectral dependence of the coarse albedo on λ is not reflected in the values of the *improved effective albedos* which are calculated using the value of $\Omega^C_{x,1000}$. We find that $R^I_{\lambda,1000} = 0.100$ for six values of λ mentioned above. On the other hand, use of the 400 mb tables leads to the following sets of values for

$R^C_{\lambda,400}$, and $R^I_{\lambda,400}$: $R^C_{\lambda,400}$ = 0.334, 0.326, 0.306, 0.293, 0.263, 0.233 and $R^I_{\lambda,400}$ = 0.356, 0.345, 0.315, 0.298, 0.263, and 0.233 for λ = 0.3125, 0.3175, 0.3312, 0.3398, 0.3600, and 0.3800 μm, respectively. This pseudo spectral dependence of $\bar{R}^I_{\lambda,400}$ on λ is due to the use of tables for a surface pressure different from that of the model under investigation. From the results presented above, we see that the *effective albedo* given by Eq. (12) will also exhibit an artificial spectral dependence in this particular case. (For the six values of λ in the increasing order of λ, $\bar{R}_\lambda$ = 0.228, 0.222, 0.208, 0.199, 0.181, and 0.167, respectively.)

For the atmospheric model No. 2 resting on a Lambert surface with a spectrally independent R of 0.8 and illuminated by the sun at 70° from the local zenith, the above-mentioned pseudo-spectral dependence of $\bar{R}_\lambda$ on λ is somewhat smaller in magnitude than the R = 0.1 subcase discussed in the preceding paragraph. For this latter case, values of $\bar{R}_\lambda$ at λ = 0.3125, 0.3175, 0.3312, 0.3398, 0.3600, and 0.3800 μm are given by 0.798, 0.797, 0.795, 0.793, 0.791, and 0.789, respectively.

We will next consider the atmospheric model No. 13 with a spectrally independent value of R of 0.1, and θ_0 = 70°. This model has a surface pressure of 400 mb, but a total ozone content (Ω_{in}) of 0.200 atm-cm when the ozone contents of the deleted layers are accounted for (Table III). The values of $\bar{R}_\lambda$ for this particular subcase which is similar to the subcase discussed in the pen-ultimate paragraph except for the difference in the surface pressure, are found to increase with an increase in λ. $\bar{R}_\lambda$ = - 0.195, - 0.173, - 0.121, - 0.092, - 0.038, and

-0.002 for $\lambda = 0.3125$, 0.3175, 0.3312, 0.3398, 0.3600, and 0.3800 μm, respectively.

6.3 *Results for the R-Independent-of-λ Cases:* In this section, we propose to compare values of the *best ozone estimate* (Ω_e) as obtained from the SITC4 procedure described in §5.1 (analysis of the simulated BUV measurements at five wavelengths), and from the SITD1 procedure described in §6.1 (analysis of the simulated SBUV/TOMS measurements at six wavelengths). This comparison will be carried out for the atmospheric models No. 2 through 11, and 13 through 22 (Table III) resting on a Lambert surface whose reflectivity R_λ is assumed to be independent of wavelength. As mentioned earlier, the quantity Ω_e was evaluated for 10 different directions of illumination of an atmospheric model from above, and for 8 different values of the Lambert reflectivity of the surface underneath the model.

Values of the *deviation* [$\Delta = 1{,}000 \times (\Omega_e - \Omega_{in})$] for the atmospheric models No. 6 and 17 with an average amount of total ozone ($\Omega_{in} = 0.400$ atm-cm) are given in Table XX and XXI, respectively, for 10 different values of the parameter θ_0, and 8 different values of the reflectivity (R_λ independent of λ). Values of Δ as obtained with the different procedures (viz, SITC4 and SITD1) are given in adjacent columns.

For the atmospheric model with 1,000 mb surface pressure (Table XX), values of the *deviation* Δ as obtained with the SITC4 and SITD1 are practically the same for low (viz, R = 0.0, and 0.1), and high (viz,

Table XX. Values of the *deviation* [$\Delta = 1{,}000 \times (\Omega_e - \Omega_{in})$] for the atmospheric model No. 6 as obtained using the SITC4 and SITD1 procedures. Ω_{in} = 0.400 atm-cm; P_0 = 1,000 mb.

Ground Reflectivity: R_λ (= R) independent of λ.

θ_0	R = 0.0		R = 0.1		R = 0.2		R = 0.3	
	SITC4	SITD1	SITC4	SITD1	SITC4	SITD1	SITC4	SITD1
0.0	0	0	0	0	0	2	1	4
45.0	0	0	0	0	0	2	1	4
60.0	0	0	0	0	0	2	1	4
70.0	0	0	0	0	0	2	1	3
75.6	0	0	0	0	-1	1	0	3
79.6	0	0	0	0	0	1	0	3
82.5	0	0	0	0	0	1	1	2
84.7	0	0	0	0	0	1	1	3
86.7	0	0	0	0	0	2	0	4
90.0	0	0	-	0	-	4	-	8

θ_0	R = 0.4		R = 0.6		R = 0.8		R = 1.0	
	SITC4	SITD1	SITC4	SITD1	SITC4	SITD1	SITC4	SITD1
0.0	4	8	15	17	28	28	33	33
45.0	4	7	13	15	26	26	30	30
60.0	3	7	11	13	21	22	26	26
70.0	3	5	9	11	17	18	20	21
75.6	1	5	6	9	14	15	16	17
79.6	1	4	5	8	10	13	12	15
82.5	2	4	5	8	10	12	11	14
84.7	2	4	6	8	12	14	13	16
86.7	2	6	8	12	15	19	18	22
90.0	-	13	8	23	21	34	24	36

Table XXI. Values of the *deviation* $[\Delta = 1{,}000 \times (\Omega_e - \Omega_{in})]$ for the atmospheric model No. 17 as obtained using the SITC4 and SITD1 procedures. Ω_{in} = 0.400 atm-cm; P_0 = 400 mb.

Ground Reflectivity: R_λ (= R) independent of λ.

θ_0	R = 0.0		R = 0.1		R = 0.2		R = 0.3	
	SITC4	SITD1	SITC4	SITD1	SITC4	SITD1	SITC4	SITD1
0.0	-	38	-	12	19	-1	4	-8
45.0	-	31	-	11	16	-1	4	-7
60.0	-	23	-	9	12	0	3	-6
70.0	-	12	-	4	6	-1	0	-5
75.6	-	11	-	3	0	-2	-2	-5
79.6	-	3	-	-1	13	-3	6	-4
82.5	-	1	-	-2	10	-3	3	-4
84.7	-	1	-	-1	11	-3	4	-4
86.7	-	4	-	-1	-	-4	10	-6
90.0	-	-	-	-3	-	-11	-	-16

θ_0	R = 0.4		R = 0.6		R = 0.8		R = 1.0	
	SITC4	SITD1	SITC4	SITD1	SITC4	SITD1	SITC4	SITD1
0.0	-4	-10	-7	-8	0	0	0	0
45.0	-3	-9	-6	-7	0	0	0	0
60.0	-3	-8	-5	-6	0	0	0	0
70.0	-3	-6	-4	-4	0	0	0	0
75.6	-3	-5	-3	-3	0	0	0	0
79.6	0	-5	-2	-3	0	0	0	0
82.5	-1	-4	-2	-3	0	0	0	0
84.7	-1	-4	-2	-3	0	0	0	0
86.7	1	-6	-2	-4	0	0	0	0
90.0	-	-15	-3	-9	0	0	0	0

R = 0.8, and 1.0) values of the parameter R. For the intermediate values of the Lambert reflectivity of the surface underlying the model, the *deviation* for a given θ_0, R combination as obtained with the SITD1 procedure, is significantly greater than that obtained with the SITC4 procedure. It may be noted that it is possible to evaluate Ω_e for four subcases ($\theta_0 = 90°$, R = 0.1, 0.2, 0.3, and 0.4) with the SITD1 procedure, but not with SITC4. The mean values of Ω_e where the means are taken over all 8 values of R, and over all 10 values of θ_0 for which an Ω_e is available, is 0.406 atm-cm and 0.409 atm-cm for the SITC4 and SITD1 procedures, respectively. Similar analysis of results for the models with 1,000 mb surface pressure suggests that the SITD1 procedure tends to over-estimate the total ozone of an atmospheric column by a significant amount when its results are compared with those obtained with the SITC4 procedure.

For the atmospheric model with 400 mb surface pressure (Table XXI), we find that the use of the SITD1 procedure results in the recovery of meaningful values for the quantity Ω_e for several subcases which were previously declared "undeterminable" by the SITC4 procedure. For the models with low surface pressures, the SITD1 procedure has a tendency of over-estimating the total ozone amounts at low values of R, but of under-estimating them at intermediate values of R.

Mean values of the *best ozone estimate* as obtained with the SITC4 and SITD1 procedures and where a mean for a given atmospheric model is taken over all available values of Ω_e (10 values of θ_0, and 8 values

of R), are given in Table XXII for the models No. 2 through 11, and 13 through 22. Results presented in this table support our findings of the preceding two paragraphs. Mean values of Ω_e as obtained with the SITD1 procedure are significantly greater (smaller) than those obtained with the SITC4 procedure for the models with 1,000 (400) mb surface pressure. Comparison of the grand means taken over a maximum of 160 subcases (2 values of P_0 × 10 values of θ_0 × 8 values of R; results presented in columns 4 and 7 of Table XXII) suggests that, on the average, the SITD1 procedure tends to provide results of somewhat better quality than the other procedure especially if Ω_{in} is small. However, this statement should not be construed to imply any superiority of the SITD1 procedure over the SITC4 procedure. A more realistic interpretation of the results presented in Tables XX, XXI, and XXII will be as follows: Errors in the values of the *best ozone estimate* (Ω_e) as obtained with the SITC4 and SITD1 procedures, are of the same magnitude for all practical purposes. The distribution of this error amongst values of Ω_e for various subcases of a given model, depends significantly on the procedure used.

6.4 *Results for the Cases with R dependent upon* λ: In §5.3, we presented results for the analysis of the simulated BUV measurements for the atmospheric models resting on a Lambert surface whose reflectivity (R_λ) is varied with wavelength. These results were presented for three distinct types of simulated reflection characteristics. The first (second) type of characteristics represents surfaces whose Lambert

Table XXII. Mean values (mean over a maximum of 80 subcases; 10 values of θ_0, and 8 values of R) of the *best ozone estimate* for atmospheric models with a given surface pressure (P_0 in mb), and a given amount of ozone (Ω_{in} in atm-cm).

Ω_{in} atm-cm	Mean Ω_e (atm-cm)					
	PROCEDURE USED: SITC4			PROCEDURE USED: SITD1		
	P_0 = 1000 mb	P_0 = 400 mb	mean of cols. 2 and 3	P_0 = 1000 mb	P_0 = 400 mb	mean of cols. 5 and 6
0.200	0.203	0.207	0.205	0.204	0.202	0.203
0.250	0.254	0.256	0.255	0.256	0.252	0.254
0.300	0.305	0.304	0.305	0.307	0.301	0.304
0.350	0.356	0.352	0.354	0.358	0.350	0.354
0.400	0.406	0.401	0.404	0.409	0.399	0.403
0.450	0.458	0.450	0.454	0.460	0.448	0.454
0.500	0.509	0.499	0.504	0.512	0.496	0.504
0.550	0.560	0.548	0.554	0.563	0.545	0.554
0.600	0.611	0.598	0.604	0.613	0.593	0.603
0.650	0.650	0.646	0.648	-	0.640	-

reflectivity increases (decreases) with an increase of wavelength, and is represented by the curves A, B, and C (D, E, and F) of Fig. 8. The third type of characteristics represents surfaces whose R_λ vs. λ curve has either a maximum (curve G), or a minimum (curve H) in the middle of the spectral region of interest, viz, 0.3100 - 0.3800 μm. These results were obtained using two different procedures named SITC6 and SITC8. We concluded that, on the average, results obtained with the SITC8 procedure are of somewhat better quality than those obtained with the SITC6 procedure.

In order to investigate the effect of the spectrally-dependent Lambert reflectivity on the *best ozone estimate* value (Ω_e) obtained with the SITD1 procedure specially developed for the analysis of the simulated SBUV/TOMS observations (§6.1), the program of the SITD1 procedure was modified to handle cases for which the Lambert reflectivity of the surface underlying the atmospheric model can be an arbitrary function of wavelength. This modified version of SITD1 will be called SITD2. Atmospheric models No. 2 through 11, and 13 through 22 (Table III) were again used to obtain values of Ω_e and $\bar{R}_\lambda$ at six wavelengths for 10 different values of θ_0 listed earlier, and 8 different R_λ vs. λ curves of Fig. 8.

For brevity, we will again restrict our discussion to a mean value of Ω_e where this mean is taken over a maximum of 20 subcases for a given value of the input ozone amount (Ω_{in}), but for 10 values of θ_0, and 2 values of the surface pressure (P_0). It should be again pointed

C-22

out that the analysis of results presented in this subsection is, by no means, complete. Other additional aspects which should be looked into, are the maximum, mean, and R.M.S. deviation of Ω_e around its mean value. The deviation $[1000 \times (\Omega_e - \Omega_{in})]$ will be found to depend very significantly on various input parameters such as Ω_{in}, θ_0, P_0, and R_λ vs. λ characteristics.

From the results presented in Table XXIII for the models resting on a Lambert surface whose reflectivity increases with an increase of wavelength, it can be seen that the availability of the additional measurement at 0.3600 μm (i.e., the use of SITD2 procedure in the place of SITC8) results in a very significant increase in the number of subcases for which a value of Ω_e can be evaluated. Mean values of Ω_e obtained with the SITD2 procedure are nearer to the corresponding values of Ω_{in} when compared to those obtained with the SITC8 procedure. This improvement is in the right direction but probably not of the expected magnitude. Since R_λ is a linear function of λ and as the new estimation procedure (SITD2) simulates this trend very accurately, one would expect Ω_{in} and the corresponding mean Ω_e for the SITD2 procedure to be exactly equal. We found that the absolute difference between the individual values of Ω_e and Ω_{in} not to exceed 0.003 atm-cm for all models with P_0 = 1,000 mb, and $\theta_0 < 86.7°$. For P_0 = 1,000 mb models, the quantity $|\Omega_e - \Omega_{in}|$ exceeded 0.003 atm-cm limit only six times, and exceeded 0.005 atm-cm limit only twice. It was never observed to exceed 0.009 atm-cm value. Thus, most of the differences between the mean Ω_e of SITD2 and

Table XXIII. Number of subcases for which the *best ozone estimate* (Ω_e) could be evaluated out of a maximum of 20 subcases (10 values of θ_0, and 2 values of P_0) for a given input ozone amount (Ω_{in}), and the corresponding mean Ω_e for these subcases as obtained with the SITC8 and SITD2 procedures.

Ground Reflectivity: R_λ is assumed to increase linearly with an increase of λ (curves A, B, and C of Fig. 8).

Number of subcases for which Ω_e could be evaluated.

Ω_{in} atm-cm	Ref. Curve A		Ref. Curve B		Ref. Curve C	
	SITC8	SITD2	SITC8	SITD2	SITC8	SITD2
0.200	17	20	17	20	15	19
0.250	17	20	15	20	13	20
0.300	15	20	12	20	8	20
0.350	10	20	9	20	8	20
0.400	9	20	8	20	5	20
0.450	9	20	8	20	0	20
0.500	8	19	7	19	0	19
0.550	7	18	6	18	0	18
0.600	7	16	5	16	0	16

Corresponding value of mean Ω_e in atm-cm.

0.200	0.211	0.204	0.214	0.205	0.221	0.208
0.250	0.262	0.255	0.264	0.256	0.272	0.260
0.300	0.312	0.304	0.311	0.305	0.315	0.309
0.350	0.362	0.353	0.357	0.354	0.367	0.358
0.400	0.405	0.402	0.408	0.405	0.417	0.409
0.450	0.455	0.452	0.458	0.454	-	0.459
0.500	0.505	0.501	0.509	0.503	-	0.508
0.550	0.555	0.550	0.559	0.552	-	0.557
0.600	0.606	0.600	0.608	0.602	-	0.606

corresponding Ω_{in} in Table XXIII are due to significant differences between the individual values of Ω_e and Ω_{in} for the models with 400 mb surface pressure. The reason for the over-estimation of Ω_e for the 400 mb models is that the corresponding $\bar{R}_\lambda$ values are very small (< 0.2), and hence the estimation procedure favors the value of $\Omega^I_{x,1000}$ over that of $\Omega^I_{x,400}$. It should be added that a subcase which is discarded by the SITC8 procedure but is accepted by the SITD2 procedure, generally carries a large value for the difference, $\Omega_e - \Omega_{in}$. As for example, for the model No. 13 resting on a Lambert surface having the reflectivity curve C of Fig. 8, and illuminated by the sun at local zenith, $\Omega_e - \Omega_{in} = 0.037$ atm-cm.

Results presented in Table XXIV for the models resting on a Lambert surface whose reflectivity decreases with an increase of the wavelength, also show a very significant increase in the number of cases for which Ω_e could be evaluated with the SITD2 procedure. The differences between the mean Ω_e and the corresponding value of Ω_{in} are very small for this second type of surfaces compared to those for the first type of surfaces. For the atmospheric models resting on Lambert surfaces with their spectral reflectivity decreasing with an increase of wavelength, we found the total ozone content of the column to be over-estimated for the models with 1,000 mb surface pressure, and to be under-estimated for those with 400 mb surface pressure. The magnitude of the over-estimation and under-estimation are practically equal for a given Ω_{in}, especially for the models resting on a surface with its R_λ vs. λ variation represented by the curve F of Fig. 8

Table XXIV. Number of subcases for which the *best ozone estimate* (Ω_e) could be evaluated out of a maximum of 20 subcases (10 values of θ_0, and 2 values of P_0) for a given input ozone amount (Ω_{in}), and the corresponding mean Ω_e for these subcases as obtained with the SITC8 and SITD2 procedures.

Ground Reflectivity: R_λ is assumed to decrease linearly with an increase of λ (curves D, E, and F of Fig. 8).

Number of subcases for which Ω_e could be evaluated.

Ω_{in} atm-cm	Ref. Curve D		Ref. Curve E		Ref. Curve F	
	SITC8	SITD2	SITC8	SITD2	SITC8	SITD2
0.200	20	20	20	20	18	20
0.250	20	20	20	20	18	20
0.300	20	20	18	20	17	20
0.350	19	20	18	20	13	20
0.400	18	20	16	20	4	20
0.450	18	20	14	20	0	20
0.500	16	20	12	20	0	20
0.550	14	20	12	20	0	20
0.600	13	19	10	19	0	19

Corresponding value of mean Ω_e in atm-cm.

0.200	0.196	0.201	0.192	0.201	0.180	0.200
0.250	0.247	0.252	0.243	0.252	0.231	0.251
0.300	0.297	0.302	0.293	0.302	0.278	0.300
0.350	0.347	0.353	0.343	0.352	0.324	0.350
0.400	0.397	0.403	0.392	0.403	0.381	0.401
0.450	0.446	0.454	0.442	0.453	-	0.451
0.500	0.497	0.504	0.491	0.503	-	0.501
0.550	0.547	0.555	0.541	0.554	-	0.550
0.600	0.597	0.604	0.591	0.603	-	0.600

When the R_λ vs. λ curves of the Lambert surface underlying an atmospheric model exhibit a strong maximum or a minimum in the middle of the spectral region of interest, use of the SITD2 procedure results in a significant increase (decrease) in the number of subcases for which Ω_e could be evaluated provided Ω_{in} is large (small). However, an increase in the number of subcases for which the Ω_e is recovered is also generally associated with a very significant under-estimation of mean Ω_e for models with surface having its R_λ vs. λ variation represented by the curve H of Fig. 8. As for example, for Ω_{in} = 0.500 atm-cm, the value of the mean Ω_e = 0.424 atm-cm. This under-estimation was generally found to be very large at large values of θ_0. As for example, for the atmospheric model No. 18 resting on a Lambert surface with the curve H type reflectivity, we found the *deviation* (Δ) to be - 58, - 44, - 28, - 63, - 53, - 50, - 54, - 70, and - 131 units for the values of θ_0 given by θ_0 = 45°, 60°, 70°, 75.6°, 79.6°, 82.5°, 84.7°, 86.7°, and 90°, respectively. Thus, we may conclude that the use of SITD2 procedure leads to better values of Ω_e compared to those obtained with SITC8 procedure provided the spectral reflectivity of the surface underlying the atmosphere increases or decreases linearly with the wavelength. For surfaces with other types of characteristics, results are of mixed quality, indeed.

6.5 *Recommendations:* A procedure for the estimation of total ozone in an atmospheric column using measurements at six wavelengths (SBUV/TOMS configuration) was outlined in §6.1. This procedure referred to as the

Table XXV. Number of subcases for which the *best ozone estimate* (Ω_e) could be evaluated out of a maximum of 20 subcases (10 values of θ_0, and 2 values of P_0) for a given input ozone amount (Ω_{in}), and the corresponding mean Ω_e for these subcases as obtained with the SITC8 and SITD2 procedures.

Ground Reflectivity: Variations of R_λ vs. λ used for these results are as shown by the curves G and H of Fig. 8.

Number of subcases for which Ω_e could be evaluated.

Ω_{in} atm-cm	Ref. Curve G		Ref. Curve H	
	SITC8	SITD2	SITC8	SITD2
0.200	15	4	15	8
0.250	7	4	14	9
0.300	5	3	9	9
0.350	0	5	6	10
0.400	0	5	4	9
0.450	0	6	0	10
0.500	0	7	0	8
0.550	0	9	0	11
0.600	0	5	0	8

Corresponding values of mean Ω_e in atm-cm.

0.200	0.231	0.208	0.173	0.181
0.250	0.275	0.259	0.226	0.233
0.300	0.325	0.306	0.275	0.280
0.350	-	0.358	0.329	0.328
0.400	-	0.404	0.376	0.375
0.450	-	0.450	-	0.418
0.500	-	0.519	-	0.424
0.550	-	0.576	-	0.502
0.600	-	0.613	-	0.549

SITD1 procedure (SITD2 procedure if the simulated measurements are for the atmospheric models resting on a Lambert surface with spectrally dependent reflectivity) contains recommendations I, III, and IV (§5.6) for a better analysis of the BUV measurements (i.e., the procedure SITC4 of §5.1) which are made at five wavelengths only. Besides, the additional measurement at 0.3600 μm is used in the SITD1 procedure for obtaining values of the *coarse* and *improved effective albedoes* at shorter wavelengths by extrapolation of the $R^{Z}_{\lambda,y}$ vs. λ curves on the longer wavelength region. Results obtained with the analysis of simulated measurements for the five, and six wavelength configurations, were compared in §6.2, §6.3, and §6.4. The following recommendations are based on the aforementioned analysis.

Recommendation I: The SITD1 procedure should be modified for computing values of $R^{I}_{\lambda,y}$ at λ = 0.3125, 0.3175, and 0.3312 μm using a linear extrapolation procedure in the place of the current quadraic extrapolation procedure (Step V of §6.1). Values of Ω_e obtained with such a modified procedure should be compared with the corresponding values of Ω_e obtained with the original procedure for all types of models discussed in §6.3 and §6.4. This additional test can assist in improving the poor quality of Ω_e values for the atmospheric models resting on surfaces with their R_λ vs. λ characteristics represented by curve H of Fig. 8 (see last paragraph of §6.4).

Recommendation II: For the SBUV/TOMS configurations, plans are made for obtaining the *best ozone estimate* values from the analysis of

measurements of intensity along directions making some angle with the local nadir direction. Sufficient evidence is presented in the preceding sections to demonstrate the unexpected (and probably unpredictable) nature of the errors in Ω_e due to absence of any information on the surface pressure, and on the spectral dependence of the surface reflectivity at the place and time of observation. We therefore recommend that the analysis of the type outlined in the preceding sections, should also be carried for several additional directions of observation.

Recommendation III: Appropriate versions of the Recommendations II, V, VI, and VII given in §5.6 should also be included for the analysis of actual SBUV/TOMS observations for the estimation of total ozone in an atmospheric column.

Recommendation IV: It is recommended that an extensive analysis of selected SBUV/TOMS data for which approximate coincidences of the highly reliable *ground-truth* measurements of total ozone are available, be carried out. Attempts should be made to encompass as many different situations as possible for this selected study. The analysis of the entire SBUV/TOMS data must await results of such a detailed study.

VII. CONCLUSION

The procedure for estimation of total ozone in an atmospheric column from the measurements of the ultraviolet radiation back-scattered along the local nadir direction by the earth-atmosphere system, makes

use of a quantity called N_c which is proportional to the logarithm of the ratio of intensities at two wavelengths. One of these wavelengths is located in the spectral region of moderate absorption by ozone, while the other is located in the region of weak absorption. This quantity given by Eq. (4), is a function of the wavelength pair used, of the amount of ozone in the atmospheric column, zenith angle of the sun, reflectivity of the underlying surface, and of the surface pressure at the bottom of the atmospheric column defined by the ground or the top of the cloud layer. Variations of N_c as a function of the various parameters listed above, and computed for models of the terrestrial atmosphere free of aerosols, water droplets, and snow crystals are discussed in §4.

The total-ozone estimation procedure currently being used at NASA/GSFC for the analysis of BUV measurements was modified for the analysis of simulated measurements of intensity. This modified total-ozone estimation procedure is described in §2.4. The original as well as the modified procedures attempt to estimate total ozone content of an atmospheric column (called the *best ozone estimate*) from the measurements of intensities at wavelength pairs for which tables of the quantity N_c are available, from a knowledge of the solar zenith angle at the place and time of observation, and from the knowledge of the so-called *effective albedo* based on measurements of intensities in the adjacent spectral regions with little or no absorption by ozone. No information is available about the surface pressure, and actual reflectivities of the underlying surface at various wavelengths of interest. Comparison of the

numerical results obtained from the analysis of simulated measurements at five wavelengths (BUV configuration) using the original procedure and several modifications to it based on the findings of §4, is made in §5.1 through §5.5. This comparison then culminates into a set of recommendations (§5.6) which are too numerous to be summarized here.

The experience gained during the investigation reported in §5 is then used to set up an estimation procedure for total ozone with the SBUV/TOMS configuration where one additional measurement of intensity is also available (§6.1). Results obtained with the final version of the procedure for the BUV configuration, and with the procedure for the SBUV/TOMS configuration are compared in §6.2, §6.3, and §6.4. Recommendations which can assist in improving the quality of ozone values obtained with the procedure described in §6.1, are then outlined in §6.5.

Analysis presented in this particular report is for the so-called Rayleigh-, or molecular-scattering models of the terrestrial atmosphere. In other words, these models are assumed to be free of any particles comparable to, or larger than, the wavelengths of the electromagnetic radiation specified for measurements. Analysis of numerical results for atmospheric models containing spherical polydispersions of known characteristics, will be the subject matter of the final report with the same title as this one.

VIII. ACKNOWLEDGMENTS

I would like to take this opportunity to express my sincere thanks to Dr. C. L. Mateer of the Atmospheric Environment Service, Toronto, Canada, to Drs. A. J. Fleig, R. S. Fraser, and Mr. L. V. Novak of NASA/GSFC, and to Dr. A. Kaveeshwar and others associated directly with the BUV analysis project at NASA/GSFC for their valuable comments and assistance at various stages of this work.

IX. REFERENCES

1. Dave, J. V., and C. L. Mateer, 1967: J. Atmos. Sci., *24*, pp. 414 - 427.

2. Mateer, C. L., D. F. Heath, and A. J. Krueger, 1971: J. Atmos. Sci., *28*, pp. 1307 - 1311.

APPENDIX A

A.1 *Description of the Program:* In §2.4, §5.1, §5.3, §6.1, and §6.4, we mentioned several programs (SITC1, SITC2, SITC3, SITC4, SITC6, SITC8, SITD1, and SITD2) for estimating total ozone from the simulated measurements of the intensity of the scattered radiation emerging at the top of an atmospheric model along the local nadir direction. These procedures are arrived at after carrying out minor changes (from the programming considerations) in a basic program, i.e., SITC1. We will therefore describe only one program (viz, SITC4), in great detail, in this section. The listing of the FORTRAN statements, and printout for a test run with simulated measurements for one atmospheric model are given in §A.2 and A.3, respectively. The subroutine OMESLO which is being called by all programs, will be described first. In Table A.I, we have given mathematical equivalence as appearing in the text and/or definitions of important variables appearing in the subroutine OMESLO, and the calling program SITC4.

Subroutine OMESLO: The function of this subroutine is to return values of the quantities $\Omega^{Z}_{x,y}$ and $S^{Z}_{x,y}$ for a given value of θ_0, and for the stated values of the subscripts x and y, as well as the superscript Z. It has 11 arguments and contains 66 statements.

The first three arguments (viz, EIC, TIC, and SBAR) are for specifying locations for the quantities $I_c(\lambda, \Omega_{in}, P_0, R_\lambda = 0.0, \theta_0)$, $T_c(\lambda, \Omega_{in}, P_0, \theta_0)$, and $\bar{S}(\lambda, \Omega_{in}, P_0)$ defined in §2.2. These are essentially

Table A.I Variables appearing in the subroutine OMESLO, and program SITC4 and their mathematical equivalence or definition.

Variable	Equivalence or Definition
A	Variable for reading in values of $I_c(\lambda, \Omega, P_0, R_\lambda = 0.0, \theta, \theta_0)$ for a given model defined by the parameters Ω and P_0. These values are available on the disc (Data File No. 16) for 18 values of θ, for 10 values of θ_0, and for 6 different wavelengths. See ¶1 and ¶2 of §2.2 for the definition.
ALBD	$R^Z_{\lambda,y}$ vector called by the subroutine OMESLO. Z = C or I (see Steps. I, II, and V of §2.4). y = 1,000 mb or 400 mb.
ALDA	Wavelength λ.
B	Variable for reading in values of $T_c(\lambda, \Omega, P_0, \theta, \theta_0)$ for a given model. See ¶1 and ¶2 of §2.2, and also the definition of the quantity A above.
BEST	*Best ozone estimate*, Ω_e; Eqs. (9), (10), and (11).
C	Variable for reading in values of $\bar{S}(\lambda, \Omega, P_0)$ for a given model. See ¶1 and ¶2 of §2.2, and also the definition of the quantity A above.
DEV	$\Omega_e - \Omega$
EFFALC	$R^C_{\lambda,y}$; *coarse effective albedo* at the wavelength λ obtained by using y mb pressure tables; see Step I and II of §2.4.

Table A.I, cont'd.

Variable	Equivalence or Definition
EFFALI	$R^{I}_{\lambda,y}$; *improved effective albedo*; see EFFALC.
EIC	$I_c(\lambda, \Omega_{in}, P_0, R_\lambda = 0.0, \theta_0)$ for 6 values of λ, 20 basic atmospheric models [the first (second) 10 values of the second subscript of EIC for 10 increasing values of Ω_{in}, but for P_0 = 1,000 (400) mb], and 10 values of θ_0 (the last subscript of EIC).
EIM	$I_m(\lambda, \theta_0)$; §2.4.
IGRP	Parameter representing the ground pressure value for the basic tables; IGRP = 1, and 2 for P_0 = 1,000, and 400 mb, respectively.
ISLT	Parameter selecting the wavelength (or wavelength pair) to be used for the next set of computations.
LAM1, LAM2	Parameters for selecting individual wavelengths of a pair; see Eq. (4) and the statement No. SITC 11.
NMOD	Model number for which values of Ω_e and $\bar{R}$ are to be obtained.
NTHETO	Serial number of the subscript of the parameter θ_0 (THETO); see the statement No. SITC 10.
OMEGA	Total ozone amount, $\Omega^{Z}_{x,y}$ for Z = C, or I; x = 1, or 2, and y = 1,000, or 400 mb.
OMEGC	$\Omega^{C}_{x,y}$; see Step III of §2.4.
OMEGI	$\Omega^{I}_{x,y}$; see Step VI of §2.4.

Table A.I, cont'd.

Variable	Equivalence or Definition
OMEGIN	Ω_{in}; see the second paragraph following Eq. (1).
RAT	N_c given by Eq. (4); for a given wavelength pair, and given values of the parameters P_0 and θ_0.
RATM	N_m; see Eq. (5).
REF	R; Lambert reflectivity of the surface underlying the atmospheric model.
SBAR	$\bar{S}(\lambda, \Omega_{in}, P_0)$ for 6 values of λ, and 20 basic atmospheric models (see definition of EIC).
SLOPE	$S^Z_{x,y}$; see Eq. (6).
SLPC	$S^C_{x,y}$; see Step III of §2.4.
SLPI	$S^I_{x,y}$; see Step VI of §2.4.
STALB	$\sum \bar{R}$ summed over all values of θ_0 for a given value of R (quantity REF above); see Eq. (12).
TEMA, TEMB, TEMC	Temporary variables.
THETO	θ_0; solar zenith angle.
TIC	$T_c(\lambda, \Omega_{in}, P_0, \theta_0)$ for 6 values of λ, 20 basic atmospheric models (see definition of EIC), and 10 values of θ_0.
TITB	Title information.

the basic tables of these quantities for six different values of wavelengths used in the SBUV/TOMS configuration (only five for the BUV configuration), ten atmospheric models with P_0 = 1,000 mb and the next ten models with P_0 = 400 mb, and for ten different values of the solar zenith angle. The input ozone amounts for these models are those listed in Table III; models No. 1 and 12 are not to be included.

The next two arguments (viz, LAM1 and LAM2) specify wavelengths λ_i and λ_j for which the measurements of $I_m(\lambda, \theta_0)$ are to be analyzed for obtaining values of $\Omega^Z_{x,y}$ and $S^Z_{x,y}$. The sixth argument (NTHETO) is for specifying one of the ten preselected (statement No. SITC 10) values of the solar zenith angle, θ_0. The seventh argument (ALBD) carries values for the quantities R_{λ_i} and R_{λ_j} to be used in computations of N_c given by Eq. (4). The eighth argument IGRP = 1 if 1,000 mb tables are to be used, and = 2 for the use of 400 mb tables. Values of $I_m(\lambda, \theta_0)$ for six wavelengths, but for a given value of θ_0 are available in the locations specified by EIM, while computed values of $\Omega^Z_{x,y}$ and $S^Z_{x,y}$ are returned in locations marked OMEGA and SLOPE, respectively.

Statements No. OMESL 3 through 41 contain comments, a format statement, a dimension statement, and a data (Ω_{in}) initialization statement. The quantity $N_m(\lambda_i, \lambda_j; \theta_0)$ given by Eq. (5) is computed at the end of successful execution of statement No. OMESL 42.

The DO LOOP 200 contained between the statements No. OMESL 43 through 56 is for computations of values of the quantity N_c for all ten values of Ω_{in}, but for the given values of the parameters λ_i, λ_j,

R_{λ_i}, R_{λ_j}, θ_0, and P_0. The quantity N_c is set to -999.99 (OMESL 55) under an unlikely condition of finding a very small ($\leq 10^{-10}$) value for the computed intensity, I_c (OMESL 49). An appropriate message (OMESL 53 and 54) is also printed out at the terminal.

Statements contained in the DO LOOP 300 (OMESL 57 through 62) are then executed for computing values of $\Omega^Z_{x,y}$ (OMEGA), and $S^Z_{x,y}$ (SLOPE) by making use of the procedure outlined in §2.3. The quantity $\Omega^C_{x,y}$ is computed by backward extrapolation if a given value of N_m is less than the first computed value of N_c which is for Ω_{in} = 0.200 atm-cm. The quantities OMEGA and SLOPE are set to 0.0, and -100.0, respectively when a given value of N_m is greater than the last computed value of N_c which is for Ω_{in} = 0.650 atm-cm (OMESL 63 and 64).

Program SITC4: This program contains a total of 235 statements. Statements No. SITC 1 through 15 contain comment cards, dimension statements, and data initialization statement. Further information about the DEFINE FILE 16 statement (SITC 13) can be found on page No. 55 of the Technical Report: I of this contract. The first 22 records of this data set contains values of I_c, T_c, $\bar{S}$ for 22 atmospheric models listed in Table III.

The input to this program is the values of I_c, T_c, and $\bar{S}$ for the 22 atmospheric models listed in Table III, and also for the atmospheric model (NMOD, see SITC 61) for which values of the *best ozone estimate* (Ω_e) and *effective albedo* ($\bar{R}$) are to be computed for 10 values of θ_0 (SITC 10), and 8 values of R (SITC 12). A given record on the data set

No. 16 contains 14 words of the title information describing the atmospheric model for which values of I_c and T_c are available for 18 values of θ and 10 values of θ_0, and of I_c, T_c, and $\bar{S}$ for 6 wavelengths.

The function of the part of the program contained between the statements SITC 40 through 59 is to read in data for 20 atmospheric models with non-zero ozone content (Table III), and to store the part of these data required for future use in appropriate locations. It should be noted that only values of I_c and T_c along the nadir direction [i.e., $\theta = 0°$; or A(1, N, L) and B(1, N, L)] are stored; values of these quantities in the remaining 17 directions are discarded. At the end of a successful execution of this part of the program, values of I_c, T_c, and $\bar{S}$ for the L-th wavelength, for the J-th atmospheric model, and for the N-th value of θ_0 (not for $\bar{S}$) can be found in the location EIC(L, J1, N), TIC(L, J1, N), and SBAR(L, J1), respectively, where J1 = J - 1 for 1,000 mb models, and J1 = J - 2 for 400 mb models.

The next input to the program (value of the parameter NMOD; the atmospheric model number for which the printout is desired) is in a conversational mode (at a terminal) under VM/CMS. Execution of the statement No. SITC 60 leads to the appearance of the following message at the terminal:

```
MODEL NUMBER PLEASE?
?
```

A value for NMOD can then be typed and entered. This value is then read

in as the value of the quantity NMOD during execution of statement No. 61.

The program is terminated if the value of the parameter NMOD read in is less than, or equal to, zero (SITC 62). For values of NMOD greater than zero, the quantities Ω_e and $\bar{R}$ are evaluated and printed out for all ten values of θ_0 and a given R during the execution of the 450 DO LOOP (SITC 71 through 227), and then this process is repeated for the remaining values of R (500 DO LOOP; SITC 67 through 230). Information about the atmospheric model under study is printed out before entering the DO LOOP 500 (SITC 64 through 66).

For a given atmospheric model NMOD, and a given value of reflectivity [REF(I)] as well as of the solar zenith angle [THETO(N)], values of $I_m(\lambda, \theta_0)$ for all six values of λ are computed during the execution of the statements contained between the statements numbered SITC 75 and 77, by making use of Eq. (1). Computed value of $I_m(0.3800, \theta_0)$ is then used for computations of the quantity $R^C_{0.3800,1000}$ [Eqs. (2) and (3)] using 1,000 mb (IGRP = 1) tables, [Note that 0.3800 μm radiation is unaffected by ozone absorption. Thus, values of EIC(6, IT, N), TIC(6, IT, N), and SBAR(6, IT) are the same for all values of the subscript IT in the range 1 through 10.], and Eqs. (2) and (3). Statements in the 158 DO LOOP (SITC 87 through 89) are then used to assign the value of $R^C_{0.3800,1000}$ to $R^C_{\lambda,1000}$ at the remaining five wavelengths (Step II of §2.4).

The section of the program contained between the statements No. SITC 97 and 108 is then used for computing values of $\Omega^C_{x,1000}$ and $S^C_{x,1000}$ for $x = 1$, and 2 [computations for the first pair ($x = 1$) are carried out only if $\theta_0 \leq 79.6°$]. The quantity $\Omega^C_{x,1000}$ is set to zero, and the quantity $S^C_{x,1000}$ is set to -100 for cases for which it is not possible to evaluate $\Omega^C_{x,1000}$ (Step III of §2.4). Computations of $\Omega^C_{x,1000}$ and $S^C_{x,1000}$ are performed by calling the subroutine OMESLO, and after using the values of $R^C_{\lambda,1000}$ (EFFALC).

If $\Omega^C_{x,1000} = 0$ for $x = 1$ and 2, i.e., none of the ozone values is available at stage SITC 109, it is not possible to proceed with computations of $R^I_{\lambda,1000}$, $\Omega^I_{x,1000}$ and $S^I_{x,1000}$ using Steps IV and V of §2.4. Under such circumstances, we assign appropriate values to these quantities, and transfer control to statement No. SITC 169. If one or both values of $\Omega^C_{x,1000}$ are available, one of the pairs (i.e., parameter ISLT) is selected for computations of $R^I_{0.3398,1000}$ during execution of the statements No. SITC 118, 119, and 120.

The part of the program contained between statements No. SITC 127 through 150 is for computations of the *improved effective albedo* represented by the symbol $R^I_{\lambda,1000}$ using the procedure outlined in Step V of §2.4. The parameter JT is assigned a value between 1 and 10 (11 and 20) if the set of computations are to be performed with 1,000 (400) mb tables. Values of $\Omega^I_{x,1000}$ and $S^I_{x,1000}$ are then obtained during the execution of statements No. SITC 157 through 168. This latter part of the program is identical to that contained between statements No.

SITC 97 through 108, except that values of EFFALI are used in the place of those for the quantity EFFALC.

A second pass through the part of the program contained between SITC 84 and SITC 169 is then made for computations of various quantities listed in Step VII of §2.4. Since this second pass is for computations with the 400 mb tables, parameters IGRP and IT are set to 2 and to 11, respectively (SITC 170 through 173).

Statements SITC 178 through 185 are used for satisfying the constraint described under SITC3 in §5.1. Values of Ω_e and $\bar{R}$ are then obtained following Step IX of §2.4 by executing statements No. SITC 186 through 221.

For computations for a given value of the Lambert reflectivity of the underlying surface (variable I of the DO LOOP 500), a summation of $\bar{R}$ for all ten values of θ_0 is accumulated at the location STALB(I). Mean values of $\bar{R}$ for each of the eight values of R are printed out after completing all work for the atmospheric model, NMOD.

A.2 *Listing of the FORTRAN Statements:*

```
C                                                                       SITC   1
C      PROGRAM FOR ESTIMATING TOTAL OZONE FROM SIMULATED OBSERVATIONS    SITC   2
C      IN THE NADIR DIRECTION FOR THE NIMBUS - 4 CONFIGURATION....      SITC   3
C                                                                       SITC   4
      REAL * 4 TITB(14),A(18,10,6),B(18,10,6),C(6),REF(8),EIC(6,20,10), SITC   5
     1 TIC(6,20,10),SBAR(6,20),ALDA(6),THETO(10),EFFALC(6,2),           SITC   6
     2 EFFALI(6,2),OMEGIN(10),OMEGC(2,2),OMEGI(2,2),SLPC(2,2),SLPI(2,2) SITC   7
     3 ,EIM(6)                                                          SITC   8
      REAL * 4 STALB(8)                                                 SITC   9
      DATA THETO /0.0,45.0,60.0,70.0,75.6,79.6,82.5,84.7,86.7,90.0/     SITC  10
      DATA ALDA /0.3125,0.3175,0.3312,0.3398,0.3600,0.3800/             SITC  11
      DATA REF /0.0,0.1,0.2,0.3,0.4,0.6,0.8,1.0/                        SITC  12
      DEFINE FILE 16 (200,8720,L,IPF)                                   SITC  13
      DATA OMEGIN /0.200,0.250,0.300,0.350,0.400,0.450,0.500,0.550,     SITC  14
     1 0.600,0.650/                                                     SITC  15
   10 FORMAT (1H1)                                                      SITC  16
   15 FORMAT (T3,'MODEL NUMBER PLEASE ?')                               SITC  17
   20 FORMAT (1H1/T30,'ATMOSPHERIC MODEL NUMBER : ',I5,T80,             SITC  18
     1 'PROGRAM USED : SITC4'///T10,                                    SITC  19
     2 'SURFACE PRESSURE (MB) : ',F10.2,T55,'TOTAL OZONE AMOUNT (ATM-CM)SITC  20
     3 : ',F10.3////T40,'D U S T     D A T A '///T9,'TYPE OF',          SITC  21
     4 T24,'SIZE DISTRIBUTION',T48,'PART OF THE REFRACTIVE INDEX',      SITC  22
     5 T86,'TOTAL'/T8,'AEROSOLS',T30,'FUNCTION',T52,'REAL',             SITC  23
     6 T62,'IMAGINARY',T85,'AMOUNT'/)                                   SITC  24
   25 FORMAT (/T4,'STRATOSPHERIC',8X,3A4,4X,0P2F15.3,1P1E20.2)          SITC  25
   30 FORMAT (/T4,'TROPOSPHERIC',9X,3A4,4X,0P2F15.3,1P1E20.2/)          SITC  26
   35 FORMAT (/T2,'THETA',T14,'USING 1,000 MB SURFACE-PRESSURE TABLES', SITC  27
     1 T71,'USING 400 MB SURFACE-PRESSURE TABLES',T120,'BEST'/         SITC  28
     2 T2,'SUB',T14,'COARSE VALUES',T42,'IMPROVED VALUES',             SITC  29
     3 T72,'COARSE VALUES',T97,'IMPROVED VALUES',T120,'OZONE'/         SITC  30
     4 T2,'ZERO',T10,'ALBEDO',T19,'OMEG.A',T27,'OMEG.B',T37,'ALBEDO',  SITC  31
     5 T46,'OMEG.A',T54,'OMEG.B',T66,'ALBEDO',T75,'OMEG.A',T83,        SITC  32
     6 'OMEG.B',T93,'ALBEDO',T102,'OMEG.A',T110,'OMEG.B',T120,'ESTI.', SITC  33
     7 T128,'DEV.'/)                                                   SITC  34
   40 FORMAT (/T10,'MODEL NUMBER :',I5,                                 SITC  35
     1 T45,'LAMBERT REFLECTIVITY OF THE UNDERLYING SURFACE = ',         SITC  36
     2 F10.3/)                                                         SITC  37
   45 FORMAT (F6.2,2X,3F8.3,3X,3F8.3,5X,3F8.3,3X,3F8.3,F9.3,F7.3)       SITC  38
      IW = 8                                                           SITC  39
      JMIN = 2                                                         SITC  40
      JMAX = 11                                                        SITC  41
  110 CONTINUE                                                         SITC  42
      DO 130 J = JMIN,JMAX                                             SITC  43
      READ (16'J) TITB,A,B,C                                           SITC  44
      J1 = J - 1                                                       SITC  45
      IF ( J .GT. 11 ) J1 = J - 2                                      SITC  46
      DO 120 L = 1,6                                                   SITC  47
      DO 115 N = 1,10                                                  SITC  48
      EIC(L,J1,N) = A(1,N,L)                                           SITC  49
      TIC(L,J1,N) = B(1,N,L)                                           SITC  50
  115 CONTINUE                                                         SITC  51
      SBAR(L,J1) = C(L)                                                SITC  52
  120 CONTINUE                                                         SITC  53
  130 CONTINUE                                                         SITC  54
      IF ( JMAX .GT. 11 ) GO TO 135                                    SITC  55
```

```
      JMIN = 13                                                          SITC  56
      JMAX = 22                                                          SITC  57
      GO TO 110                                                          SITC  58
  135 CONTINUE                                                           SITC  59
  140 WRITE (6,15)                                                       SITC  60
      READ (5,*) NMOD                                                    SITC  61
      IF ( NMOD .LE. 0) GO TO 1000                                       SITC  62
      READ (16'NMOD) TITB,A,B,C                                          SITC  63
      WRITE (IW,20) NMOD,TITB(1),TITB(2)                                 SITC  64
      WRITE (IW,25) TITB(9),TITB(10),TITB(11),TITB(5),TITB(6),TITB(3)    SITC  65
      WRITE (IW,30) TITB(12),TITB(13),TITB(14),TITB(7),TITB(8),TITB(4)   SITC  66
      DO 500 I = 1,8                                                     SITC  67
      STALB(I) = 0.0                                                     SITC  68
      WRITE (IW,40) NMOD,REF(I)                                          SITC  69
      WRITE (IW,35)                                                      SITC  70
      DO 450 N = 1,10                                                    SITC  71
C                                                                        SITC  72
C      COMPUTE SIMULATED MEASUREMENTS OF THE INTENSITY....               SITC  73
C                                                                        SITC  74
      DO 150 L = 1,6                                                     SITC  75
      EIM(L) = A(1,N,L) + B(1,N,L) * (REF(I)/(1.0 - C(L) * REF(I)))      SITC  76
  150 CONTINUE                                                           SITC  77
C                                                                        SITC  78
C      COMPUTE VALUES OF THE COARSE EFFECTIVE ALBEDO USING 1,000 MB      SITC  79
C      (IGRP=1) TABLES, OR 400 MB (IGRP=2) TABLES.                       SITC  80
C                                                                        SITC  81
      IGRP = 1                                                           SITC  82
      IT = 1                                                             SITC  83
  155 CONTINUE                                                           SITC  84
      TEMA = EIM(6) - EIC(6,IT,N)                                        SITC  85
      EFFALC(6,IGRP) = TEMA/(TIC(6,IT,N) + SBAR(6,IT) * TEMA)            SITC  86
      DO 158 J = 1,4                                                     SITC  87
      EFFALC(J,IGRP) = EFFALC(6,IGRP)                                    SITC  88
  158 CONTINUE                                                           SITC  89
C                                                                        SITC  90
C      ESTIMATE COARSE TOTAL-OZONE AMOUNTS FOR BOTH WAVELENGTH PAIRS,    SITC  91
C      AND DECIDE THE PAIR FOR DETERMINING IMPROVED EFECTIVE ALBEDO.     SITC  92
C                                                                        SITC  93
C                                                                        SITC  94
C      DO NOT USE THE FIRST PAIR IF THETA SUB ZERO IS GREATER THAN 79.6. SITC  95
C                                                                        SITC  96
      IF ( N .LE. 6 ) GO TO 159                                          SITC  97
      OMEGC(1,IGRP) = 0.0                                                SITC  98
      SLPC(1,IGRP) = -100.0                                              SITC  99
      GO TO 160                                                          SITC 100
  159 CONTINUE                                                           SITC 101
      CALL OMESLO (EIC,TIC,SBAR,1,3,N,EFFALC,IGRP,EIM,OMEGA,SLOPE)       SITC 102
      OMEGC(1,IGRP) = OMEGA                                              SITC 103
      SLPC(1,IGRP) = SLOPE                                               SITC 104
  160 CONTINUE                                                           SITC 105
      CALL OMESLO (EIC,TIC,SBAR,2,4,N,EFFALC,IGRP,EIM,OMEGA,SLOPE)       SITC 106
      OMEGC(2,IGRP) = OMEGA                                              SITC 107
      SLPC(2,IGRP) = SLOPE                                               SITC 108
      IF(OMEGC(1,IGRP) .GT. 0.0 .OR. OMEGC(2,IGRP) .GT. 0.0) GO TO 165   SITC 109
      OMEGI(1,IGRP) = 0.0                                                SITC 110
```

```
      OMEGI(2,IGRP) = 0.0                                                SITC 111
      SLPI(1,IGRP) = -100.0                                              SITC 112
      SLPI(2,IGRP) = -100.0                                              SITC 113
      DO 162 J = 1,4                                                     SITC 114
      EFFALI(J,IGRP) = EFFALC(J,IGRP)                                    SITC 115
  162 CONTINUE                                                           SITC 116
      GO TO 190                                                          SITC 117
  165 CONTINUE                                                           SITC 118
      ISLT = 2                                                           SITC 119
      IF ( SLPC(1,IGRP) .GT. SLPC(2,IGRP) ) ISLT = 1                     SITC 120
C                                                                        SITC 121
C      COMPUTE VALUES OF THE IMPROVED EFFECTIVE ALBEDO..                 SITC 122
C                                                                        SITC 123
C                                                                        SITC 124
C      INTERPOLATE BETWEEN TWO OZONE VALUES.                             SITC 125
C                                                                        SITC 126
      TEMA = OMEGC(ISLT,IGRP)                                            SITC 127
      DO 170 J = 2,10                                                    SITC 128
      IF ( TEMA .GT. OMEGIN(J) ) GO TO 170                               SITC 129
      JT = (IGRP-1) * 10 + J - 1                                         SITC 130
      GO TO 175                                                          SITC 131
  170 CONTINUE                                                           SITC 132
      JT = (IGRP-1) * 10 + 10                                            SITC 133
  175 CONTINUE                                                           SITC 134
      TEMB = EIM(4) - EIC(4,JT,N)                                        SITC 135
      TEMB = TEMB/(TIC(4,JT,N) + SBAR(4,JT) * TEMB)                      SITC 136
      JT = JT + 1                                                        SITC 137
      IF ( IGRP .EQ. 2 ) GO TO 176                                       SITC 138
      IF ( JT .GT. 10 ) JT = 10                                          SITC 139
      GO TO 177                                                          SITC 140
  176 IF ( JT .GT. 20 ) JT = 20                                          SITC 141
  177 CONTINUE                                                           SITC 142
      TEMC = EIM(4) - EIC(4,JT,N)                                        SITC 143
      TEMC = TEMC/(TIC(4,JT,N) + SBAR(4,JT) * TEMC)                      SITC 144
      JT = JT - 1                                                        SITC 145
      IF ( JT .GT. 10 ) JT = JT - 10                                     SITC 146
      EFFALI(4,IGRP) = TEMB + 20.0 * (TEMC - TEMB) * (TEMA - OMEGIN(JT)) SITC 147
      DO 180 J = 1,3                                                     SITC 148
      EFFALI(J,IGRP) = EFFALI(4,IGRP)                                    SITC 149
  180 CONTINUE                                                           SITC 150
C                                                                        SITC 151
C      ESTIMATE IMPROVED TOTAL OZONE AMOUNTS FOR BOTH WAVELENGTH PAIRS.  SITC 152
C                                                                        SITC 153
C                                                                        SITC 154
C      DO NOT USE THE FIRST PAIR IF THETA SUB ZERO IS GREATER THAN 79.6. SITC 155
C                                                                        SITC 156
      IF ( N .LE. 6 ) GO TO 185                                          SITC 157
      OMEGI(1,IGRP) = 0.0                                                SITC 158
      SLPI(1,IGRP) = -100.0                                              SITC 159
      GO TO 187                                                          SITC 160
  185 CONTINUE                                                           SITC 161
      CALL OMESLO (EIC,TIC,SBAR,1,3,N,EFFALI,IGRP,EIM,OMEGA,SLOPE)       SITC 162
      OMEGI(1,IGRP) = OMEGA                                              SITC 163
      SLPI(1,IGRP) = SLOPE                                               SITC 164
  187 CONTINUE                                                           SITC 165
```

```
      CALL OMESLO (EIC,TIC,SBAR,2,4,N,EFFALI,IGRP,EIM,OMEGA,SLOPE)      SITC 166
      OMEGI(2,IGRP) = OMEGA                                             SITC 167
      SLPI(2,IGRP) = SLOPE                                              SITC 168
  190 CONTINUE                                                          SITC 169
      IF ( IGRP .EQ. 2 ) GO TO 200                                      SITC 170
      IGRP = 2                                                          SITC 171
      IT = 11                                                           SITC 172
      GO TO 155                                                         SITC 173
C                                                                       SITC 174
C      SELECT THE BEST ESTIMATE..                                       SITC 175
C                                                                       SITC 176
  200 CONTINUE                                                          SITC 177
      DO 210 K = 1,2                                                    SITC 178
      DO 205 J = 1,2                                                    SITC 179
      TEMA = ABS(OMEGI(J,K) - OMEGC(J,K))                               SITC 180
      IF ( TEMA .LT. 0.030 ) GO TO 205                                  SITC 181
      OMEGI(J,K) = 0.0                                                  SITC 182
      SLPI(J,K) = -100.0                                                SITC 183
  205 CONTINUE                                                          SITC 184
  210 CONTINUE                                                          SITC 185
      IPAIRA = 0                                                        SITC 186
      IPAIRB = 0                                                        SITC 187
      IF (OMEGI(1,1) .GT. 0.0 .AND. OMEGI(1,2) .GT. 0.0) IPAIRA = 1     SITC 188
      IF (OMEGI(2,1) .GT. 0.0 .AND. OMEGI(2,2) .GT. 0.0) IPAIRB = 1     SITC 189
      IF (IPAIRA .EQ. 1 .AND. IPAIRB .EQ. 1) GO TO 300                  SITC 190
      IF (IPAIRA .EQ. 1) GO TO 230                                      SITC 191
      IF (IPAIRB .EQ. 1) GO TO 270                                      SITC 192
      BEST = 0.0                                                        SITC 193
      TEMA = 0.5 * (EFFALI(4,1) + EFFALI(4,2))                          SITC 194
      IF ( TEMA .GT. 0.2 ) GO TO 215                                    SITC 195
      BEST = AMAX1 (OMEGI(1,1),OMEGI(2,1))                              SITC 196
      GO TO 380                                                         SITC 197
  215 IF ( TEMA .LT. 0.8 ) GO TO 380                                    SITC 198
      BEST = AMAX1 (OMEGI(1,2),OMEGI(2,2))                              SITC 199
      GO TO 380                                                         SITC 200
  230 ISLT = 1                                                          SITC 201
      GO TO 330                                                         SITC 202
  270 ISLT = 2                                                          SITC 203
      GO TO 330                                                         SITC 204
  300 ISLT = 2                                                          SITC 205
      IF (SLPI(1,1) .GT. SLPI(2,1) .AND. SLPI(1,2) .GT. SLPI(2,2))     SITC 206
     1 ISLT = 1                                                         SITC 207
  330 CONTINUE                                                          SITC 208
      TEMA = 0.5 * (EFFALI(4,1) + EFFALI(4,2))                          SITC 209
      IF ( TEMA .GT. 0.2 ) GO TO 340                                    SITC 210
      BEST = OMEGI(ISLT,1)                                              SITC 211
      GO TO 380                                                         SITC 212
  340 IF ( TEMA .GE. 0.8 ) GO TO 360                                    SITC 213
      BEST = (1.0/0.6) * ((0.8-TEMA) * OMEGI(ISLT,1) +                  SITC 214
     1 (TEMA-0.2) * OMEGI(ISLT,2))                                      SITC 215
      GO TO 380                                                         SITC 216
  360 BEST = OMEGI(ISLT,2)                                              SITC 217
C                                                                       SITC 218
C     PRINT OUT..                                                       SITC 219
C                                                                       SITC 220
```

```
 380 CONTINUE                                                                    SITC 221
     STALB(I) = STALB(I) + TEMA                                                  SITC 222
     DEV = BEST - TITB(2)                                                        SITC 223
     WRITE (IW,45) THETO(N),EFFALC(4,1),(OMEGC(K,1),K=1,2),                      SITC 224
    1 EFFALI(4,1),(OMEGI(K,1),K=1,2),EFFALC(4,2),(OMEGC(K,2),K=1,2),             SITC 225
    2 EFFALI(4,2),(OMEGI(K,2),K=1,2),BEST,DEV                                   SITC 226
 450 CONTINUE                                                                    SITC 227
     STALB(I) = 0.1 * STALB(I)                                                   SITC 228
     IF ( I .EQ. 2 .OR. I .EQ. 5 .OR. I .EQ. 8 ) WRITE (IW,10)                   SITC 229
 500 CONTINUE                                                                    SITC 230
     WRITE (IW,502) (STALB(I),I=1,8)                                             SITC 231
 502 FORMAT (/T4,'EIGHT MEAN IMPROVED ALBEDOES : ',8F8.3)                        SITC 232
     GO TO 140                                                                   SITC 233
1000 RETURN                                                                      SITC 234
     END                                                                         SITC 235
```

```
      SUBROUTINE OMESLO (EIC,TIC,SBAR,LAM1,LAM2,NTHETO,                 OMESL  1
     1 ALBD,IGRP,EIM,OMEGA,SLOPE)                                       OMESL  2
C                                                                       OMESL  3
C       SUBROUTINE FOR ESTIMATING TOTAL OZONE AND THE SLOPE             OMESL  4
C       OF THE N - OMEGA CURVE IN THE REGION OF THE ESTIMATED OZONE...  OMESL  5
C                                                                       OMESL  6
C       EIC,TIC, AND SBAR AT 6 WAVELENGTHS, VIZ. 0.3125,0.3175,         OMESL  7
C       0.3312,0.3398,0.3600, AND 0.3800 MICROMETERS.                   OMESL  8
C                                                                       OMESL  9
C       EIC,TIC, AND SBAR FOR 10 DIFFERENT OZONE AMOUNTS (0.200(0.050)  OMESL 10
C       0.650) FOR  1,000 MB SURFACE-PRESSURE MODELS, AND THEN FOR      OMESL 11
C       400 MB SURFACE-PRESSURE MODELS....                              OMESL 12
C                                                                       OMESL 13
C       EIC AND TIC FOR 10 DIFFERENT VALUES OF THETA SUB ZERO...        OMESL 14
C                                                                       OMESL 15
C       LAM1 : SERIAL NUMBER OF THE SHORTER WAVELENGTH.                 OMESL 16
C       LAM2 : SERIAL NUMBER OF THE LONGER WAVELENGTH.                  OMESL 17
C                                                                       OMESL 18
C       NTHETO : SERIAL NUMBER OF THETA SUB ZERO.                       OMESL 19
C                                                                       OMESL 20
C       ALBD : MEASURED ALBEDOES AT 6 WAVELENGTHS, AND FOR TWO GROUND   OMESL 21
C       PRESSURES...                                                    OMESL 22
C                                                                       OMESL 23
C       IGRP = 1 : USE TABLES CORRESPONDING TO 1,000 MB.                OMESL 24
C       IGRP = 2 : USE TABLES CORRESPONDING TO 400 MB.                  OMESL 25
C                                                                       OMESL 26
C       EIM : MEASURED INTENSITIES AT 6 WAVELENGTHS.                    OMESL 27
C                                                                       OMESL 28
C       OMEGA : ESTIMATED OZONE AMOUNT; SET TO 0.0 IF NO ESTIMATION     OMESL 29
C               IS POSSIBLE.                                            OMESL 30
C                                                                       OMESL 31
C       SLOPE : SLOPE OF THE N - OMEGA CURVE IN THE REGION OF THE       OMESL 32
C               ESTIMATED TOTAL OZONE; SET TO -100.0 IF OMEGA = 0.0.    OMESL 33
C                                                                       OMESL 34
   20 FORMAT (/T5,'NOT POSSIBLE TO DETERMINE N VALUE FOR'/              OMESL 35
     1 T5,'IGRP,NTHETO,LAM1,LAM2,TEMA,TEMB =',4I5,1P2E12.4/             OMESL 36
     2 T5,'EFFECTIVE ALBEDO AT LAM1 AND LAM2 =',2F12.5)                 OMESL 37
      REAL * 4 EIC(6,20,10),TIC(6,20,10),SBAR(6,20),ALBD(6,2),          OMESL 38
     1 EIM(6),RAT(10),OMEGIN(10)                                        OMESL 39
      DATA OMEGIN /0.200,0.250,0.300,0.350,0.400,0.450,0.500,           OMESL 40
     1 0.550,0.600,0.650/                                               OMESL 41
      RATM = 100.0 * ALOG10 (EIM(LAM2)/EIM(LAM1))                       OMESL 42
      DO 200 J = 1,10                                                   OMESL 43
      JJ = (IGRP - 1) * 10 + J                                          OMESL 44
      TEMA = EIC(LAM1,JJ,NTHETO) + TIC(LAM1,JJ,NTHETO) *                OMESL 45
     1 (ALBD(LAM1,IGRP)/(1.0 - SBAR(LAM1,JJ)*ALBD(LAM1,IGRP)))          OMESL 46
      TEMB = EIC(LAM2,JJ,NTHETO) + TIC(LAM2,JJ,NTHETO) *                OMESL 47
     1 (ALBD(LAM2,IGRP)/(1.0 - SBAR(LAM2,JJ)*ALBD(LAM2,IGRP)))          OMESL 48
      IF (TEMA .LE. 1.0E-10 .OR. TEMB .LE. 1.0E-10) GO TO 150           OMESL 49
      RAT(J) = 100.0 * ALOG10(TEMB/TEMA)                                OMESL 50
      GO TO 200                                                         OMESL 51
  150 CONTINUE                                                          OMESL 52
      WRITE (6,20)IGRP,NTHETO,LAM1,LAM2,TEMA,TEMB,ALBD(LAM1,IGRP),      OMESL 53
     1 ALBD(LAM2,IGRP)                                                  OMESL 54
      RAT(J) = -9999.99                                                 OMESL 55
```

```
200 CONTINUE                                                          OMESL 56
    DO 300 J = 1,9                                                    OMESL 57
    IF ( RATM .GT. RAT(J+1) ) GO TO 300                               OMESL 58
    SLOPE = (RAT(J+1) - RAT(J)) * 20.0                                OMESL 59
    OMEGA = OMEGIN(J) + (RATM - RAT(J))/SLOPE                         OMESL 60
    GO TO 350                                                         OMESL 61
300 CONTINUE                                                          OMESL 62
    OMEGA = 0.0                                                       OMESL 63
    SLOPE = -100.0                                                    OMESL 64
350 RETURN                                                            OMESL 65
    END                                                               OMESL 66
```

A.3 *Output from a Test Run:*

ATMOSPHERIC MODEL NUMBER : 5

SURFACE PRESSURE (MB) : 1000.00 TOTAL OZONE AMOUNT (ATM-C

D U S T D A T A

TYPE OF AEROSOLS	SIZE DISTRIBUTION FUNCTION	PART OF THE REFRACTIVE INDEX REAL	IMAGINARY
STRATOSPHERIC		1.000	0.0
TROPOSPHERIC		1.000	0.0

MODEL NUMBER : 5 LAMBERT REFLECTIVITY OF THE UNDERLY

THETA SUB ZERO	USING 1,000 MB SURFACE-PRESSURE TABLES COARSE VALUES ALBEDO	OMEG.A	OMEG.B	IMPROVED VALUES ALBEDO	OMEG.A	OMEG.B	USING 400 COARSE VA ALBEDO	OMEG.A
0.0	0.0	0.350	0.350	-0.000	0.350	0.350	0.105	0.34
45.00	0.0	0.350	0.350	-0.000	0.350	0.350	0.120	0.35
60.00	0.0	0.350	0.350	-0.000	0.350	0.350	0.140	0.36
70.00	0.0	0.350	0.350	-0.000	0.350	0.350	0.167	0.36
75.60	0.0	0.350	0.350	-0.000	0.350	0.350	0.187	0.37
79.60	0.0	0.350	0.350	-0.000	0.350	0.350	0.201	0.37
82.50	0.0	0.0	0.350	-0.000	0.0	0.350	0.205	0.0
84.70	0.0	0.0	0.350	-0.000	0.0	0.350	0.198	0.0
86.70	0.0	0.0	0.350	-0.000	0.0	0.350	0.180	0.0
90.00	0.0	0.0	0.350	-0.000	0.0	0.350	0.147	0.0

MODEL NUMBER : 5 LAMBERT REFLECTIVITY OF THE UNDERLY

THETA SUB ZERO	USING 1,000 MB SURFACE-PRESSURE TABLES COARSE VALUES ALBEDO	OMEG.A	OMEG.B	IMPROVED VALUES ALBEDO	OMEG.A	OMEG.B	USING 400 COARSE V ALBEDO	OMEG.A
0.0	0.100	0.350	0.350	0.100	0.350	0.350	0.183	0.34
45.00	0.100	0.350	0.350	0.100	0.350	0.350	0.194	0.35
60.00	0.100	0.350	0.350	0.100	0.350	0.350	0.211	0.35
70.00	0.100	0.350	0.350	0.100	0.350	0.350	0.233	0.36
75.60	0.100	0.350	0.350	0.100	0.350	0.350	0.250	0.36
79.60	0.100	0.350	0.350	0.100	0.350	0.350	0.263	0.37
82.50	0.100	0.0	0.350	0.100	0.0	0.350	0.267	0.0
84.70	0.100	0.0	0.350	0.100	0.0	0.350	0.262	0.0
86.70	0.100	0.0	0.350	0.100	0.0	0.350	0.247	0.0
90.00	0.100	0.0	0.350	0.100	0.0	0.350	0.217	0.0

AL OZONE AMOUNT (ATM-CM) : 0.350

A

E REFRACTIVE INDEX IMAGINARY | TOTAL AMOUNT

0.0 | 0.0

0.0 | 0.0

CTIVITY OF THE UNDERLYING SURFACE = 0.0

.B	USING 400 MB SURFACE-PRESSURE TABLES COARSE VALUES ALBEDO	OMEG.A	OMEG.B	IMPROVED VALUES ALBEDO	OMEG.A	OMEG.B	BEST OZONE ESTI.	DEV.
50	0.105	0.346	0.305	0.166	0.324	0.275	0.350	0.000
50	0.120	0.353	0.319	0.189	0.332	0.291	0.350	0.000
50	0.140	0.360	0.333	0.216	0.339	0.309	0.350	0.000
50	0.167	0.366	0.345	0.244	0.346	0.326	0.350	0.000
50	0.187	0.372	0.352	0.259	0.350	0.336	0.350	0.000
50	0.201	0.379	0.356	0.260	0.354	0.342	0.350	0.000
50	0.205	0.0	0.356	0.252	0.0	0.345	0.350	0.000
50	0.198	0.0	0.356	0.239	0.0	0.344	0.350	0.000
50	0.180	0.0	0.360	0.226	0.0	0.340	0.350	0.000
50	0.147	0.0	0.450	0.241	0.0	0.0	0.350	0.000

CTIVITY OF THE UNDERLYING SURFACE = 0.100

.B	USING 400 MB SURFACE-PRESSURE TABLES COARSE VALUES ALBEDO	OMEG.A	OMEG.B	IMPROVED VALUES ALBEDO	OMEG.A	OMEG.B	BEST OZONE ESTI.	DEV.
50	0.183	0.348	0.318	0.233	0.336	0.302	0.350	0.000
50	0.194	0.353	0.327	0.252	0.340	0.311	0.350	0.000
50	0.211	0.357	0.337	0.275	0.345	0.322	0.350	0.000
50	0.233	0.363	0.347	0.299	0.349	0.333	0.350	0.000
50	0.250	0.367	0.352	0.312	0.352	0.341	0.350	0.000
50	0.263	0.373	0.355	0.313	0.355	0.345	0.350	-0.000
50	0.267	0.0	0.356	0.307	0.0	0.347	0.350	-0.000
50	0.262	0.0	0.356	0.295	0.0	0.347	0.350	0.000
50	0.247	0.0	0.358	0.284	0.0	0.344	0.350	0.000
50	0.217	0.0	0.405	0.290	0.0	0.0	0.350	0.000

MODEL NUMBER : 5 LAMBERT REFLECTIVITY OF THE UNDERLYI

THETA SUB ZERO	USING 1,000 MB SURFACE-PRESSURE TABLES COARSE VALUES ALBEDO	OMEG.A	OMEG.B	IMPROVED VALUES ALBEDO	OMEG.A	OMEG.B	USING 400 M COARSE VA ALBEDO	OMEG.A
0.0	0.200	0.350	0.350	0.200	0.350	0.350	0.264	0.353
45.00	0.200	0.350	0.350	0.200	0.350	0.350	0.271	0.355
60.00	0.200	0.350	0.350	0.200	0.350	0.350	0.284	0.358
70.00	0.200	0.350	0.350	0.200	0.350	0.350	0.302	0.361
75.60	0.200	0.350	0.350	0.200	0.350	0.350	0.316	0.364
79.60	0.200	0.350	0.350	0.200	0.350	0.350	0.327	0.369
82.50	0.200	0.0	0.350	0.200	0.0	0.350	0.332	0.0
84.70	0.200	0.0	0.350	0.200	0.0	0.350	0.328	0.0
86.70	0.200	0.0	0.350	0.200	0.0	0.350	0.317	0.0
90.00	0.200	0.0	0.350	0.200	0.0	0.350	0.290	0.0

MODEL NUMBER : 5 LAMBERT REFLECTIVITY OF THE UNDERLYI

THETA SUB ZERO	USING 1,000 MB SURFACE-PRESSURE TABLES COARSE VALUES ALBEDO	OMEG.A	OMEG.B	IMPROVED VALUES ALBEDO	OMEG.A	OMEG.B	USING 400 M COARSE VAL ALBEDO	OMEG.A
0.0	0.300	0.350	0.350	0.300	0.350	0.350	0.347	0.358
45.00	0.300	0.350	0.350	0.300	0.350	0.350	0.352	0.358
60.00	0.300	0.350	0.350	0.300	0.350	0.350	0.361	0.359
70.00	0.300	0.350	0.350	0.300	0.350	0.350	0.374	0.361
75.60	0.300	0.350	0.350	0.300	0.350	0.350	0.385	0.363
79.60	0.300	0.350	0.350	0.300	0.350	0.350	0.394	0.366
82.50	0.300	0.0	0.350	0.300	0.0	0.350	0.399	0.0
84.70	0.300	0.0	0.350	0.300	0.0	0.350	0.398	0.0
86.70	0.300	0.0	0.350	0.300	0.0	0.350	0.389	0.0
90.00	0.300	0.0	0.350	0.300	0.0	0.350	0.365	0.0

MODEL NUMBER : 5 LAMBERT REFLECTIVITY OF THE UNDERLYIN

THETA SUB ZERO	USING 1,000 MB SURFACE-PRESSURE TABLES COARSE VALUES ALBEDO	OMEG.A	OMEG.B	IMPROVED VALUES ALBEDO	OMEG.A	OMEG.B	USING 400 M COARSE VAL ALBEDO	OMEG.A
0.0	0.400	0.350	0.350	0.400	0.350	0.350	0.434	0.363
45.00	0.400	0.350	0.350	0.400	0.350	0.350	0.435	0.362
60.00	0.400	0.350	0.350	0.400	0.350	0.350	0.440	0.361
70.00	0.400	0.350	0.350	0.400	0.350	0.350	0.448	0.361
75.60	0.400	0.350	0.350	0.400	0.350	0.350	0.457	0.362
79.60	0.400	0.350	0.350	0.400	0.350	0.350	0.464	0.364
82.50	0.400	0.0	0.350	0.400	0.0	0.350	0.469	0.0
84.70	0.400	0.0	0.350	0.400	0.0	0.350	0.469	0.0
86.70	0.400	0.0	0.350	0.400	0.0	0.350	0.464	0.0
90.00	0.400	0.0	0.350	0.400	0.0	0.350	0.444	0.0

CTIVITY OF THE UNDERLYING SURFACE = 0.200

	USING 400 MB SURFACE-PRESSURE TABLES						BEST	
	COARSE VALUES			IMPROVED VALUES			OZONE	
B	ALBEDO	OMEG.A	OMEG.B	ALBEDO	OMEG.A	OMEG.B	ESTI.	DEV.
50	0.264	0.353	0.332	0.303	0.346	0.323	0.350	-0.000
50	0.271	0.355	0.336	0.318	0.348	0.327	0.350	-0.000
50	0.284	0.358	0.342	0.337	0.350	0.333	0.350	-0.000
50	0.302	0.361	0.349	0.357	0.352	0.340	0.350	0.000
50	0.316	0.364	0.353	0.368	0.353	0.345	0.350	0.000
50	0.327	0.369	0.355	0.370	0.356	0.348	0.350	-0.000
50	0.332	0.0	0.356	0.365	0.0	0.349	0.350	-0.000
50	0.328	0.0	0.356	0.355	0.0	0.349	0.350	-0.000
50	0.317	0.0	0.357	0.345	0.0	0.347	0.350	-0.000
50	0.290	0.0	0.388	0.348	0.0	0.0	0.0	-0.350

CTIVITY OF THE UNDERLYING SURFACE = 0.300

	USING 400 MB SURFACE-PRESSURE TABLES						BEST	
	COARSE VALUES			IMPROVED VALUES			OZONE	
B	ALBEDO	OMEG.A	OMEG.B	ALBEDO	OMEG.A	OMEG.B	ESTI.	DEV.
50	0.347	0.358	0.344	0.377	0.354	0.339	0.351	0.001
50	0.352	0.358	0.345	0.388	0.354	0.340	0.351	0.001
50	0.361	0.359	0.348	0.402	0.354	0.342	0.351	0.001
50	0.374	0.361	0.352	0.418	0.355	0.346	0.351	0.001
50	0.385	0.363	0.354	0.428	0.355	0.349	0.351	0.001
50	0.394	0.366	0.356	0.429	0.357	0.351	0.350	0.000
50	0.399	0.0	0.356	0.426	0.0	0.352	0.350	0.000
50	0.398	0.0	0.356	0.419	0.0	0.351	0.350	0.000
50	0.389	0.0	0.357	0.410	0.0	0.350	0.350	-0.000
50	0.365	0.0	0.380	0.411	0.0	0.0	0.0	-0.350

CTIVITY OF THE UNDERLYING SURFACE = 0.400

	USING 400 MB SURFACE-PRESSURE TABLES						BEST	
	COARSE VALUES			IMPROVED VALUES			OZONE	
.B	ALBEDO	OMEG.A	OMEG.B	ALBEDO	OMEG.A	OMEG.B	ESTI.	DEV.
50	0.434	0.363	0.354	0.455	0.361	0.351	0.354	0.004
50	0.435	0.362	0.353	0.461	0.359	0.350	0.354	0.004
50	0.440	0.361	0.354	0.471	0.358	0.350	0.353	0.003
50	0.448	0.361	0.355	0.483	0.357	0.351	0.353	0.003
50	0.457	0.362	0.356	0.491	0.357	0.352	0.353	0.003
50	0.464	0.364	0.356	0.493	0.358	0.353	0.351	0.001
50	0.469	0.0	0.357	0.491	0.0	0.353	0.351	0.001
50	0.469	0.0	0.357	0.486	0.0	0.354	0.351	0.001
50	0.464	0.0	0.357	0.479	0.0	0.353	0.351	0.001
50	0.444	0.0	0.375	0.480	0.0	0.348	0.349	-0.001

MODEL NUMBER : 5 LAMBERT REFLECTIVITY OF THE UNDERLYIN

THETA SUB ZERO	USING 1,000 MB SURFACE-PRESSURE TABLES COARSE VALUES ALBEDO	OMEG.A	OMEG.B	IMPROVED VALUES ALBEDO	OMEG.A	OMEG.B	USING 400 M COARSE VAL ALBEDO	OMEG.A
0.0	0.600	0.350	0.350	0.600	0.350	0.350	0.617	0.371
45.00	0.600	0.350	0.350	0.600	0.350	0.350	0.610	0.369
60.00	0.600	0.350	0.350	0.600	0.350	0.350	0.607	0.366
70.00	0.600	0.350	0.350	0.600	0.350	0.350	0.607	0.363
75.60	0.600	0.350	0.350	0.600	0.350	0.350	0.609	0.362
79.60	0.600	0.350	0.350	0.600	0.350	0.350	0.612	0.363
82.50	0.600	0.0	0.350	0.600	0.0	0.350	0.617	0.0
84.70	0.600	0.0	0.350	0.600	0.0	0.350	0.622	0.0
86.70	0.600	0.0	0.350	0.600	0.0	0.350	0.624	0.0
90.00	0.600	0.0	0.350	0.600	0.0	0.350	0.610	0.0

MODEL NUMBER : 5 LAMBERT REFLECTIVITY OF THE UNDERLYIN

THETA SUB ZERO	USING 1,000 MB SURFACE-PRESSURE TABLES COARSE VALUES ALBEDO	OMEG.A	OMEG.B	IMPROVED VALUES ALBEDO	OMEG.A	OMEG.B	USING 400 M COARSE VAL ALBEDO	OMEG.A
0.0	0.800	0.350	0.350	0.800	0.350	0.350	0.813	0.377
45.00	0.800	0.350	0.350	0.800	0.350	0.350	0.800	0.374
60.00	0.800	0.350	0.350	0.800	0.350	0.350	0.788	0.370
70.00	0.800	0.350	0.350	0.800	0.350	0.350	0.779	0.366
75.60	0.800	0.350	0.350	0.800	0.350	0.350	0.774	0.364
79.60	0.800	0.350	0.350	0.800	0.350	0.350	0.774	0.363
82.50	0.800	0.0	0.350	0.800	0.0	0.350	0.779	0.0
84.70	0.800	0.0	0.350	0.800	0.0	0.350	0.788	0.0
86.70	0.800	0.0	0.350	0.800	0.0	0.350	0.797	0.0
90.00	0.800	0.0	0.350	0.800	0.0	0.350	0.789	0.0

MODEL NUMBER : 5 LAMBERT REFLECTIVITY OF THE UNDERLYIN

THETA SUB ZERO	USING 1,000 MB SURFACE-PRESSURE TABLES COARSE VALUES ALBEDO	OMEG.A	OMEG.B	IMPROVED VALUES ALBEDO	OMEG.A	OMEG.B	USING 400 M COARSE VAL ALBEDO	OMEG.A
0.0	1.000	0.350	0.350	1.000	0.350	0.350	1.026	0.382
45.00	1.000	0.350	0.350	1.000	0.350	0.350	1.006	0.379
60.00	1.000	0.350	0.350	1.000	0.350	0.350	0.985	0.374
70.00	1.000	0.350	0.350	1.000	0.350	0.350	0.966	0.369
75.60	1.000	0.350	0.350	1.000	0.350	0.350	0.954	0.366
79.60	1.000	0.350	0.350	1.000	0.350	0.350	0.951	0.365
82.50	1.000	0.0	0.350	1.000	0.0	0.350	0.956	0.0
84.70	1.000	0.0	0.350	1.000	0.0	0.350	0.970	0.0
86.70	1.000	0.0	0.350	1.000	0.0	0.350	0.986	0.0
90.00	1.000	0.0	0.350	1.000	0.0	0.350	0.985	0.0

EIGHT MEAN IMPROVED ALBEDOES : 0.114 0.193 0.273 0.355 0.439 0.61

128

ECTIVITY OF THE UNDERLYING SURFACE = 0.600

	USING 400 MB SURFACE-PRESSURE TABLES						BEST	
	COARSE VALUES			IMPROVED VALUES			OZONE	
G.B	ALBEDO	OMEG.A	OMEG.B	ALBEDO	OMEG.A	OMEG.B	ESTI.	DEV.
350	0.617	0.371	0.368	0.624	0.370	0.368	0.364	0.014
350	0.610	0.369	0.366	0.621	0.368	0.365	0.362	0.012
350	0.607	0.366	0.363	0.622	0.365	0.362	0.360	0.010
350	0.607	0.363	0.360	0.625	0.362	0.359	0.358	0.008
350	0.609	0.362	0.359	0.629	0.360	0.357	0.357	0.007
350	0.612	0.363	0.358	0.631	0.360	0.357	0.355	0.005
350	0.617	0.0	0.358	0.632	0.0	0.357	0.355	0.005
350	0.622	0.0	0.358	0.632	0.0	0.357	0.355	0.005
350	0.624	0.0	0.360	0.629	0.0	0.358	0.356	0.006
350	0.610	0.0	0.372	0.631	0.0	0.361	0.357	0.007

ECTIVITY OF THE UNDERLYING SURFACE = 0.800

	USING 400 MB SURFACE-PRESSURE TABLES						BEST	
	COARSE VALUES			IMPROVED VALUES			OZONE	
G.B	ALBEDO	OMEG.A	OMEG.B	ALBEDO	OMEG.A	OMEG.B	ESTI.	DEV.
350	0.813	0.377	0.378	0.813	0.377	0.378	0.377	0.027
350	0.800	0.374	0.374	0.801	0.374	0.374	0.374	0.024
350	0.788	0.370	0.370	0.792	0.370	0.370	0.370	0.020
350	0.779	0.366	0.365	0.786	0.366	0.365	0.365	0.015
350	0.774	0.364	0.362	0.786	0.363	0.362	0.363	0.013
350	0.774	0.363	0.360	0.788	0.362	0.359	0.359	0.009
350	0.779	0.0	0.360	0.793	0.0	0.359	0.359	0.009
350	0.788	0.0	0.361	0.797	0.0	0.360	0.360	0.010
350	0.797	0.0	0.362	0.799	0.0	0.362	0.362	0.012
350	0.789	0.0	0.374	0.803	0.0	0.368	0.368	0.018

ECTIVITY OF THE UNDERLYING SURFACE = 1.000

	USING 400 MB SURFACE-PRESSURE TABLES						BEST	
	COARSE VALUES			IMPROVED VALUES			OZONE	
G.B	ALBEDO	OMEG.A	OMEG.B	ALBEDO	OMEG.A	OMEG.B	ESTI.	DEV.
350	1.026	0.382	0.383	1.025	0.382	0.383	0.382	0.032
350	1.006	0.379	0.380	1.003	0.379	0.380	0.379	0.029
350	0.985	0.374	0.375	0.984	0.374	0.375	0.374	0.024
350	0.966	0.369	0.369	0.969	0.369	0.369	0.369	0.019
350	0.954	0.366	0.365	0.964	0.365	0.364	0.365	0.015
350	0.951	0.365	0.362	0.968	0.363	0.361	0.363	0.013
350	0.956	0.0	0.361	0.975	0.0	0.360	0.360	0.010
350	0.970	0.0	0.362	0.984	0.0	0.361	0.361	0.011
350	0.986	0.0	0.365	0.992	0.0	0.364	0.364	0.014
350	0.985	0.0	0.376	0.998	0.0	0.372	0.372	0.022

73 0.355 0.439 0.614 0.798 0.993